Scuola Internazionale Superiore di Studi Avanzati - Trieste

Gene Therapy for Arterial Restenosis Using AAV Vectors

Thesis submitted for the degree of

"Doctor Philosophiae"
in
Molecular Genetics and Biotechnology

Candidate:
Genaro Antonio Ramirez Correa

Supervisors:
Mauro Giacca
Lorena Zentilin

SISSA – Via Beirut 2-4 – 34014 TRIESTE – ITALY

Gene Therapy for Arterial Restenosis Using AAV Vectors

a thesis submitted for
Ph. D. degree in Molecular Genetics
S.I.S.S.A., Trieste, Italy

Genaro Antonio Ramirez-Correa

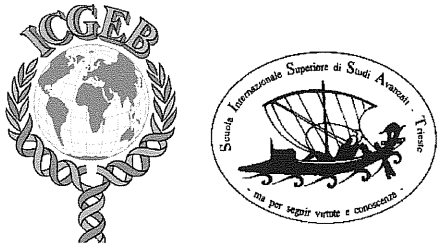

International Centre for Genetic Engineering and Biotechnology

October 2003

ABSTRACT

Gene Therapy for Arterial Restenosis Using AAV Vectors

Genaro Antonio Ramirez-Correa

The work I will describe in this thesis concerns the study of the properties of AAV vectors both as a gene transfer system and as a therapeutic vector in the context of a restenosis model. The gene transfer properties of AAV are evaluated *in vitro* and *in vivo*, directly exposing recombinant AAV vectors (rAAV) in cells and tissues. Complementary to these studies, the rAAV transfer properties are also evaluated *in vitro* and in *organ culture* conditions using intracoronary sents as scaffolds for gene delivery.

The main focus of the thesis was to evaluate the effects of two different AAV vectors, AAV-Timp1 and AAV-PTX3, in blocking arterial stenosis. AAV-Timp1 vector encodes for the human Tissue-inhibitor of metalloproteinases 1, which blocks the metalloproteinases (MMPs) and AAV-PTX3 vector encodes for the human long-pentraxin 3, which inhibits Fibroblast growth factor 2 (FGF-2) induced proliferation. Both MMPs and FGF-2 are involved in the pathogenesis of restenosis and atherosclerosis.

Chapter 1 offers an introduction to the characteristics of the normal and atherosclerotic vessels, angioplasty and restenosis. It reviews the available animals models for restenosis and pathogenesis. The functional properties of MMPs, Timps and PTX3 are also reviewed. The history of gene transfer to the vessel wall and other gene therapy approaches for restenosis together with the characteristics of the AAV vectors are described.

Chapter 2 covers both the details of experimental techniques and materials. The rat animal model was the main tool for *in vivo* evaluation. In Chapter 3 the experimental results are exposed and Chapter 4 includes their discussion. In Chapter 5 the rationale and the proof of principle of AAV attachment to coated intracoronary stents are described.

The novelty of this thesis is three-fold. First, from the point of view of gene therapy, this is the first time that AAV is used as a therapeutic vector in a restenosis model. Second, from the point of view of investigating the role of a new protein, this is the first time that PTX3 is overexpressed in the vascular wall and its effects reported. Third, this is the first time that an AAV gene delivery system using stent-based gene therapy has been reported. AAV gene delivery is a powerful new approach for site-specific expression of genes aiming to block restenosis or in-stent restenosis.

ACKNOWLEDGEMENTS

I would like to express a sincere thanks to my supervisors, Mauro Giacca and Lorena Zentilin. They have both given me constant stimulus since early days as a visiting undergraduate student, they show me how to face scientific challenges, and provide me advice and patience throughout all this four years of my Ph.D. I would also like to thank ICGEB for awarding me with a pre-doctoral fellowship.

To Giacca's Lab I would like to take this opportunity to express all my gratefulness to everybody in the lab for the friendly and lively environment (almost to loudly Lusič but thanks for doing the DJ thing), also to all my friends (old and new) from the ICGEB, from back home (Monterrey and Mexico City), from the American Football, from the Aikido and elsewhere. Especial thanks to Ramiro for encouraging my application and having advised me on numerous experiments. Also many thanks to Serena, Elena, Palacios, Vindigni, Marco, Maurizio, Renata and Capullo for sharing good moments, hopes and principally for giving me comfort in difficult moments.

I am indebted to the members of the ULIEG and Biochemistry Departments, especially to Hugo Barrera who open to me first the gate to the molecular medicine.

Unmeasurable thanks go to my closest friends, Ernesto, Sheila, Dalila, Rafa, Azeneth, Lalo, Chicharo, Davis, Armendariz, Homero, Ivan and many others who have made always believe the distance and the time does not matter when a true friendship has born.

I am very grateful to Maša for her trust in me, her enormous support and love over all these very important three years, of course in similar extent to her family particularly to Marco and Breda.

Por ultimo me gustaría agradecer eternamente a Dios, a Papá y Mama por su apoyo incondicional desde que la memoria me registra, a Paco y a la Beba por ser mis hermanos y dejarse sentir cercanos durante todo este tiempo, a mi abuela y a mi tía Martha a Rita y a todos mis tíos, tías, primos y primas (tengo una familia grande), especialmente a Bibis que nunca dejo de contactarme, todos ellos han siempre han creído en mí. Obviamente dedico esta tesis a ellos, a mis padres a a la Ani y a mis seres queridos que ya se fueron; mis abuelos (Pancho, Chole y Baldomero), a Chabelita y a Andrea...también a ellos les dedico esta tesis. El recuerdo de los que se fueron alimentan el anhelo de mi sueño.

Contents

List of Figures

Chapter 1

Introduction

1.1 Aim and scope of the thesis

The aim of this thesis is to demonstrate the potential of recombinant adeno-associate viruses (rAAV) as efficient *in vivo* vectors for gene therapy approaches to block restenosis. The potential of AAV to infect the vessel wall and express gene markers is explored after direct intraluminal injection and after stent-based gene delivery. The *in vivo* effects of specific gene products are evaluated with a morphometry analysis. Finally, the effects of AAV-Timp1 and AAV-PTX3 are compared for both single and dual vector administration.

This introductory chapter provides the scientific background for the thesis and describes first the normal blood vessels, the changes that lead to atherosclerosis and the restenosis process. Further, it reviews the therapeutic strategies that have been used in the past and the potential targets for future therapies. Finally, it describes the structure and the biology of AAV vectors and their use for gene transfer in the vascular system.

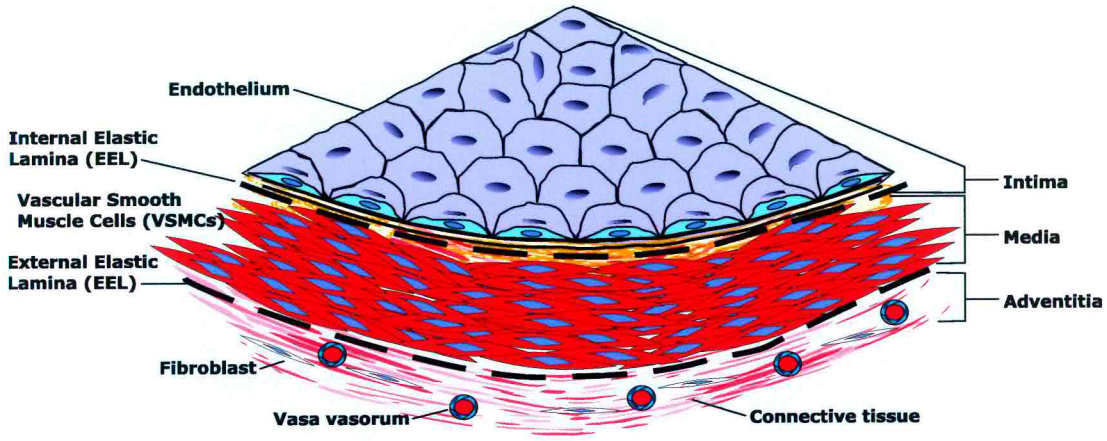

Figure 1.1: **Composition of normal arterial vascular wall:** schematic representation of the main components of the vascular wall of a muscular artery.

1.2 Normal blood vessels

1.2.1 Histological characteristics

The arteries are composed mainly of endothelial cells, smooth muscle cells and an extracellular matrix, which includes elastin, collagen and proteoglycans. Arterial vasculature is composed of arteries, arterioles (20 to 100 μm) and capillaries (7 to 8 μm). Arteries are divided into three types, depending on their diameter and main wall composition: i) large or elastic arteries, including aorta, common carotid and iliac, ii) medium or muscular, including coronary and renal, iii) small arteries that are distributed mainly as a part of organ parenchyma and that have an average diameter of less than 2 mm. Arteries are composed of three concentric layers: intima, media and adventitia as shown in Figure 1.1. The *intima* is adjacent to the lumen, composed of endothelial cells (EC) and a thin subendothelial connective tissue. The *media* is separated from the intima by the internal elastic lamina (IEL), contains vascular smooth muscle cells (VSMCs) and the outer limit is defined by external elastic lamina (EEL). The adventitia is composed by connective tissue, fibroblasts, nerve fibers and vasa vasorum, in bigger arteries [1].

1.2.2 Physiology of arterial cell types

Endothelial cells

The endothelial system occupies the largest area of the human body and could be considered as the largest organ. This system is formed by a monolayer of endothelial cells (EC) that are in general of polygonal shape, elongated and joined by specialized organelles. The endothelial cells exert pleiotropic functions, from the physical isolation of the vessel wall to the synthesis of key regulators of the cardiovascular system. In particular they play a role in; 1) Control of macromolecular trafficking by acting as semipermeable membrane, 2) Control of coagulation and haemostasis, 3) Modulation of vascular reactivity and blood flow by synthesizing specific molecules, 4) Metabolism of hormones, 5) Regulation of cell trafficking during inflammation, 6) Modification of lipoproteins and 7) Control of growth of vascular smooth muscle cells (VSMCs) and other cell types [1].

Vascular smooth muscle cells (VSMCs)

This cell type is generally present only in the wall of arteries and arterioles. In the resting state VSMCs have a spindle shape morphology and a single elongated nucleus. VSMCs can be recognized by their hemostatic role and their plastic ability. The later property provides them with the capacity of responding to hemodynamic stress and injury.

These cells exert several important functions, that can be summarized as follows: 1) Modulation of vascular reactivity and blood flow by direct vasoconstriction and vasodilatation, 2) Modulation of extracellular matrix metabolism (synthesis/degradation) within the vessel wall, 3) Synthesis of growth factors and cytokines, 4) Modulation of proliferation and migration by autocrine/paracrine mechanisms in normal vascular repair and pathological processes and 4) Anti-apoptotic effects [2].

There are different types of VSMCs depending on the type of environmental influence. They may proliferate and hence give rise to hyperplasia (increase in cell number), become hypertrophic (increase in cell size), endoduplicate (increase in DNA content with normal size) or undergo premature apoptosis.

VSMCs, derived form mesenchyma, and in normal conditions, are quiescent cells in resting state(G_0). Although morphologically indistinguishable, the VSMCs population within the vessel wall is phenotypically and functionally heterogeneous. It is worthy to mention that VSMCs is not the only cell type found in the media of muscular arteries. Campbell and colleagues [3] introduced first the term, "contractile" and "synthetic", to distinguish the normal spindle-shaped VSMCs phenotype which correlates with the"contractile"function from the epithelioid VSMCs phenotype which correlates wit the"synthetic"ability. Recently, Fird et al [4] identified at least four different phenotypes, two non-muscle and two smooth muscle cell phenotype. The two non-muscle cell types were located one closer to the luminal side and one in the outer side of medial layer, they were of rhomboidal and rounded morphology, respectively, and of fast growth in serum. The two smooth muscle cell types were located in the middle and outer part of the medial layer, were of sindle shape morphology and of slow growth in serum. They both expressed alpha-SM-actin, SM-myosin and only the one located in the outer media expressed metavinculin.

1.3 Atherosclerotic blood vessels

1.3.1 Histopathological features

Arteriosclerosis comes from the Greek words athero (meaning gruel or paste) and sclerosis (hardness), and means literally *hardening of the arteries.* It is a generic term for different patterns of vascular diseases, that have in common wall thickening, lumen loss and loss of elasticity. The most frequent pattern is *atherosclerosis*, which is followed

by *Mönckenberg medial calcific sclerosis* and then by a disease of small arteries, *hyperplastic* or *hyaline arteriosclerosis.* These two anatomic variants are more frequently secondary to diabetes mellitus and hypertension. Hyperplastic arteriosclerosis is the most common complication post-organ transplantation, being the cause of more than half of transplantation failures.

Atherosclerosis is characterized by *fibrous plaque* or *fibrofatty plaques.* The plaque probably originates from an initial lesion called *fatty streak* and can be found already in the first life decade. The key features of the atherosclerosis are intimal thickening and lipid accumulation, which in turn give rise to a focal plaque. As lesion grows, a core rich in lipids forms (cholesterol, cholesterol esters and necrotic cells), covered by a fibrous cap. Slowly, this lesion protrudes into the lumen predisposing thrombosis, plaque rupture or hemorrhage.

The main components of an atherosclerotic plaque are cells, including VSMCs, macrophages (Mϕ), leukocytes, connective tissue extracellular matrix (ECM), including collagen, elastic fibers, proteoglycans and intracellular-extracellular lipid deposits (see Figure 1.2).

The typical lesion in the vessel wall is eccentrical, the superficial *fibrous cap* is composed mainly of VSMCs, few leukocytes and a dense layer of connective tissue. Beneath this surface there is an area called *Shoulder* that has a cellular layer (VSMCs, Mϕ, T Lymphocytes) and a *necrotic core.* The *necrotic core* is variable in size and composition, there is a disorganized mass of lipid material, cholesterol clefts, cellular debris, lipid-laden foam cells, fibrin deposits, thrombus and plasmatic proteins. Around this lesion there is usually some evidence of neovascularization, seen in the proliferation of small blood vessels [1].

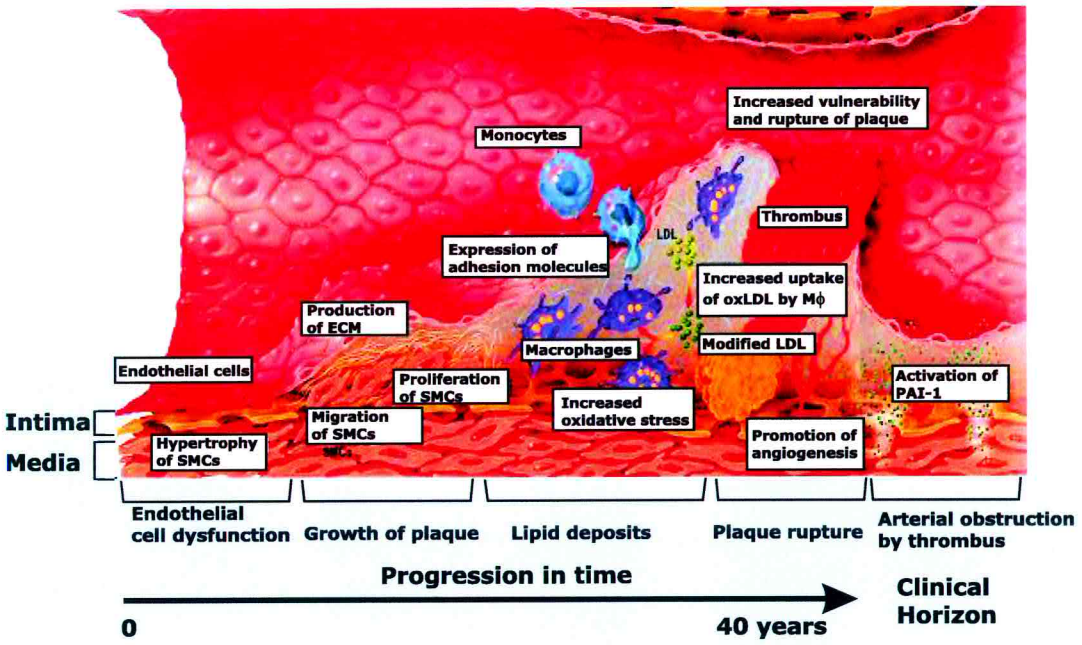

Figure 1.2: **Atherosclerosis progression**: Schematic diagram of the sequence of events leading to the progression of atherosclerosis in response to the injury hypothesis. Main events are depicted making reference to time elapsed in the natural history towards an obscure clinical horizon.

1.3.2 Atherogenesis

Atherosclerosis is currently considered a chronic inflammatory disease [5]. Atherosclerosis has a very complex aetiology and only certain factors have been directly linked to the development of the disease. However, for atherogenesis as for many other diseases, there are initial stimuli that trigger the *initiation* of the process, several factors that may influence its *progression* and severity of the lesions and *late complications* that give rise to clinical syndromes and many fatal clinical events, such as stroke, hemorrhage, heart attack and hypertension.

Endothelial contribution

The endothelial injury is the cornerstone of the *initiation* of the process, as atherosclerosis has preferred sites and it is believed that hemodynamic forces are responsible for the initial increase of endothelial permeability. Chronic endothelial injury may be

caused by one or more of the following factors, 1) hyperlipidemia, 2) hypertension, 3) smoking, 4) homocysteinemia, 5) hemodynamic forces, 6) mechanical endothelial denudation, 7) toxins, 8) viral infection, 9) bacterial infections, and 10) immune reactions. This stimuli have in focal areas the following pathological consequences: 1) increased endothelial permeability, namely low-density lipoproteins (LDLs) later modified by oxidation, 2) increased leukocyte adhesion and migration: T lymphocytes, monocyte that transform in macrophages (Mϕ) and foam cells, 3) platelets adhesion in denuded areas and to adherent leukocytes, 4) release of factors from activated platelets, (Mϕ) or vascular cells that provoke migration of VSMCs from media to intima, 5) proliferation of VSMCs within the intima with synthesis of extracellular matrix (ECM) leading to accumulation of collagen and proteoglycans, 6) accumulation of lipids within cells (Mϕ and VSMCs) and extracellularly [6].

Once the initial lesion is established the progression is favored by the development of a chronic inflammatory reaction. A key event for triggering the inflammatory reaction is the accumulation of oxidized LDL (oxLDL) that stimulates endothelial cells to produce pro-inflammatory molecules. The presence of this molecules ensures the recruitment of lymphocytes and monocytes by inducing the endothelial cells to express the following factors 1) chemotactic proteins (i.e. monocyte chemotactic protein (MCP-1)), 2) growth factors (i.e. macrophage colony-stimulating factor (M-CSF)) and 3) leukocyte adhesion molecules (i.e. ICAM-1, P-selectin, E-selectin, PCAM-1, VCAM-1, β2 integrin, VLA-4). oxLDL affect endothelial cells through the inhibition of production of nitric oxide (NO), a master molecule for the vessel haemostasia, and activation of NF-κB pathway [7].

Macrophages contribution to Atherosclerosis

Foam-cell formation starts as soon as macrophages (Mϕ) differentiated from monocytes phagocyte highly oxidized LDL. The oxidation of LDL is mediated by reactive

oxygen species (ROS), sphingomyelinase (SMAse), secretory phospholipase 2 (sPLA2) and myeloperoxidase (MPO). Rapid take up of oxLDL by Mϕ is mediated by specific receptors, SR-A and CD36 that recognize modified LDL (oxLDL). In addition, oxLDLs are by themselves chemotactic, inhibit Mϕ motility, are cytotoxic for EC and VSMCs and are immunogenic, inducing the production of antibodies. On the other hand, Mϕ have a multifunctional role in the development of atherosclerosis, in inducing proliferation in the intima and amplification of the inflammatory reaction by producing and secreting growth agonists, growth antagonists and chemoattractants [7].

Vascular smooth muscle cells contribution

VSMCs have a complex origin and represent an heterogeneous cell population. In humans within this cell population two morphological phenotypes, spindle-shaped and epithelioid, can be described. The spindle-shaped phenotype functionally correlates with the contractile function whereas the epithelioid correlates with the synthetic ability. Different myosin filaments distribution and secretory protein apparatus characterize the two phenotypes. Contractile VSMCs express high levels of myosin and low levels of *alpha*-actin. In contrast, synthetic VSMCs express high levels of *alpha*-actin, extracellular matrix (ECM) and low levels of myosin [2]. Each VSMCs subtype responds to different agents; contractile phenotype react to endothelin (ET), cathecolamines, angiotensin II (A-II), PGE, PGI2, neuropeptides, leukotrienes and NO, whereas synthetic phenotype responds to numerous growth-regulatory molecules and cytokines [6].

Endothelial cells (EC), activated macrophages (Mϕ), VSMCs and aggregating platelets (Plts) release factors that provoke VSMCs migration to the intima. Other molecules, which originate form the same cell types, such as IL-1, TNF-α, TGF-β and PDGF, stimulate synthetic VSMC to proliferate and to produce PDGF-AA, creating an autocrine loop and stimulating also neighboring cells [6].

Bone marrow derived cells contribution

There is a growing body of evidence that recruitment of bone marrow (BM) derived cells, such as monocytes [8] and hematopoietic derived stem cells (HSCs) [9], is involved in the pathogenesis of atherosclerosis. A similar event has been observed in other accelerated atherosclerotic syndromes such as vein graft failure [10], post-angioplastic [11, 12], post-transplant restenosis [13, 14, 15] and post-transplant arteriosclerosis [16]. These observations depend on the model and strategy employed, likewise, the level of HSCs contribution to lesions progression varies from author to author [17, 9]. The specific cell type(s) that serve(s) as progenitor(s) in atherosclerotic lesions is at the moment obscure.

Nevertheless, the relevance of this process resides in the recent identification of alternative mechanism by which plaque progression can be influenced. The HSCs contribution to plaque formation has been well documented among others by Sata and colleagues, in the ApoE knockout mice. In this animal model the presence of BM-derived vascular cells varies within the vessel wall, being maximum at neointimal layer [9]. On the other hand, in the cardiac rat allograft the contribution of the recipient cells to the endothelial cells (ECs) replacement is not a general phenomenon, whereas in aortic allograft neointimal ECs and VSMCs are of recipient origin. These data suggests that the level of HSCs contribution might be related to the severity of the initial graft endothelial damage [16].

The detailed understanding of these new mechanisms could expand the opportunities to identify and design potential new therapeutic approaches.

Lesion progression

VSMCs migrate into the intima at an early stage of the lesion formation and contribute to foam-cell development by engulfing lipids eventually yielding to aggregates of foam cells which can be recognized macroscopically as *fatty streaks*. As long as

hypercholesterolemia and/or other endothelial injurious stimuli persist, VSMCs proliferation and matrix depositions in the intima will continue. Some of the foam cells may die releasing lipids and cellular debris. Progressive deposition of collagen and proteoglycans produce a fibrous cap in the surroundings of the lesion, evolving from cellular-fatty atheroma to the fibrous cap. With additional cellular proliferation and connective tissue reorganization lesions finally evolve to fibrous plaques, acquiring the above described characteristics and growing first outward and then inward occluding slowly the arterial lumen [1].

Variation on histological features depend on factors that control VSMCs and Mϕ proliferation, migration, apoptosis, involve different levels of lipid deposit, oxidative stress, neo-angiogenesis, and extracellular matrix metabolism (collagen and proteoglycans). Among other causes of variability that could influence the natural history of atherosclerosis, there is the genetic heterogeneity of MMP. For instance, MMP-9 is essential for VSMC proliferation, migration [18] and proper geometrical remodelling [19].

1.3.3 Clinical syndromes

Atherosclerosis is affecting a big proportion of world population, it is the principal cause of heart attack, stroke and gangrene of the extremities and it is responsible for 50% of all mortality in USA, Europe, Japan [6] and other westernized countries. After a slow and sustained progression, atherosclerosis can give rise to a variety of symptomatic manifestations. Some of them include coronary heart disease (CHD), namely *angina pectoris* or chronic ischaemic heart disease and chronic hind limb ischaemia. Some others are silent manifestations, such as atherosclerotic lesion in aorta branches, carotid, brain tree arteries and hypertension.

Coronary heart disease

Only in the USA, this year about 1.1 million Americans will have a first or recurrent coronary attack. About 515,000 of these people will die and 250,000 of them before they reach a hospital. In this nation coronary heart disease (CHD) is the number one single leading cause of death. In addition, about 7.6 million Americans aged 20 and older have survived a heart attack (myocardial infarction). About 6.6 million Americans have angina pectoris (chest pain or discomfort due to reduced blood supply to the heart) [20].

In Europe cardiovascular disease (CVD) is the main cause of death, more than 50% in both women and men, men deaths predominate in all 49 countries except in France. In particular CVD causes more than 50% of deaths in women in 27 countries, mostly in Central and Eastern Europe but they also include Greece and Germany. CVD causes more than 50% of deaths in men in five countries: Georgia, Bulgaria, Romania, the Czech Republic and Macedonia.

Coronary heart disease (CHD) by itself is the most common cause of death in Europe: accounting for nearly 2 million deaths in Europe each year. Around 20% of both, male and female, die from the disease. CHD by itself is also the most common cause of death in the European Union (EU): accounting for over 600,000 deaths in the EU each year. In men around 17% and in women around 15% die from CHD. The source of this data is the British Heart Foundation Statistics (www.heartstats.org).

Late complications

Plaques keep growing and develop several complications such as calcification, focal rupture or gross ulceration at luminal surface resulting in a highly thrombogenic stimulus. The formation of a thrombus in partially occluded vessels, results in a myocardial infarction, when it affects coronary arteries, a cerebral stroke, when it occurs in brain artery or acute hind limb ischaemia, when it affects leg arteries.

Usually, such clinical events are triggered by plaque disruption. There is strong evidence to support the hypothesis that disregulation of matrix metalloproteinases (MMPs) metabolism contribute to weakening of atherosclerotic plaques [21]. Thus, converting MMPs in an interesting therapeutical target to prevent plaque disruption and by consequence acute cardiovascular events.

The major determinants of vascular remodelling such as hemodynamic forces, endothelial injury, inflammation and oxidative stress are also part of the initiator factors of atherogenesis and regulators of MMPs expression and activity. In this way MMPs role in vascular remodelling underlies the pathogenesis of major cardiovascular diseases, such as atherosclerosis and restenosis, see section 1.4.6 [21].

1.4 Angioplasty and restenosis

1.4.1 Angioplasty

Description of coronary angioplasty

Angioplasty is a non-surgical medical procedure where a specialized device (balloon catheter) is used to dilate narrowed or occluded coronary arteries in order to restore blood supply. There are alternative names to make reference of the same procedure, for instance Balloon angioplasty, Percutaneous Transluminal Coronary Angioplasty (PTCA), Heart artery dilatation. The indication for angioplasty is the narrowing of arteries as a consequence of an advanced coronary atherosclerosis or sudden occlusion by the formation of a thrombus.

The approach is, as the name indicates, percutaneous through the femoral artery and follows towards the coronary tree. The localization of the catheter is made by the use of real time X-Ray (fluoroscopy) in order to localize the occluded vessel and give the right position to the tip of the catheter, see Figure 1.3. The dilatable balloon is at the tip of the catheter; after localizing the sick vessel a dilatation of the balloon is

performed at high pressure, usually from 3 to 7 atmospheres according to the hardness of the plaque. When the procedure is performed in the presence of an acute event, like a heart attack, thrombolytic therapy is given at the same time to dissolve the thrombus. Nowadays, if there are no contraindications, an intravascular prothesis called stent is placed in the site of dilatation, see Figure 1.4.

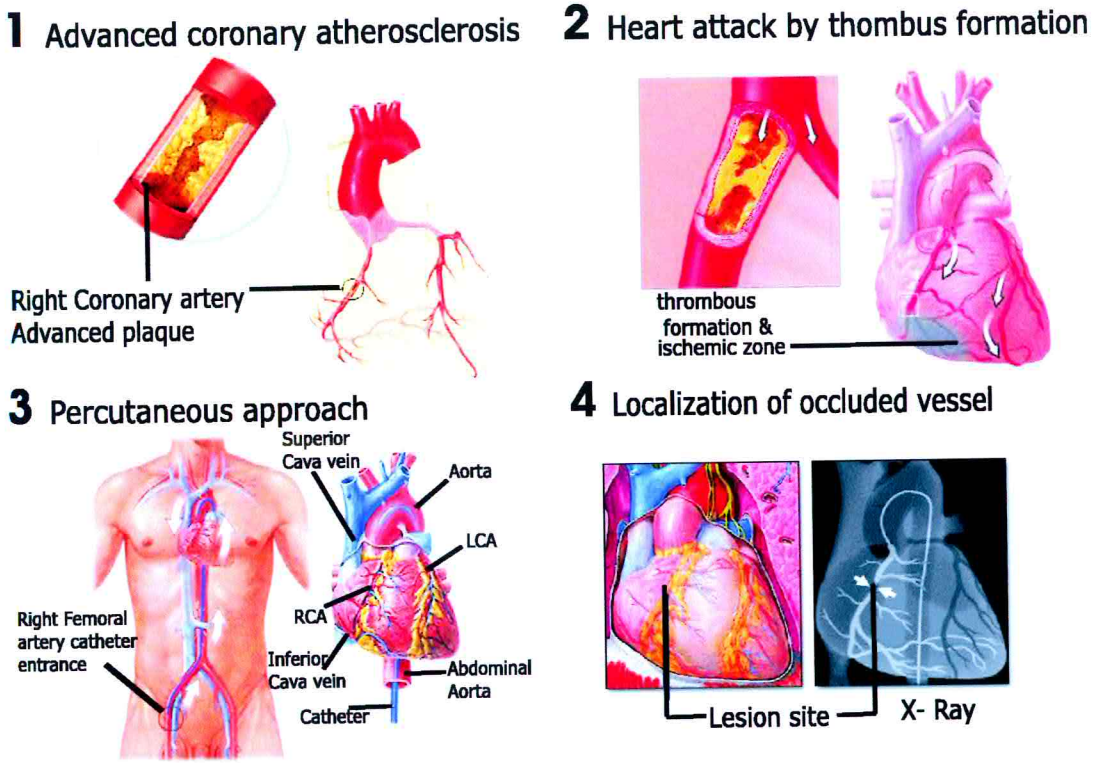

Figure 1.3: **Illustration of the sequence for coronary angioplasty (PTCA) part I:** 1) and 2) represent a usual site of coronary lesion, making emphasis in the chronic advanced atherosclerotic coronary lesion that is clinically manifested as an *angor pecotris*, simultaneously the lesion can get complicated by plaque rupture and superimposed thrombosis, 3) Shows schematically the place where catheter is inserted at the level of right femoral artery and the trajectory that follows towards the coronary tree, 4) Represents the image obtained of the heart under direct X-Ray visualization (fluoroscopy) to localize the vessel to be treated by balloon dilatation. Images adapted from MedlinePlus from US National Library of Medicine and National Institute of Health, images created by A.D.A.M. under American Accreditation Health Care Commission.

History and evolution of PTCA

In 1964 Dotter and Judkins performed the first angioplasty for the treatment of hind limb ischaemia [22]. By the year of 1977 Gruntzing did the first percutaneous translu-

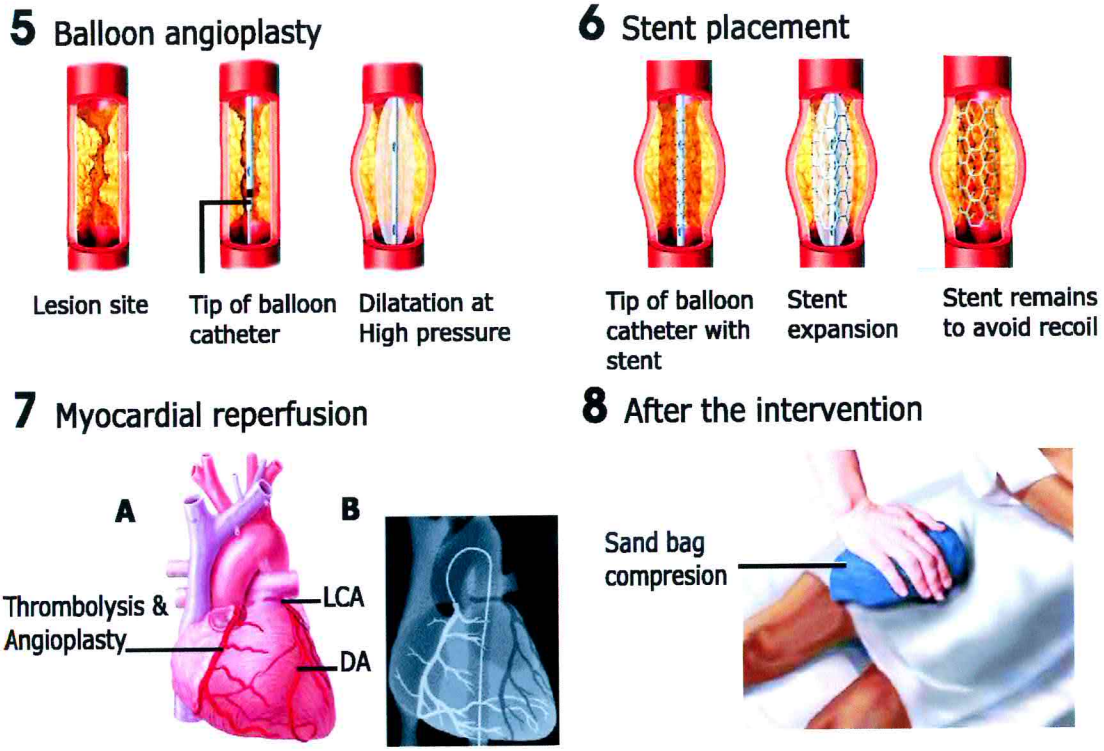

Figure 1.4: **Illustration of the sequence for coronary angioplasty (PTCA) part II:** 5, 6) represent two possible PTCA strategies (5) only balloon angioplasty or (6) adapted for stent placement, 7) A, Shows schematically the reperfusion of the previously ischemic region, B, Representation of coronary angiography to show the success achieved after the procedure, 8) Represents the care for haemostasia after PTCA. Images adapted from MedlinePlus from US National Library of Medicine and National Institute of Health, images were created by A.D.A.M. under American Accreditation Health Care Commission.

minal coronary angioplasty (PTCA) with a modified dilatation catheter [23], developed by himself in the early 70's for coronary use. Since then, PTCA has become the most common method of coronary revascularization in patients with coronary artery disease, including stable and unstable angina, and acute myocardial infraction [24]. This non surgical technique has improved greatly the quality of life of many people but bears a complication called restenosis. In an attempt to prevent restenosis after successful PTCA in 1986 Sigwart was the first to introduce the coronary stents [25], which significantly improved the short and long-term results of PTCA. Although initially limited to PTCA, percutaneous coronary interventions (PCI) now includes other new techniques capable of relieving coronary narrowing such as rotational atherectomy, directional atherectomy, extraction atherectomy, laser angioplasty, intracoronary stents

and other catheter devices. Despite the improvements in techniques and equipment, the development of novel strategies and design of intelligent mechanical devices, with the exception of sirolimus-coated stents [26], all the attempts to prevent restenosis have failed.

1.4.2 Restenosis

Restenosis is a hyperplastic and remodelling response that reduces the luminal size after an intravascular interventional procedure. Frequently restenosis is defined as the loss of more than 50% of lumen gain in post-PTCA angiogram. The lumen of narrowed arteries is usually less than 0.5 mm and after the intervention it is enlarged rapidly to 3 mm or more. If coronary arteries respond to this injury, this happens in a period of 1 to 6 months. Restenosis typically occurs one to three months after PTCA, and in 95% of the patients, it occurs within 6 months after the procedure [24]. It is uncommon for it to occur less than one month or more than six months after PTCA [27], see Figure 1.5.

Restenosis hampers several therapeutical procedures and is associated with angioplasty, vein graft failure after bypass grafting, stenting and transplant atherosclerosis after organ transplantation. Although this thesis is focused mainly on post-PTCA restenosis without exploring the other variants, some insights into pathogenesis of in-stent restenosis will be given.

In 1984, the National Heart, Lung, and Blood Institute's PTCA registry reported a restenosis rate of 33.6% and identified male gender, new unstable angina, diabetes mellitus, and treatment of bypass graft stenosis as risk factors [29]. In the year 2002 more than 1.5 million of PTCA were practiced worldwide, however, Post-PTCA and/or In-stent restenosis cases in the practical cardiology remained unacceptably high [26].

According to the American College of Cardiology and American Heart Association (ACC/AHA) practice guidelines it is recommended that patients who develop restenosis following an initially successful PTCA should be considered to repeat PCI

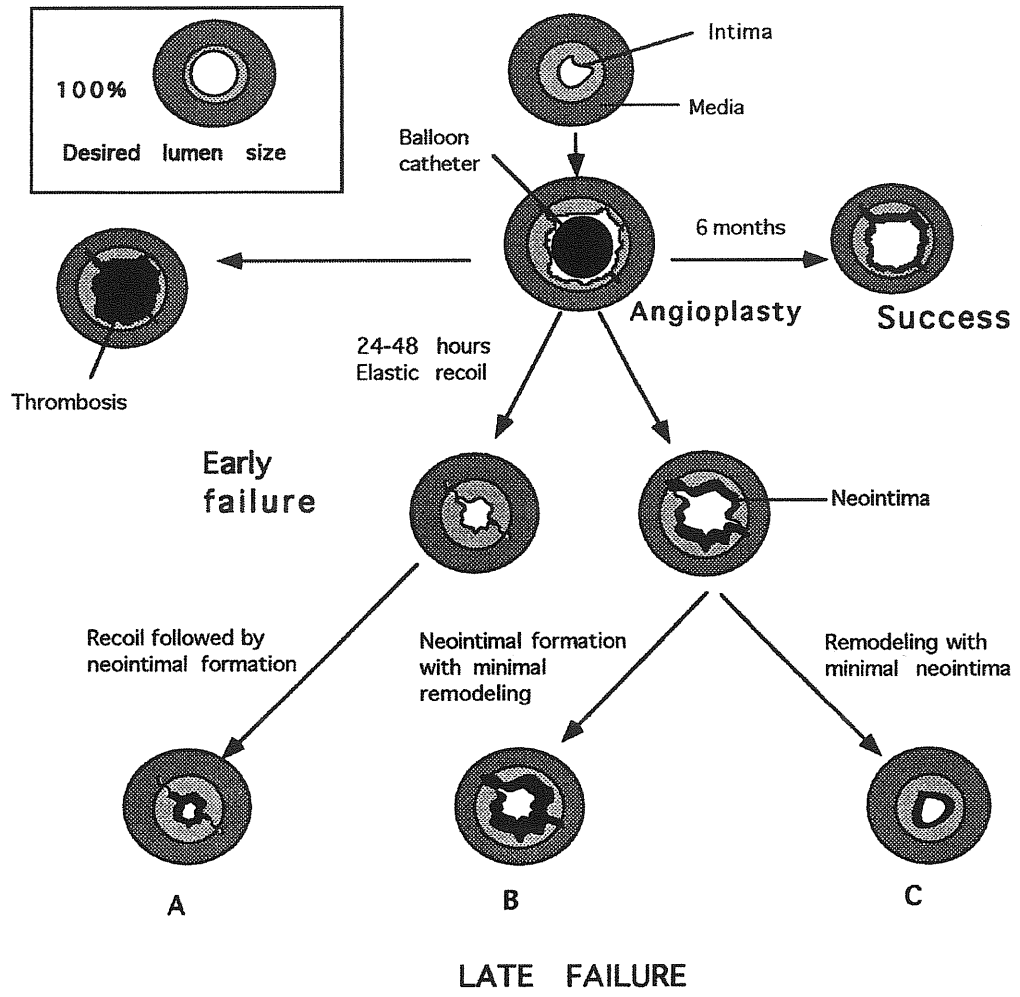

Figure 1.5: **Possible outcomes after angioplasty**: this flow chart shows possible outcomes after angioplasty and mechanisms responsible for restenosis. It is important to note that an increase in neointimal mass may not necessarily cause restenosis if sufficient remodelling of the vessel occurs, and remodelling also may result in restenosis with minimal increase in neointimal mass (as in C). Inset shows desired lumen size. Taken from Bennett et al. 1995. [28].

with stent placement [30]. In the case of restenosis after stent implantation (In-stent Restenosis), intravascular radiation with either gamma or beta radiation is a promising therapy for in-stent restenosis at this time, reducing the chances of recurrence from 50 to 60% (other method) to 25 to 35% (intravascular radiation) [30].

Today restenosis still occurs in 33% of the patients, is still associated with recurrent angina, and occurs usually within several months after a successful intervention [31].

1.4.3 Pathophysiology and pathogenesis of restenosis

The general risk factors associated with restenosis start from the initial therapeutic approach, either with or without a stent, the number of stents used, lesion localization (left anterior descending is more susceptible to restenosis), kind of lesion to be treated (either simple or complex lesion: diffuse atheromasia, ostial lesion, lesions at bifurcation, small vessel disease), residual stenosis and coexisting diseases such as diabetes [32, 26].

Neointimal hyperplasia arises from multiple pathophysiological stimuli including thrombus formation, inflammation, intimal and medial dissections. Acute arterial wall recoil or "*elastic recoil*" is the initial response of the elastic fibers of the vascular wall to overstretching induced by the balloon catheter and this process is responsible for acute lumen loss. Vascular remodelling is a gradual dynamic process mediated by adventitial myofibroblasts. Adventitia, like neointima, thickens to become fibrotic, leading to a change in the vessel size by constrictive remodelling that causes vessel shrinkage without an overall change in tissue volume. The so-called "*negative remodelling*" contributes to the loss of lumen at later times [33, 34, 35]. This is the principal cause of post-PTCA restenosis when a stent is not present to resist the constriction. Stents prevent remodelling but enhance neointimal formation, this neointima is the principal responsible for in-stent restenosis (IR) [36, 33, 37, 32].

The factors that regulate vascular remodelling and neointimal hyperplasia are not fully understood. However, insights have been gained on the importance of MMPs/Timps balance and ECM metabolism in vascular remodelling. Human genetic polymorphisms related to MMPs have been associated with development of post-PTCA restenosis and animal models have shown that MMP-9 is essential for VSMC proliferation and migration [18] and proper geometrical remodelling [19]. Despite the lack of knowledge about the exact mechanisms governing neointmal hyperplasia after stent placement, some recent studies suggest that greater neointimal proliferation is associated with deeper

medial stent struts penetration [38]. This contradicts the idea that "The Bigger, the Better", regarding the concept that the larger lumen achieved after PTCA diminishes the rate of restenosis. In addition, arterial medial disruption and lipid core penetration by stent struts is associated with greater inflammation whereas medial damage and stent oversizing relative to reference arterial lumen are associated with increased neointimal growth [39, 38]. A recent study has shown that the greater neointimal hyperplasia found in diabetic patients could be related to the effect of RAGE (radical glycosylation end products) upon the expression of growth factors [40].

1.4.4 Animal models of restenosis

Studies in human necropsy specimens are of great value to understand the pathological events that originate from certain diseases and treatment complications, however this material is often limited. To gain more understanding from particular processes that characterize human disease various animal models have been developed. However, by mimicking human diseases we can reproduce in the animal models some but not all the features of the human pathology. The knowledge of the pathophysiology of accelerated atherosclerotic syndromes, in particular of restenosis post-angioplasty, has been accumulated for more than twenty years, mostly from observations made in animal models.

The animal models most commonly used in vascular biology research include, rodent, mammalian non-primate and non-human primate species. Rodents represent an attractive model because they are inexpensive, easy to maintain, available in pure bred lines and suitable to most surgical interventions. Rabbits are perhaps the most widely used animals in vascular research and this model has proven its efficiency principally in the study of atherosclerosis formation and hyperlipidemia [41]. In the setting of angioplasty model, the lesion is influenced by the type of diet and may vary morphologically from a lesion of lose, lipid-rich connective tissue and thrombus, to those with

predominantly fibrocellular nature [42]. However, studies of therapeutic measures in rabbit angioplasty models have not fully correlated with the rat model. Porcine models, in spite of their size and expense of maintenance, have proven useful in all aspects of vascular research [43], in particular in the study of in-stent restenosis (IR).

One of the best characterized animal models is balloon angioplasty of the rat carotid artery [44]. The rat model is easy to perform, rat carotid responds rapidly to injury forming a neointimal layer and is an optimal model to study cell proliferation. This correlates with much shorter time course of intimal lesion formation (14-21 days) after arterial balloon injury. However, they respond with much higher levels of VSMCs proliferation than found in human lesions, they do not develop atherosclerosis, and they are resistant to hyperlipidemia effects and lack other pathophysiological features important in humans, such as thrombosis.

The real kinetics and interplay among the different cellular and molecular factors that determine restenosis is extremely large and complex, varying from one animal model to another. In order to have an idea of the pathogenesis of human restenosis, the rat and the porcine model will be briefly described.

In rats, a number of *in vivo* studies have defined the morphology, kinetics and control of the hyperplastic response after controlled injury to normal arteries [45, 46]. A definition of "four waves" of smooth muscle cell response to injury have been established by Libby et al. in 1992 and the molecules playing a role in each of this waves have been partially identified [41]. In the rat, the balloon injury induces a complete destruction of endothelium and extensive smooth muscle cell death. The "*first wave*" of events consists of medial smooth muscle cell proliferation, beginning around 24 hours after the injury and lasting from day 0 to day 3. The main phenomena observed during this phase is replication of VSMCs within the media. The migration of smooth muscle cells across the internal elastic lamina contributes to the formation of the intima; this constitutes the "*second wave*". Smooth muscle cells are readily observed at the luminal

side of internal elastic lamina (IEL) 4 days after the injury and this phase is considered to last from day 3 to day 14. Once the smooth muscle cells arrive in the intima of the rat artery, neointimal cells located near to the lumen replicate for weeks or months, this replication phase is called "*third wave*" and it lasts from day 7 to 1 month. However, formation of neointima in rats is not representative of the formation of neointima in humans; although platelet adhesion occurs in rats thrombus formation and leukocyte infiltration are minimal. A better model to understand the role of thrombosis in human restenosis is the porcine model.

The role of thrombus in vascular response to injury remains only partially understood. In the porcine model the formation of in-stent restenosis derives from the hemostatic plug, this becomes permanent and it is substituted by neointimal tissue obstructing the vessel. The cellular event form thrombus to neointima are summarized below. A definition of three stages has been proposed by Schwartz et al. 2003 [32].

The stage I is called "Thrombotic phase" and is characterized by rapid thrombus formation following the injury. This initial response includes explosive activation, adhesion, aggregation and platelet deposition and last from day 0 to day 3. Two morphologic features are prominent, platelet/fibrin and fibrin/red cell thrombus. The stage II is called "Recruitment" phase, it is characterized by the formation of an endothelial cell layer over the thrombus and lasts from day 3 to day 8. It is unclear whether the cells are truly endothelial despite their histological appearance. Shortly after this, an intense cellular infiltration occurs. The infiltration is mainly composed of monocytes that become macrophages, although lymphocytes are also present. Both cell types infiltrate from luminal side to the injured artery and migrate progressively deeper into the mural thrombus. The stage III is called "Proliferative phase" is characterized by the appearance of alpha actin-positive cells that colonize the residual thrombus from lumen, forming a "cap", it lasts from day 8 to final healing. These cells progressively proliferate towards the injured media, reabsorbing completely the thrombus and replac-

ing it by neointimal cells. At this point the healing is complete. In the pig this process requires 21 to 40 days, depending on residual thrombosis thickness. Healing progresses in the human coronary artery occur in a manner similar to that of the pig [32]. Experimental animal model studies suggest important relationships among inflammation, vascular injury and neointimal growth. Results from porcine animal model appear to mimic those of human studies, but differences in injury must be better understood at both cellular and molecular levels, and the implications respected in the design of new therapies.

In general, awareness of the similarities and differences between animal models and human disease, and between various species and strains within species (for example the limitations of rat animal model and key features of human disease), is crucial to properly interpret the data obtained. Despite its limitations, the rat model is still relevant to the understanding of physiological and molecular biology aspects [43] of angioplasty restenosis and In-stent restenosis (IR) [47], with special regard to intimal hyperplasia that has been shown to be the prime cause of IR. Therefore, the rat model is key to test experimental therapies, such as in the case of this thesis, gene therapy with adeno-associate vectors.

Influence of growth factors, cytokines and oxidative stress

A cytokine-growth factor cascade model for restenosis pathobiology has been proposed by Libby et al. in 1992 [41] in order to explain the features of human restenosis. According to this model PTCA would produce acute local thrombosis and/or mechanical injury that triggers cytokine/growth factor gene expression by resident macrophages and smooth muscle cells. This early event evokes a secondary cytokine and growth factor response that establishes a positive, self-stimulatory (autocrine) and/or paracrine feed-back loop that would amplify and sustain the proliferative response. This model could explain the lag phase between injury and restenosis. Another important concept

is that macrophage content in individual lesions could determine in part the propensity to develop restenosis. The typical factors involved in this model of restenosis include FGFs (FGF1 and FGF2), PDGF, TNF, Angiotensin II, IL-1, TGF- α and HB-EGF (from activated macrophages and VSMCs) [41].

Many growth factors and cytokines involved in the pathogenesis of atherosclerosis and restenosis post-PTCA up-regulate VEGF, favor fibronectin-EDA(+) isoform and up-regulate $\alpha_5\beta_1$ integrin expression and function. These cytokines are produced by activated endothelial cells (EC), macrophages (Mϕ), VSMCs and fibroblasts.

The cytokine group that modulates VEGF include PDGF, TNF-α, TGF-α, TGF-β, FGF-4, EGF, IGF-1, IL-1α, IL-1β and IL-6. Some growth factors (PDGF, TGF-β and angiotensin II), cytokines (IL-1β, IL-6) and radical oxygen species (ROS) (12(S)-HETES) favor the synthesis of both FN-EDA (+) and VEGF, whereas other oxidation products such as 4- HNES modulate only VEGF [48, 49, 50, 51]. TGF-β, IL-1β, TNF-α and INF-γ are also able to up-regulate $\alpha_5\beta_1$ integrin expression by VSMCs, thus increasing their ability to respond to migratory and trophic stimuli [52].

Interestingly, oxidized LDL, angiotensin II and lipopolysacharides (LPS) have also been reported to induce vascular cell apoptosis, the initial event of atherosclerosis development. In addition, it has been reported that LPS and FN-EDA domain activate the Toll-Like receptor 4 (TLR4) [53], a receptor expressed in adventitial fibroblasts, macrophages and endothelial cells of human atherosclerotic plaques. TLR4 activation mediates inflammation through NF-κB pathway leading to the production of various cytokines that influence VSMCs and fibroblast (myofibroblast) proliferation and migration, thus contributing importantly to neointima formation [49]. This evidence supports the existence of a link between the inflammatory, growth factor and oxidative stress axis.

Hematopoietic stem cells (HSCs) recruitment to restenotic lesions

As mentioned above for atherosclerosis, there is a growing body of evidence that points out the contribution of bone marrow derived cells to arterial lesion development in restenosis. In a wire injury model the level of contribution of BM-derived cells was as high as 63% in the neointima and 45.9% in the media. These results strongly suggest that BM-derived cells contribute to arterial remodelling after mechanical injury [9] and support the hypothesis that BM-derived cells are recruited in vascular healing as a complementary source of smooth muscle-like cells when the media is severely damaged [17].

Several local and remote progenitors have been proposed to contribute to arterial neointimal lesions ranging from adventitial myofibroblasts [11, 54], artery wall resident cells that transdifferentiate [55] to circulating endothelial progenitor cells. However, specific progenitor(s) of neointimal lesions and the kinetics of the recruitment of such a progenitor has not been described yet.

1.4.5 Therapeutical interventions against restenosis

Since its first description, restenosis was often treated with a second PTCA. In 1994 the only two procedures approved by FDA for percutaneous coronary vascularization were PTCA and directional coronary atherectomy.

After stents introduction in 1986 by Sigwart, the first major clinical trials STRESS (Stent Restenosis Study) conducted in USA and BENSTENT (Belgium Netherlands Stent Trial) conducted in Europe (eight years later), demonstrated that stenting after PTCA indeed reduces the incidence of restenosis. Despite these results and the lower rate of the initial complication, restenosis occurs in approximately 15-20% within 6 months after intervention and some times it is necessary to repeat the PTCA [56].

Systemic administration of drugs after PTCA has proven to be effective in preventing restenosis development in the rat model [57, 58, 59, 60] and in other animal

models. However, in human clinical trials all the drug treatments including antiplatelet agents, anticoagulants (comadin and aspirin in C-HEART Group), corticosteroids, ACE inhibitors (cilazapril in MERCATOR), statins (fluvastatin in FLARE), calcium channel blockers (diltiazem), tranilast (PRESTO) trail, antioxidants, hirudin and angiopeptin [61, 62, 63, 64, 65, 66] have shown to be ineffective. PRESTO (from 2000 to 2001, gained relevance serving as a model in designing more recent ongoing trials [65].

Three major clinical trials have clearly demonstrated that cholesterol reduction is an efficient risk-reduction strategy for prevention of coronary artery disease (CAD) (West of Scotland Coronary Prevention Study (WOSCOPS), Scandinavian Simvastatin Survival Study (4S) and Cholesterol and Recurrent Events (CARE) [67, 68, 69]. However, in the early 1990's data from animal model suggested that HMG-CoA reductase inhibitors (statins) might reduce restenosis after balloon angioplasty in both normolipemic and hyperlipemic animals, with a mechanism independent of the effect that is compound exerts on LDL cholesterol levels [70, 71, 72].

Despite the promising results of experimental studies and the outcome of large prospective placebo-controlled prevention trials (LTR, APPLE, PREDICT), the role of HMG-CoA reductase inhibitors remains unclear in the prevention or delay of restenosis after conventional PTCA [73, 74]. Very little information is available about the plausible role of statins on preventing restenosis after coronary stenting. However, Walter et al. have shown promising results [75] and large clinical trials have already been designed to verify their findings. Other clinical trials have shown partial benefits after the lowering of plasma homocysteine levels [76]

After the description of restenosis developed after stent application (In-stent restenosis) several strategies in order to solve this "new" problem have been designed and applied, such strategies include "brachytherapy" which involves the implantation of stents able to emit radiation. The spectra of stents material include the β-emitters ^{90}Y, Sr/^{90}Y, ^{32}P [77, 78] and γ-radiation . In particular γ-radiation has proven to

be efficient in three different double-blind, randomized clinical trials [79, 80, 81, 82]. On this basis, in the year of 2000 the FDA approved unanimously γ-radiation to treat in-stent native coronary artery restenosis.

The successful strategy of inhibition of VSMCs proliferation by drug-eluting stents was first reported by Morice and colleagues their study compared coronary stents sirolimus-coated with standard uncoated stents in the RAVEL study, with impressive data: restenosis rate of 26.6% in the standard group versus 0% in the drug-stent group [83]. Moreover, the beneficial impact was still present at 2 years follow-up [84]. Sirolimus is also known by the commercial name of rapamycin or rapamune, a well studied immunosuppressor durg that binds to mTOR complex and stops cell proliferation. Sirolimus may be the first drug to show success in the prevention of restenosis, but many other drugs are under evaluation, including other immunosuppressants, antineoplastic agents, vascular endothelial growth factor (VEGF) and 17-β-oestradiol. Paclitaxel is an anti-neoplastic agent also known by the commercial name of taxol, this drug inhibits the polymerization of microtubules and also stops the cell proliferation. Paclitaxel-coated stents have also been shown effective in the prevention of restenosis after stent implantation [85, 86]. In the Figure 1.6 are depicted the details of sirolimus and paclitaxel mechanisms of action. Despite the promising results obtained from sirolimus and paclitaxel trials, these data should be considered preliminary and caution should be taken until other potential systemic or local toxic effects will be ruled out.

Despite the initial enthusiasm of intravascular therapy there is evidence that points against the use this devices. In patients treated with brachytherapy it has been reported late coronary occlusion and thrombosis [87, 88]. These effects seen in humans have been related to the prolonged deendothelialization observed in animal models with irradiated arteries [89]. In similar way, low frequencies of late acute thrombosis have been associated with the implantation of drug eluting stents in humans [90]. The basis

of these effects in humans could be related to recent animal model studies. These studies have demonstrated that paclitaxel and rapamycin induce direct inhibition of both, reendothelialization [91] and EC proliferation [92], respectively.

These findings imply that the inhibition of the endothelial recovery may have undesirable consequences and support the idea that endothelial functions, such as barrier regulation of permeability, thrombogenicity, and leukocyte, may be essential for the prevention of neointimal proliferation [6].

Other anti in-stent restenosis strategies have not been successful, these include; rotational atherectomy (ARTIST), glycoprotein IIb/IIIa blockade, abciximab (ERASER) and heparin-coated stents (SISCA). Whereas for others strategies even deleterious effects have been reported and trials suspended, these include dactinomycin, QUADS-QP2 taxane and batimastat, which have shown late thrombosis, delayed restenosis and aneurysm formation [93, 94].

1.4.6 Metalloproteinases (MMPs) and endogenous inhibitors (TIMPs)

Metalloproteinases (MMPs)

The matrix metalloproteinases (MMPs) are zinc and calcium-dependent proteases that degrade collagen and most of the components of extracellular matrix. In 1962 a "collagenase activity" in tadpole tail was reported by Gross et al. [95] and in by 1970 Jeffrey was able to purify an enzyme from mammals [96]. The MMPs are an expanding family of proteins that share common functional domains and mechanisms of action. In humans the family includes 23 gene products which cleave within a polypeptide (endopeptidase) [97]. There are also two other large families of proteins that have major roles in extracellular proteolysis, the ADAM family (A disintegrin and metalloprotease domain, in humans about 33 members) and the ADAMSTS family (A disintegrin-like and metalloproteinase domain with thrombospondin type I repeats, 19 members).

The first cloning of an MMP occurred in 1984 [98]. MMPs genes are struc-

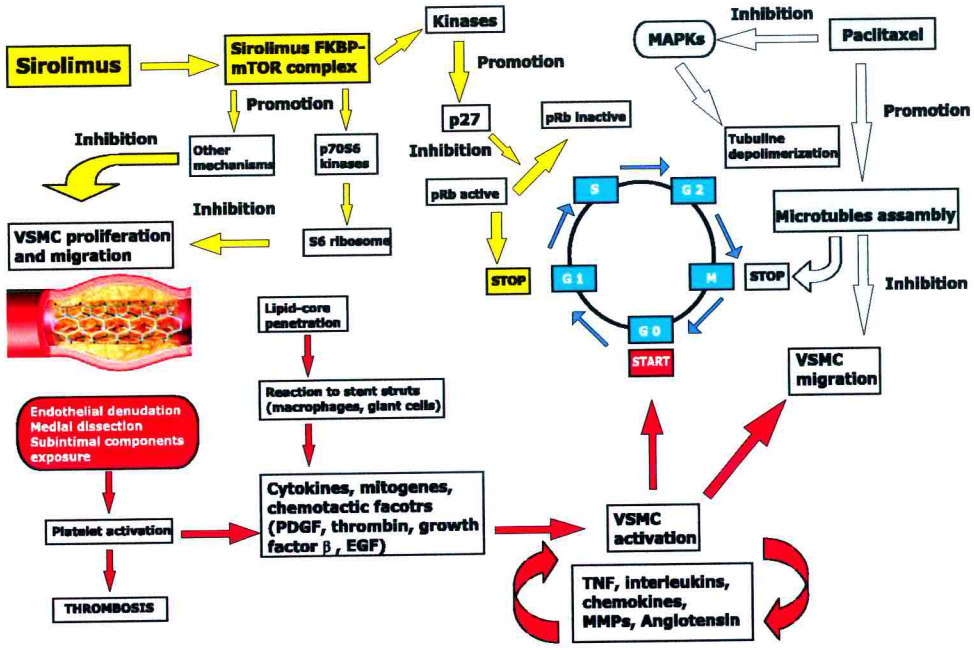

Figure 1.6: **Sirolimus and paclitaxel mechanism of action**: Is this cartoon are depicted the mechanisms by which the principal sirolimus and paclitaxeln eluting stents inhibit the mitosis. The events responsible for VSMCs activation, proliferation and migration are identified by the red box and arrows The cellular pathways related to sirolimus mechanism of action are identified by yellow boxes and arrows. The cellular pathways related to paclitaxel are distinguished by light blue boxes and arrows. Adapted from Fattori et al. 2003. [26].

turally similar, of about 10kb in length and contain 10 exon and 11 introns. A group of them (MMP-1, MMP-3, MMP-7, MMP-8, MMP-10, MMP-12, MMP-13, MMP-20 and MMP-26) is located in a cluster on the chromosome 11 (11q21-23) [99, 100, 101]. MMP-2 and MMP-9 show some diversity, they contain three extra exons that encode fibronectin-like domains and are localized on chromosomes 16 and 20, respectively [102].

The similarity of MMPs genes indicates that they derived by the divergent duplication and evolution of common ancestral genes [99, 100], as it is evident by the conservation of their domain structure, shown in Figure 1.7, and of their mechanism of catalysis and regulation.

The term "cysteine switch" was introduced in 1990 by Van Wart and colleagues to describe the mechanism that MMPs use to maintain enzyme latency [104]. The

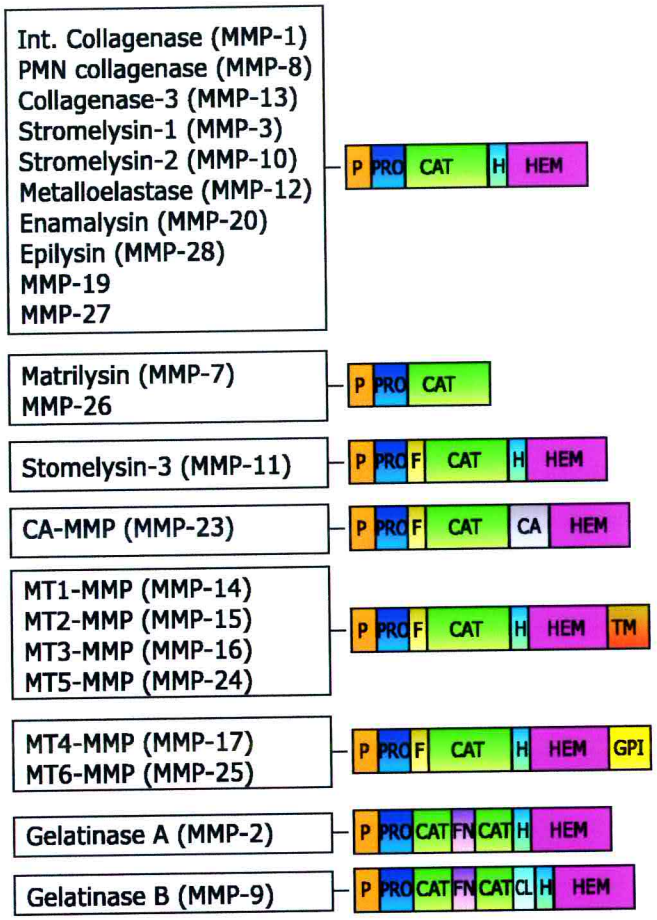

Figure 1.7: **Domain structure of MMP family**: all except MMP-7 and MMP-26 consist of two domain connected by a flexible proline-rich hinge peptide (H). The domains comprise a protease domain and helper domain HE and FN (Hemopexin and fibronectin like repeat). The protease domain contains a signal peptide (P), the pro-domain (PRO)and catalytic module (CAT). MMP-2 and MMP-9 have three tandem fibronectin type II repeats (FN) in the CAT, which modulate gelatin binding, MMP-9 has a collagen V like domain (CL) which its function is unknown. They are anchored to the cell surface by a transmembrane domain (TM) or by a glycosylphosphoinositol anchor (GPI). CA, cysteine array, F, furin cleavage consensus sequence, Ig, immunoglobulin-like domain. Adapted from Brinckerhoff et al. 2002. [103].

cysteine in the pro-domain (PRO), see Figure 1.7, forms a bridge with the catalytic zinc and prevents enzymatic activity. This enzymatic activation, which occurs when this link is chemically disrupted, can be done by proteases, such as plasmin or MT-MMPs, or through autolysis secondary to conformational changes. Therefore, MMP activity is regulated at multiple levels: gene transcription and synthesis of zymogenes, trafficking of membrane-bound forms (secretion and endocytosis), extracellular binding of proteins and interactions with endogenous inhibitors, such as tissue inhibitors of

metalloproteinases (TIMPs) [105, 106].

MMPs play key roles in the response of a cell to its microenvironment. By affecting proteolytic degradation or activation of the cell surface and ECM, they can modulate cell-cell and cell-ECM interactions, which influence cell differentiation, migration, proliferation and survival [107]. Other non-matrix substrates, whose activity is regulated by MMPs, include TNF-α [108], growth factors and their receptors [109], plasminogen and their activators [110, 111], and endothelin [112]. Physiological processes in which MMPs are important include, angiogenesis and ovulation; in addition they are essential in the continuous normal modelling and remodelling of connective tissues [103].

An extensive body of literature indicates an association of MMPs with cancer, arthritis, numerous other inflammatory or autoimmune disorders, cardiovascular, cerebrovascular and fibrotic diseases [97].

Physiological and pathological vascular remodelling needs degradation and reorganization of the extracellular matrix (ECM) scaffold of the vessel wall. The contribution of MMPs has been extensively studied in vascular disease that relay on wall remodelling, including atherosclerosis, restenosis, arterial aneurismal dilatation, vein graft failure and atherosclerotic plaque disruption. The major drivers of vascular remodelling represented by hemodynamics, injury, inflammation and oxidative stress, regulate MMPs expression and activity [21].

Tissue Inhibitors of Metalloproteinases (TIMPs)

Tissue inhibitors of metalloproteinases (TIMPs) are the major cellular inhibitors of the matrix metalloproteinases (MMPs) and can be found in the extracellular space and body fluids. TIMPs have a broad inhibitory activity against many MMPs and exhibit different tissue expression patterns and modes of regulation. Among other inhibitors there are proteins with less inhibitory activity against some MMPs, including

domains of netrins, procollagen C-terminal proteinase enhancer (PCPE), reversion-inducing cysteine-rich protein with Kazal motifs (RECK), tissue factor inhibitor (TFPI-2). However, their physiological significance is still not clear. Some others, such as α_2-Macroglobulin, thrombospondin-1 and thrombospondin-2 can also bind some MMPs and remove them from extracellular environment. Lastly, few effective inhibitors of disintegrin metalloproteinases (ADAMs) have been identified [106].

The first member of the TIMP family was isolated in 1979 by Welgus as "fibroblast anti-collagenase" [113] and cloned in 1985 by Docherty [114]. The TIMP family is constituted by four members, which have molecular weights around 20-30kDa and are glycosylated at various degrees. They have six disulphide bonds and comprise a three-loop N-terminal domain and an interacting three-loop C-subdomain. Most of their biological functions can be attributed to their sequence within the N-terminal domain, although the C-subdomains mediate interactions with the catalytic domains of some MMPs and with HE domain of MMP-2 and MMP-9 [105]. They act by forming a 1:1 complex with the activated catalytic zinc binding in a substrate-like manner. A schematic representation of the interactions of metalloproteinases inhibitors in the pericellular environment is shown in Figure 1.8

All four TIMPs inhibit active forms of all MMPs with binding constants in the picomolar range. They have no significant activity against the astacins, however, TIMP-1 inhibits ADAM 10. See detailed the effects of TIMPs in Appendix A.

TIMPs affect cell growth and survival, which can not always be clearly related to TIMPs ability to block MMP activity [106]. Therefore, the MMP-TIMPs story is not as simple as it may seem and the non-MMP inhibitory functions of TIMPs is a story that is still "unfolding" [103].

As illustrated in the Appendix A TIMPs have shown to have paradoxical roles in tumor progression, cell proliferation, apoptosis and angiogenesis. Several experimental approaches have tried to address the role of MMP:TIMP balance in diseases progres-

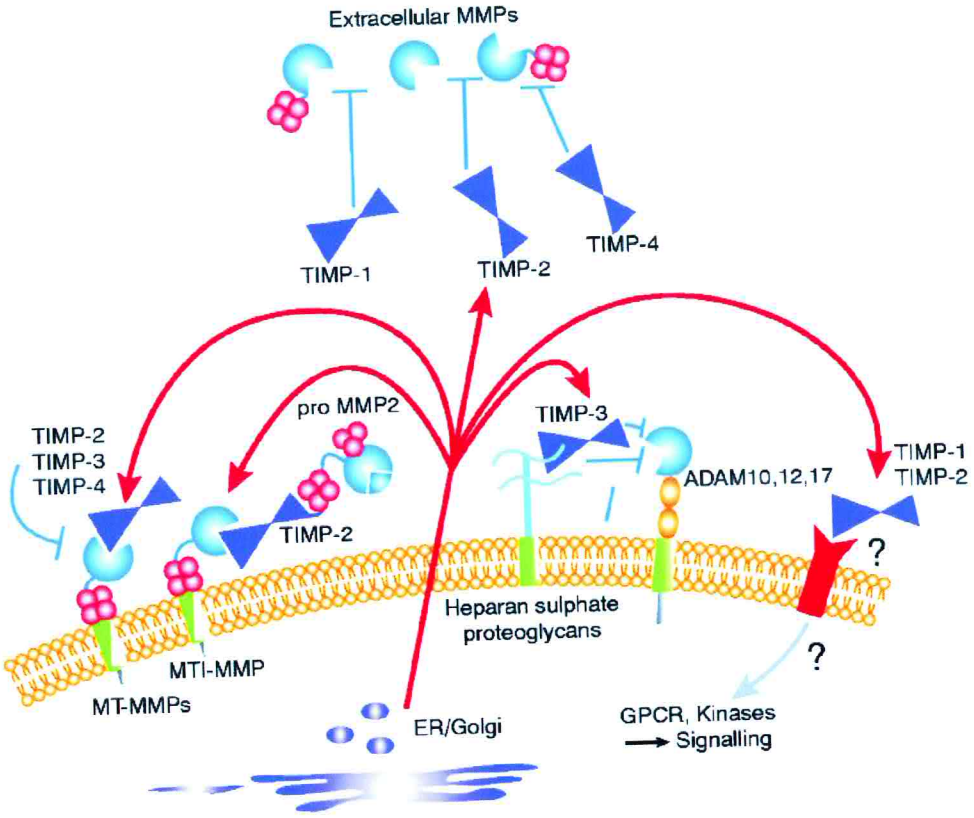

Figure 1.8: **Tissue inhibitors of metalloproteinases (TIMPs)**: TIMPs-1-4 are largely matrix metalloproteinase (MMP) inhibitors modulating the activity of soluble, matrix bound and cell associated MMPs. TIMP-3 is an extracellular matrix protein, probably bound to heparan sulphate proteoglycans and is a potential inhibitor of the function of some membrane-associated ADAM s (a disintegrin and a metalloproteinase). TIMP-2 acts in conjunction with MT1-MMP as a receptor for the pro-form of MMP-2 at the cell surface, allowing an efficient activation and focussing of the active form of this soluble proteinase. In some cell types, TIMP-1 and TIMP-2 may have receptors directly linked to intracellular signalling pathways regulating cell behavior. Adapted from Baker et al. 2002. [106].

sion, from administration of small synthetic inhibitors to TIMPs, either by recombinant protein administration or by gene transfer. The majority of clinical trials using synthetic MMP inhibitors have proven disappointing, probably due to a lack of specificity and to unwanted side effects.

The effects of MMPs blockade or abrogation have been widely studied in acute and chronic cardiovascular diseases. These include atherosclerosis [115], myocardial infarction, heart failure [116], development and rupture of aneurisms [117], post-PTCA

restenosis [118, 119] and vein graft failure [120].

Considered as obvious targets for therapy in the cardiovascular system, MMPs modulation has been tried in many experimental approaches. These include systemic administration of adenoviral vector expressing Timp1 (Ad-TIMP1) [121, 122], local administration of adenoviral vectors expressing Timp1 and other TIMP family members [123, 124, 125, 126, 127] and implantation of of Timp1 overexpressing VSMCs [128].

Systemic Ad-TIMP-1 administration has resulted in reduction of the severity of atherosclerotic lesion in the ApoE -/- knock out mice [121] and reduction of post-PTCA restenosis [122]. However, the limitation of this approach is the transient nature of adenoviral-mediated gene transfer and risky hepatic or systemic effects after its systemic administration [129]. The other approaches with local adenoviral TIMP1- overexpression and implantation of retroviral transduced TIMP1-overexpressing VSMCs have contributed to prove the effectiveness of this molecule in the prevention of VSMCs migration; however the long-term benefits of these treatments have not been fully established. On the contrary, local overexpression of TIMPs (TIMP-1, TIMP-2, TIMP-3) in a human vein graft model prevented efficiently MMP-induced neointima formation [123, 125, 126, 127], whereas *in vivo* overexpression of TIMP-3 inhibited diseases progression through the promotion of apoptosis [127]. Two recent studies in a double (TIMP-1-/-:ApoE -/-) knock-out mice have highlighted new roles for TIMP-1 in atherosclerosis formation. One study demonstrated the lack of Timp1 influenced a reduction in atherosclerotic lesion size and an increase in the incidence of aneurysms [130], whereas the other showed an increase in elastic medial ruptures and no changes in atherosclerotic lesion size [131].

In addition, synthetic MMP inhibitors have failed to prevent post-PTCA and In-stent restenosis despite their ability to block early VSMCs migration [132], and constrictive remodelling in several relevant animal models [133]. All of this examples are important demonstrations of how superior can be the therapeutical potential of

TIMP family members over small synthetic MMP inhibitors, probably due to non related MMP-inhibition mechanisms of the TIMPs.

1.4.7 Pentraxin 3 as a new therapeutic target

Pentraxin 3 (PTX3) was first identified, during the search for genes that could serve as markers of inflammatory reactions in the vessel wall, as a protein induced by TNF in cultured fibroblast; the partially characterized protein was denominated "tumor necrosis factor-stimulated gene sequence-14'(TSG14)" [134]. Later in 1992, Breviario and colleagues cloned the human full length long pentraxin 3 cDNA from a library of human umbilical vein endothelial cells (HUVEC) after interleukin-1β induction. The structure of the PTX3 gene contains 3 exons and is transcribed as a 1,861bp mRNA; it was mapped to chromosome 3q25 by somatic cell hybrid analysis and fluorescence in situ hybridization (FISH) [135]. The promoter region of the PTX3 contains in the 5' portion, several binding sites for TNF, IL1β and NF-κ_B [136]. PTX3 belongs to the "long pentraxins" protein family [136], characterized by the C-terminal pentraxin domains and by novel amino-terminal domains.

PTX3 is known to bind to C1q in N-glycosylated-multimeric form, binds also several pathogenes such as *A. fumigatus*, *P. aeruginosa* and *S. typhimurium* [137], monocytes and dendritic cells. It facilitates the interaction between conidia and mononuclear phagocytes. Conidia rapidly induces PTX3 production by monocytes and dendritic cells, but not in endothelial cells, neutrophiles or fibroblast. A PTX3 knock-out mice reveal increased susceptibility to invasive pulmonary Aspergiliosis. The authors concluded that PTX3 acts as a soluble pattern-recognition receptor and proposed that it may have therapeutic potential in bone marrow transplantation and similar immunodeficiency context [138].

Recently PTX3 has been associated to the pathogenesis of human atherosclerosis [139] and it has been suggested as a clinical predictor of myocardial infraction [140].

1.5 Gene transfer to artery wall

1.5.1 History of gene transfer to artery wall

In the late 1980's the pioneers of gene transfer to the artery wall, E. G. Nabel and G. J. Nabel, demonstrated for the first time the feasibility of this approach by transducing *ex vivo* porcine endothelial cells with retroviral vectors encoding β-galactosidase gene and reintroducing the cells in injured syngenic arteries [141].

After this breakthrough, a variety of viral and non-viral strategies have been tried with a different degree of success in many models, including organ culture. Several different strategies have been tested for the efficient transfer of potentially therapeutic genes into the wall arteries; these include the use of viral vectors derived from retrovirus and adenovirus or non-viral vectors (plasmid DNA) and oligonucleotides administrated as naked DNA, in association with liposomes or together with the hemagglutinating virus of Japan (HVJ). Other strategies entail the *in vivo* implantation of autologous cells modified *in vitro*. Encouraging results were obtained in animal models by using antisense or decoy oligonucleotides, designes to specifically inhibit genes implicated, at different levels, in the process of restenosis (see bellow 1.5.2). In particular, it is worth to mention the strategy used by Mann and colleagues, who demonstrated the efficacy of "decoy oligonucleotides" in restenosis, targeting PCNA, cdc2 kinase and E2F. The later was approved by FDA in 1996 to treat neointimal hyperplasia in the vein bypass graft [142].

Among the viral strategies, the one which utilize vectors based on adenovirus has shown the higher efficacy in transducing the vessel wall [143]. Indeed, adenoviral vectors are very effective in transducing non-replicating cells, including vascular smooth muscle cells and endothelial cells *in vivo* as well as *in vitro*. However, adenoviral vectors harbor several drawbacks, such as their short term expression of up to several weeks and the fact that they induce an important inflammatory reaction. Previously,

Lafont et al reported vasomotor dysfunction after exposure of normal arteries to an adenovirus vector [144]. More recently, Channon et al documented time- and titer-dependent impairment of endothelium-dependent relaxation after adenoviral vectors infection [145]. Since impairment of endothelium-dependent relaxation is well known to cause cardiovascular events [146], these findings have important implications in the design of future gene therapy clinical protocols aiming to use adenoviral vectors for the cardiovascular system.

Rekhter et al [147] demonstrated that gene transfer to normal and atherosclerotic human blood vessel is feasible by adenoviral vectors in organ culture conditions. In addition, they found that areas of plaque rupture and thrombus are sites of predilection for expression of recombinant genes, suggesting that discontinuity of endothelium allows penetration of viral particles and consequently transduction of intimal cells. Importantly they also found that collagenase and elastase treatment of carotid plaques increased the percentage of transgene expression by 7-fold, suggesting that the pattern of gene expression was affected by the amount of surrounding extracellular matrix. This study highlighted that endothelial integrity and extracellular matrix (ECM) can actually act as important barriers to adenoviral gene delivery to the actual normal and atherosclerotic human vessels of clinical interest.

1.5.2 Gene therapy for restenosis

After the initial studies of Nabel and colleagues, the first strategy tried was the cytotoxic-suicide gene therapy in several normolipemic animal models with adenoviral vectors [148, 149]. Preliminary studies settled the basis that vascular gene therapy could be possible in normal and diseased vessels [150, 151]. In the race to stop restenosis many other targets were tried including **a)** cell cycle regulators: Rb [152, 153], pRb2/p130 [154], p21 [155, 156, 157, 158], p27 [159, 160, 161], c-myb, c-myc [162], PCNA, cdc2, cdk2 [163] and others **b)** intracellular signal transducers: H-ras [164], N-ras, A-Raf, C-Raf [165]

and others, **c)** transcription factors: NF-κB through p65 [166], E2F [167], Gax [153, 168], GATA-6 [169] and others, **d)** cytokines and growth factors: β-interferon [170], VEGF [171], Antisense targeting of bFGF [172] or PDGF-β [173, 174], **e)** vasoprotection by means of overexpression of Nitric Oxide (NO) [175, 176, 177, 178, 179] and **f)** induction of apoptosis by Fas ligand overexpression [158].

Recently, Hedman and colleagues [180] described stimulating results of a phase II randomized, placebo-controlled, double-blind study. They suggested that catheter-mediated intracoronary gene transfer approach is feasible and tolerable. They performed a PTCA, with standard methods, in patients with coronary heart disease (CHD), followed by gene transfer with a perfusion-infusion catheter. Ninety percent of the patients were given stents; 37 patients received VEGF adenovirus, 28 patients received VEGF plasmid liposome, and 38 control patients received Ringers lactate. Although VEGF gene therapy to prevent restenosis after coronary stenting did not influence the incidence of post-PTCA angioplasty (around 6%), it did improve myocardial perfusion in the VEGF-Adv treated group.

From this anti-restenosis clinical trials we have learned that the next target in preventing restenosis could be endothelial recovery [181]. The enthusiasm in the field of understanding and developing therapies to prevent restenosis has been reflected by nearly 900 papers published [181]. However, to achieve real success many aspects of clinical gene therapy have to be still defined, such as safety of gene transfer method to be employed (viral vectors vs non viral methods), efficiency of transduction of sick vessels to stop diseases progression and/or normal vessels as a long term reservoir and even more important to find specific gene targets for every disease.

1.6 Adeno-Associated Virus (AAV)

1.6.1 Structure of AAV

Adeno-associated Virus (AAV) is a member of the family Parvoviridae [182], which belongs to the genous of Dependovirus. AAVs were discovered as a contaminant of adenovirus (Ad) stocks, and did not productively infect cells unless there was a coinfection with Ad or other type of herpesvirus [183]. Currently 6 distinct serotypes have been described, 5 of them were isolated as contaminant of Ad [184]. Epidemiological data indicate that all known serotypes are endemic to primates [185] and they can be found in many mammals, including humans. Around 90% of adults are seropositive, but in no case the virus has been associated with any disease.

AAVs are small, nonenveloped, icosahedral viruses of about 20-26 nm in diameter, see Figure 1.9, and contain a linear, single strand DNA molecule of $\sim$ 4.7-6 kb. Plus and minus strands of DNA are packaged into virons and are equally infectious [186]. At each end of their genome there is a 145 base terminal repeat sequence, which folds back to form a T-shaped three way junction. These inverted terminal repeated sequences (ITRs) represent the only viral cis-acting elements essential for several viral biological functions, including initiation of DNA replication, viral genome site-specific integration, rescue from integrated state, packaging of AAV DNA [187, 188]. Moreover, ITRs may also function as transcriptional promoter since they contain elements with several Sp1 sites [189].

The single-stranded AAV2 genome of 4680 base pairs is organized in two open reading frames (ORFs), one at the right half (*Cap*) that encodes three structural capsid proteins with overlapping amino acid sequences (VP-1, -2 and -3) and one at the left half (*Rep*) that encodes for non-structural proteins with overlapping amino acid sequences (Rep78,68, 52 and 40) [191, 192]. The Rep78 and Rep68 proteins are translated from unspliced and spliced mRNAs that originate from p5 promoter. They are essential for

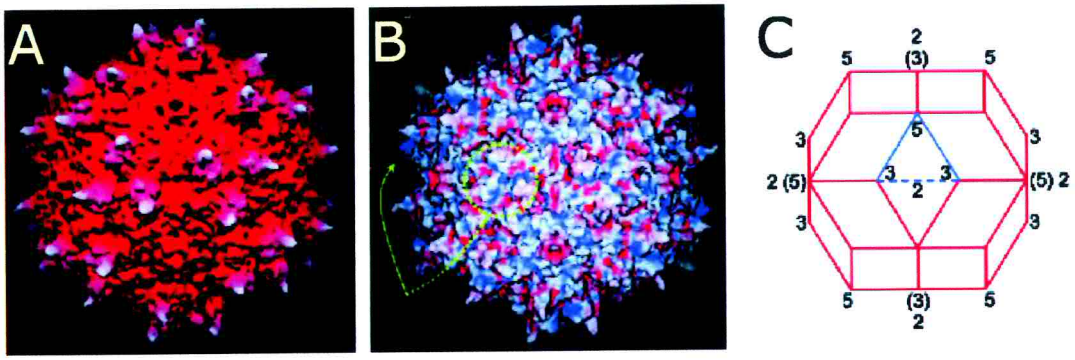

Figure 1.9: **Surface topology and electrostatics of AAV-2**: A, Show surface of AAV-2 colored according to distance from the viral center. B, Shows the electrostatic surface potential of AAV-2 . The putative receptor-binding sites are positively charged patches on the side of each threefold-proximal peak, viewed edge-on (arrowed). C, A rhombic triacontahedron showing schematically the viral orientation, the view is down a twofold axis (center of the virus) with three-fold left and right of center, five-fold above and below. Adapted from Xie Qing et al. 2002. [190].

viral DNA replication, where they exert an endonuclease and helicase activity, and are implicated in a variety of other functions, including the ability to bind to specific sites within the AAV ITR, DNA-RNA helicase activity, and ATPase activity. Rep 78/68 also negatively and positively regulate the steady-state levels of mRNA transcribed from p5, p19 and p40 promoters, as well as can inhibit or elevate RNA levels from heterologous promoters. The Rep52 and Rep40 are translated from similarly spliced mRNAs that originate from p19 promoter; they play a role in the accumulation of single-stranded progeny genomes used for packaging. The VP proteins are translated from two differentially spliced mRNAs that originate from p40 promoter, (see Figure 1.10 for details about AAV genome organization).

1.6.2 Biology of AAV2 infection

The life cycle of AAV is not completely understood yet. Since its discovery in the 1960's, AAV was considered to be a defective virus with a propensity for latency in the absence of helper virus coinfection. Further work demonstrated that AAV is not strictly a defective virus, but it rather preferentially establishes a latent infection in

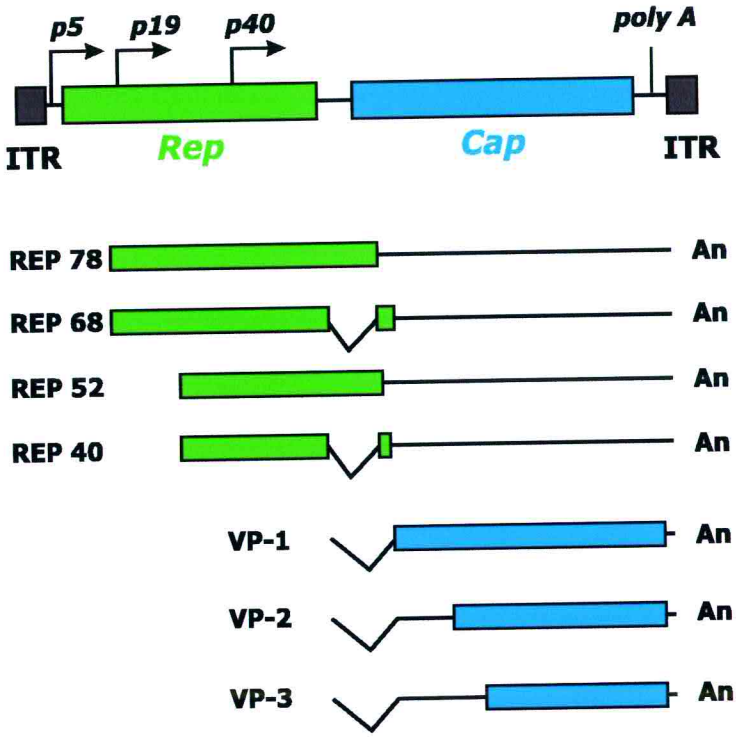

Figure 1.10: **AAV-2 genomic organization**: The genome of AAV is 4.7kb long and is characterized by the presence of two inverted terminal repeats (ITR), flanking two open reading frames (ORFS). Rep (green) and Cap (blue) genes are represented with their transcripts for the replication proteins, Rep78, 68, 52 and 40 and for the capsid proteins, VP-1, 2 and 3 respectively. Such different transcripts are produced by usage of different viral promoters (p5 and p19 for Rep and p40 for Cap transcripts) and by alternative splicing.

healthy cell and is only induced to undergo productive multiplication when the host cell is stressed, either by helper co-infection or by genotoxic agents (UV radiation,γ-irradiation, chemical carcinogens, and metabolic inhibitors) [193].

After infection in the absence of helper functions, AAV enters the cell nucleus, where its genome is uncoated. Transcription of Rep regulatory proteins (Rep 68, 78) occurs at low levels. These pleiotropic proteins are able, when present in low amounts, to exert a negative regulation over viral replication; this enhances the integration of the viral genome into the genome of the host cell, thus establishing a latent infection [194, 195, 196]. Latency can be maintained indefinitely, thus perpetuating the viral genetic

information. In humans AAV wild-type integrates at a high frequency (>70%) [197], in site-specific manner at the chromosome 19 (q13.3-qter), in an 8.2kb fragment called AAVS1 sequence [198, 199], see Figure 1.14. The specificity of this reaction depends on the AAV replication (Rep) proteins [200, 201] Rep78 and Rep68 [202, 203]. AAV is the first example of exogenous DNA which preferentially integrate at a specific site in the human genome.

The replicative or productive infection phase occurs in the presence of infection by a helper virus, either an Ad or herpesvirus [204, 183]. The role of the helper virus is, in general, to alter the intracellular milieu in order to allow the expression of AAV genes which are required for progeny production (Rep and Cap). The helper infection can either precede that of AAV, occur at the same time or involve a superinfection. In the case of herpes virus, its infection can not precede far ahead that of AAV, due to their rapid lytic nature. For Ad and HSV the genes involved in the helper effect have a common denominator, as they are all genes affecting regulation of gene expression. All Adenoviral early genes involved in the regulation can provide helper function. E1A transactivates several genes including Rep and Cap; E1B regulates mRNA maturation and transport; E4 and ORF6 facilitate AAV DNA replication and VA and E2A stimulate the translation of AAV viral genome [197]. Rescue of AAV genome after helper virus superinfection leads to replication of AAV DNA. The model initially described for *wt* AAV DNA replication is shown in Figure 1.11 [205, 206].

In conclusion, the current model of AAV life cycle can be summarized as follows: 1) In AAV life cycle the latent infection is a major component; the viral genome in the cell is perpetuated by this phase, 2) When host cell is healthy, AAV gene expression is repressed and the latent state is maintained, 4) If the cell is stressed, the intracellular milieu is altered so that stress response gene are expressed, 3) The regulatory state which permits the expression of the cellular response gene also permits the expression of the AAV genes which are required for viral replication, 4) Progeny virions are produced

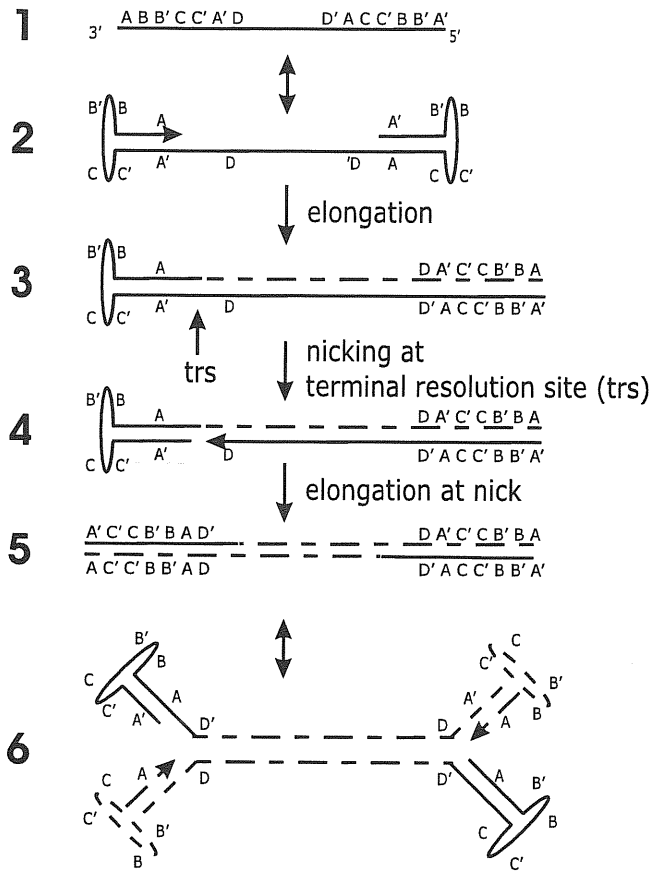

Figure 1.11: **Model of adeno-associated virus (AAV) replication:** The ITRs function as the origin of DNA replication and also serve as primers. Replication is initiated from the 3' end of the T-shaped hairpin structure to generate a duplex molecule in which one of the ends is covalently closed. The covalently closed ends are replicated by a process called terminal resolution, which involves a site-specific, strand-specific endonuclease cut at the terminal resolution sites (trs) followed by unwinding of the hairpin, so that the end can be replicated. The Rep78/68 proteins exert the ATP-dependent trs endonuclease activity, which plays an important role in the terminal resolution process. They also have an ATP-dependent helicase activity that plays a role in DNA replication. The ability of Rep protein(s) to recognize and cut the trs sequence plays an important role also in the rescue of the viral genome from the integrated state. Adapted from Berns et al. 1990. [206].

and released to infect new, healthy cells in order to reestablish the latent state.

Cell entry of AAV-2

The AAV-2 virus is able to enter very rapidly into the cell after 4 to 5 initial contacts [207]. The viral internalization was first reported to occur in 10 minutes [208],

but it seems that it occurs within seconds [207]. The process of internalization involves receptor mediated-endocytosis, with heparan sulfate proteoglycans (HSPG) used by AAV-2 as the primary receptor [209] and fibroblast growth factor receptor and $\alpha v\beta 5$ integrin as co-receptors [210, 211]. Other AAV sero-types use different receptors. AAV endocytosis occurs via clathrin-coated pits and requires dynamin, a 100-kDa cytisolic GTPase that selectively regulates clathrin-mediated endocytosis [208, 212]. In general, it appears that the mode or the efficiency of intracellular trafficking of AAV depends on the cell type being infected.

Several reports indicate that AAV uses endosomes for intracellular trafficking to the nucleus [208, 213, 214]. From this compartment the viral particles may escapes through acidification or they may be routed to the late endosomal compartment. Seisenberger and colleagues [207] used-real time single-molecule imaging of labelled virus to demonstrate that a substantial fraction of virus had a diffusion coefficient consistent with the presence of free virus particles in the cytoplasm shortly after infection.

It has been demonstrated that AAV virons use the cytoskeletal network of the cell (microtuble and microfilaments) to travel towards the nucleus through a Rac1 / phosphatidylinositol3-kinase (PI3-kinase) - dependent mechanism [215]; a similar mechanism is used by AAV helper viruses HSV1 and Adenovirus [216, 217].

Bartlett propose a model, where following endosomal release, AAV accumulates rapidly (within 30 minutes) in the perinuclear space and can be found in the nucleus 2 hours after infection, thus explaining *in vitro* transgene expression after 3 or 4 hours. See Figure 1.12 for schematic representation of AAV infectious entry pathway.

Xiao and colleagues sustain that AAV enters the cell rapidly and escapes from early endosomes within 10 min postinfection. In the absence of Ad coinfection, cytoplasmically distributed AAV accumulates outside the nucleus and viral uncoating occurs before or during the slow nuclear entry around 16 h postinfection. In the presence of Ad coinfection, cytosolic AAV quickly translocates into the nucleus as intact

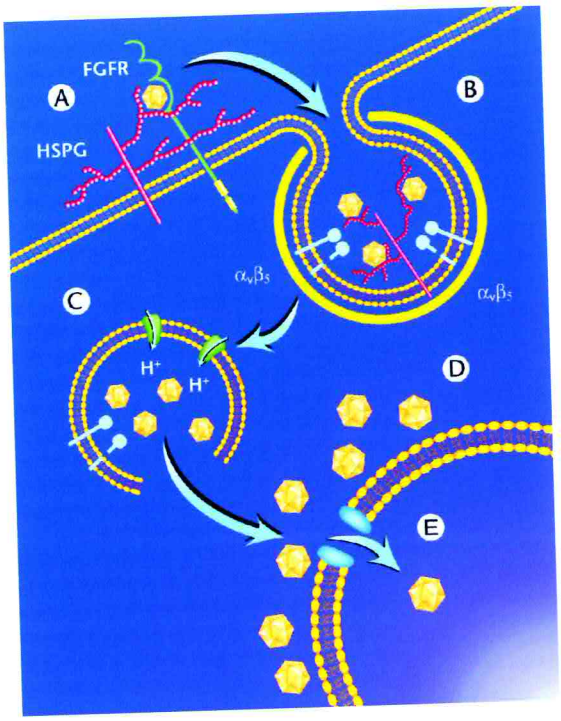

Figure 1.12: **AAV-2 infectious entry pathway:** 1. Schematic representation of AAV entry and endocytic trafficking in HeLa cells. A, Following binding to cell surface HSPG, B, AAV is rapidly internalized via clathrin-coated pits through a process involving $\alpha_v\beta_5$ integrin. C, Once internalized, the virus encounters a weakly acidic environment which is sufficient to allow penetration into the cytosol. D, Following endosome release, AAV accumulates perinuclearly and E, slowly penetrates through the NPC into the nucleus and 2. Cy-3 labelled viral capsid visualized after 2 hours of AAV-2 infection in HeLa cells. Adapted from Bartlett et al. 2000. [208].

particles, and this process is not blocked by the NPC inhibitors. This suggest the existence of two alternative trafficking patterns, depending on whether Ad is present, and is consistent with the life cycle mode of AAV [218].

1.6.3 AAV based vectors

Adeno-associated virus has gained recent interest as a viral vector for gene therapy on the basis of its lack of pathogenicity. Indeed, DNA vectors based on AAV are currently the most useful for in vivo gene therapy. The appealing features that render them so attractive include the ability to infect non dividing cells and the absence of induction of inflammatory reaction [219] since vectors keep less than 10% of the viral genome and do not code viral proteins. Moreover, AAV vectors are able to sustain

expression of the transduced gene for long periods of time (more than 4 years) [220]. AAV genome structure allows easy manipulation, including insertion of inducible [221], physiological [222] and tissue-specific promoters [223]. AAVs have a broad host range infectivity; it efficiently transduce many cell types *in vitro* [224, 225, 201, 226, 189] and *in vivo*, including muscle, liver and brain [227, 228, 229, 230, 231, 232] and capsid modifications for AAV specific retargeting have been reported [233]. rAAV vectors persist mostly as episome and less frequently integrates into host genome [234]and no adverse effects related to insertional mutagenesis have ever been reported.

The technical feasibility of cloning infectious AAV genomes [235] and the earliest AAV vectors were reported in the early 1980's [192, 236]. In the year 1994 the first clinical trial employing an AAV vector for the treatment of Cystic Fibrosis (CF) was approved by NIH [237]. AAV based vectors have achieved therapeutical potential in humans disease such as Haemophilia B [238, 220] and Cystic Fibrosis phase II clinical trials [239] have confirmed AAV safety profile.

Nowadays, many pre-clinical trials are undergoing and the risk of cancer in current AAV trials is negligible, on the basis of infrequent integration efficiency and the quiescent nature of the target tissues [240]. Although the experts on the field recommend additional long-term safety studies, up to now there are no reports of adverse effects of recombinant AAV vectors.

Production of AAV based vectors

The basic elements for production of recombinant Adeno-associated virus vectors involves at least three components: 1) Tissue culture cells, 2) Rep, Cap and the essential helper virus proteins and 3) the vector DNA. The basic notions of AAV vector production and purification are schematically represented in the Figure 1.13.

The classical strategy for the production of AAV vectors involves the use of HEK 293 cells infected with adenovirus that provides helper functions. Adenoviral infection

is combined with the transient transfection of a vector plasmid that contains viral ITRs and the gene of interest and a second plasmid codifying for the structural and non structural proteins of AAV without the ITRs [241]. Production of AAV stocks free of adenovirus contamination is problematic with this method. This problem has been overcome by providing to the packaging cell cultures only the adenoviral genes that are required for the enhancement of AAV replication: E2a, E4orf6 and VA. E1a and E1b genes, also important for efficient AAV production, are stably integrated and expressed by HEK 293 cell genome. Currently, the most common AAV production protocols entail the use both of a single helper/packaging plasmid, that codifies for all AAV (Rep and Cap) and Ad functions, or two distinct helper and packaging plasmids. The vectors have been traditionally purified through a $CsCl_2$ equilibrium gradient centrifugation. However, this procedure is time consuming and does not allow the scaling-up nor the production of clinical grade of vector's stocks.

Alternative protocols for AAV purification have been developed to overcome problems with toxicity, particles infectivity ratio, low titers and time consuming procedures. Iodixanol gradient separation shortened the centrifugation period to 3 hr. Iodixanol is an X-ray contrast solution, and resulted in reproducible concentration and purification of rAAV-vector stocks [242]. Iodixanol gradient prior to affinity chromatography has brought significant improvements over $CsCl_2$ gradient centrifugation, improving virus recovery and infectivity of preparations [243, 244]. A scalable two-steps purification procedure using ion-exchange chromatography followed by sulphate chromatography has been also developed and column-purified rAAV showed preparation with purity greater than 90%, free of any detectable contaminating adenovirus and biologically active [245]. Affinity chromatography for AAV-2 by gravity flow was based on its affinity to heparin, without ultracentrifugation and showed high titers, infectivity, and purity [246]. However, this methods were designed to purified only AAV type 2. Other sero-types such as AAV4 and AAV5 require sialic acid for binding and transduction [247] and have proven

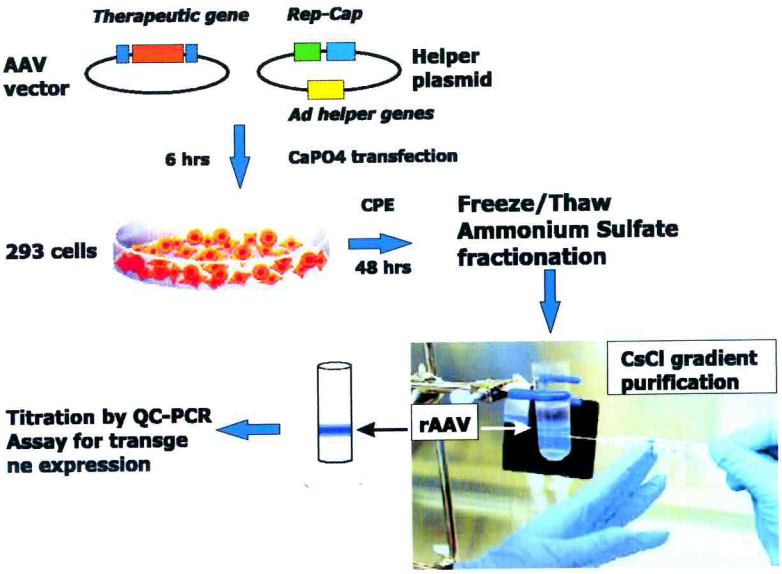

Figure 1.13: **Production of recombinant AAV vectors:** The protocol of production of recombinant AAV vectors by dual transfection is represented schematically. AAV vector plasmid and pDG plasmid (Helper plasmid) are transfected in 293 cells, cytopathic effect can be seen after 48 hours and cells are then harvested. Through freeze/thaw cycles and ammonium sulfate fractionation rAAV are released and purified through $CsCl_2$ gradient centrifugation. Fractions are then recovered, dialyzed and tittered by quantitative PCR. Functional assay is also performed to evaluate the quality of stock preparation.

to be more efficient in transducing certain cell types than AAV2 [248]. Serotypes other than AAV2 are clinically relevant due to the high prevalence of neutralizing antibodies against AAV-2 in the population [249] and the possibility that this antibodies could hamper AAV-2 vector-mediated gene transfer in a large number of patients. For that reason broader and effective methods are needed, Klaudov and colleagues have develop a simple method based in ion exchange to purify different AAV serotypes (AAV2, AAV4 and AAV5), this method is fast, reproducible, efficient, yield highly pure stocks and is amenable for large-scale production of clinical grade vectors [250].

The large-scale production of AAV vectors for clinical use requires ideally the availability of a stable packaging cell line. Attempts to produce such a cell lines have been reported, Clark and colleagues developed a cell line containing the ORF Rep

and Cap [251], but the cytostatic activity of rep and the need of adenoviral infection rendered the system not sufficiently practical. Qiao and colleagues [252] reported a cell line with E1a and E1b inducible genes, together with the stable transfection of AAV Rep and Cap genes and the AAV-GFP vector genome. They demonstrate E1a induction by DOX and infection with replicative defective Adenovirus could produce rAAV-GFP. Although this system is feasible, the cell lines obtained were not stable and the vector yields were not high. One of the latest development involves the production of rAAV in invertebrate cells. Sf9 cells were coinfected in suspension cultures with three recombinant baculoviruses (a Rep-baculovirus, a VP-baculovirus, and an AAV ITR vector genome baculovirus) and, 3 days later, rAAV was recovered. This system yield $5x10^4$ genome-containing particles per cell, which means that 1L of cultured Sf9 cells produced the equivalent to 500 to 1000 $175cm^2$ flask of 293 cells. High titer of $1.8 \text{ X } 10^{13}$ were generated by $CsCl_2$ equilibrium gradient centrifugation followed by a purification in a heparin column [253].

These recent advances in the production and purification of high-titer recombinant AAV vector stock will facilitate the preclinical experimentation and the transition to human clinical trials.

Cell processing of AAV genomes

Vectors that integrate into the host genome can provide stable transgene expression, a condition that is required for many applications. But this event can have unwanted effects, as recently shown by the development of leukemias in children treated with a retroviral vector that integrated near, and apparently activated, an oncogene [254].

Vectors based on AAV (rAAV) generally persist as episomes but occasionally integrate into the host genome. Unfortunately, the site-specific integration property of the wild type virus is lost in the absence of the Rep protein expression. Understanding how and where AAV vectors integrate has paramount implications in its future appli-

cations in gene therapy. The ultimate goal of AAV basic research is the design of a therapeutical AAV vector able to site-specific integration.

As mention above, only wt AAV has the site-specific integration ability, that relays on the presence of Rep protein [200, 201]. wt AAV integrates into an "actively transcribed" muscle-specific region that is closely linked to AAVS1 [255], corresponding to the slow skeletal troponin T gene, TNNT1 and TNNI3.

Whereas AAV proviruses integrate in multiple chromosomal locations in HeLa cells, rAAVs in mouse hepatocytes preferentially integrates in actively transcribed gene-rich regions and in a hot spot of 22-Mb in chromosome 19 [256, 257]. Nakai et al observed that 72% of rAAV integration events interrupted an actively expressed gene in mice liver, this suggesting that AAV "loves active genome" regions [234, 257].

AAV vectors do not encode proteins that catalyze integration but use host factors instead. There is no vector-encoded nuclease to cleave the host chromosome, and so AAV must take advantage of existing chromosomal breaks [234]. This requirement explains earlier observations that a variety of DNA-damaging agents increase transduction frequencies and integration of AAV vectors [258]. These observations suggest that could be a link between transcription and DSB.

Recombinant AAV vectors seem to use the NHEJ machinery to integrate at chromosomal DSBs. Some host-cell proteins from DNA double-stranded break (DSB) repair pathways have been involved in the processing of AAV genomes, including Ku86, Rad52 [259] and DNA-PK [260]. Further support for the connection between DSB and non-homologous end-joining (NHEJ) are *in vitro* and *in vivo* studies, showing that induced DSB enhance human gene targeting and that episomal circularization of input vectors genomes is at least in part dependent on DNA-PKs [260, 261]. These findings led to the proposal of a model for AAV mechanism of integration by Russell [234], see Figure 1.14.

The molecular mechanism responsible for efficient rAAV transduction are still

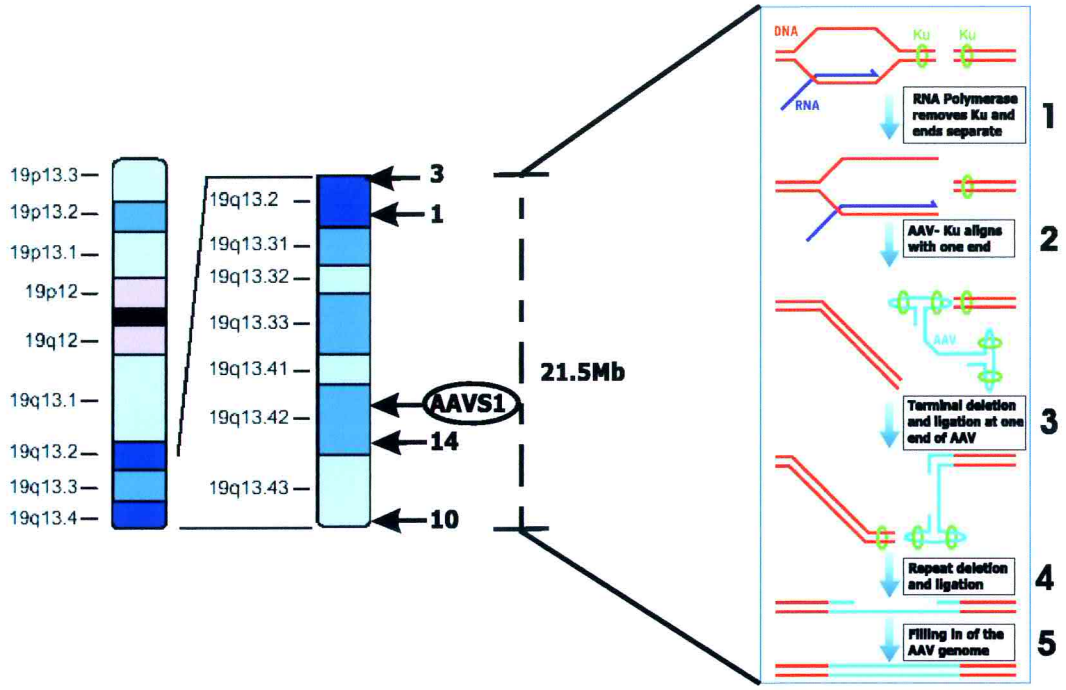

Figure 1.14: **Integration of AAV-2**: The left panel represents the q arm of chromosome 19, together with zoom of a 21.5Mb region of the cytogenetic map where the AAVS1 locus is located. AAVS1 is circled, arrows indicate other positions where integration occurs. The right panel represents the model proposed by Russell to explain AAV vector integration In this model, (1) transcription through a DSB displaces the DSB-binding Ku heterodimer,which forms a ring structure around the DNA end. The two chromosomal ends will be further separated if the transcribed region upstream of the DSB attaches to the nuclear matrix differently from the non-transcribed region downstream of the DSB. (2) One chromosomal end can then align with a single-stranded AAV vector genome, which has bound Ku at the base-paired inverted terminal repeats. (3) Ligation at this DSB by NHEJ will produce terminal deletions of the vector genome and chromosome end. (4) Ultimately the transcribed chromosomal end will also ligate to the other AAV vector end, and (5) the single-stranded region of the AAV genome will be filled in by DNA synthesis. Not shown in the figure are the other NHEJ proteins DNA-PKcs and ligase IV/XRCC4. Adapted form Russell and Miller 2003. [234, 256].

poorly defined. However, it is known that functional transduction is limited at different steps, including escape from endosomes and nuclear transport [262, 214], uncoating [208], and conversion from single-stranded to double-stranded DNA [263, 264, 265, 266].

A cellular protein that binds the immunosuppressant drug FK506, termed the FK506-binding protein (FKBP52) or single-stranded D-sequence-binding protein (ssD-BP), interacts with the single-stranded D sequence within the AAV inverted terminal

repeats and seems to play a central role in AAV-mediated transgene expression, FKBP5 inhibits viral second-strand DNA synthesis and consequently limits high-efficiency transgene expression [267]. FKBP52 can be phosphorylated by epidermal growth factor receptor protein tyrosine kinase at both tyrosine and serine/threonine residues, but only the phosphorylated forms of FKBP52 interact with the D sequence [268]. Furthermore, the tyrosine-phosphorylated FKBP52 can inhibit AAV second-strand DNA synthesis by more than 90%, whereas the dephosphorylated FKBP52 has no effect on AAV second-strand DNA synthesis.

Qing and colleagues [269] have also identified that the tyrosine-phosphorylated form of FKBP52 is a substrate for the cellular T-cell protein tyrosine phosphatase (TC-PTP). Overexpression of the murine wild-type (wt) TC-PTP gene, caused tyrosine dephosphorylation of FKBP52, leading to efficient viral second-strand DNA synthesis and resulting in a significant increase in AAV-mediated transduction efficiency in HeLa cells *in vitro*. Whereas *in vivo* hematopoietic stem/progenitor cells from TC-PTP-transgenic mice were successfully transduced by recombinant AAV vectors. This confirms the proposed role for this protein.

Long-term gene expression after *in vivo* rAAV gene transfer may relay mostly on persistent circular and linear AAV episomes [270, 264, 229, 271, 272], and to a lesser extent by integration into host genome [273]. This process of intermolecular concatamerization and recombination seems to be different among tissues. In muscle tissue the predominant form is head-to-tail circular AAV episomes [270, 261] whereas in the liver it appears that episomal linear genomes are responsible for most of the transgene expression [229, 271, 272]. The requirement for this complex molecular processing could explain in part why even in highly permissive tissues, such as skeletal muscle and brain, transgene expression takes several weeks to reach maximal level and is often preceded by a lag period [231, 232].

AAV gene transfer to artery wall

The first report of AAV based gene transfer into the vascular system appeared in 1996. This work reported gene expression in rat myocardium and in rat myocardial cells, as well as in pig myocardium 6 months after AAV intracoronary delivery [274]. In 1997 Gnatenko and colleagues [275] observed that rAAV could infect most of human umbilical vein endothelial cells (HUVEC) *in vitro*, and endothelial (EC) and vascular smooth muscle cells (VSMCs) *in vivo*, in non injured rat carotid arteries. These authors suggested also high-rates of transduction in the vessel wall. However, they used in situ PCR to establish infection efficiency and contamination with Adenoviral helper virus of used vector stock could not be excluded. Maeda and colleagues [276] using an AAV-*LacZ* vector observed *in vitro* up to 50% of transduction in rat VSMCs, and in *ex vivo* studies to infect thoracic aorta, beta-galactosidase positivity was shown in endothelial and adventitial but not in medial VSMCs cells. Rolling and colleagues showed AAV gene transfer of *beta*-gal into medial and adventitial cells of rat arteries; in this case transduction efficiency was associated with injury [277]. Lynch and colleagues [278], reported that rAAV was able to transduce the adventitial microvessels of non-human primate atherosclerotic arteries by adventitial or by intraluminal rAAV delivery and that balloon injury enhanced the adventitial rate of transduction. Later on in 2000 Richter and colleagues [279] reported transduction of mostly VSMCs in intact rabbit artery with a rAAV-CWRAP (encoding human placental alkaline phosphatase and driven by a Rous sarcoma promoter) and claimed that under optimal conditions one-third to 58% of subendothelial VSMCs can be transduced. Despite the contradictory results reported by these research groups, all together have shown that AAV can infect and achieve transgene expression in all the cell types of the normal and atherosclerotic blood vessels, and they all agree that AAV is a promising vector for the treatment of vascular diseases.

Chapter 2

Materials and methods

2.1 Characterization of rAAV vectors

2.1.1 Cloning and production of rAAV vectors

The first part of this work consisted in the subcloning of *E.Coli LacZ* gene by N. Arsic, human Timp1 and human long pentraxin 3 (PTX3) by S. Zacchigna into pTR-UF5 backbone. The results of cloning and production of the rAAV-Timp1 can be found in detailed in S. Zacchigna's degree thesis [280].

Briefly, pAAV-LacZ was obtained by inserting the *LacZ* gene from plasmid pCH110 (Pharmacia, Uppsala, Sweden) into the pTR-UF5 backbone. pAAV-Timp1 was constructed by cloning the human Timp1 cDNA, obtained by RT-PCR amplification from HeLa cell total RNA, into the original plasmid pTR-UF5 to substitute the GFP and neomycin-resistance genes, as shown in Figure 2.1B. pTR-UF5 was kindly provided by N. Muzyczka (University of Florida, Gainesville, FL). Cloning and propagation of AAV plasmids was carried out in the JC 8111 *E. coli* strain.

The cloning of pAAV-PTX3 was performed in similar way as for pAAV-Timp1. From human total RNA the cDNA of human long pentraxin 3 (PTX3) was amplified as a 1,200bp fragment with the primers forward (5'GTGCTCTCTGGTCTGCAGTG3')

and reverse (5'GAGCTCCTCCATGTGGCTG3') and cloned in the plasmid vector pTR-UF5 vector using the *Xba*I-*BamH*I sites. The cloning of rAAV-Timp1 and rAAV-PTX3 is schematically shown in Figure 2.1C.

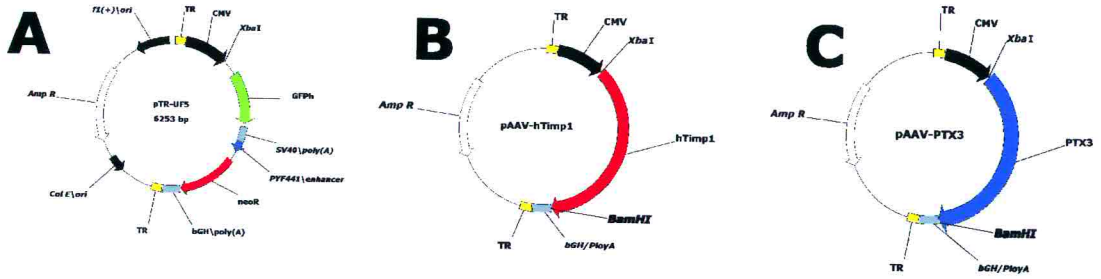

Figure 2.1: **Schematic representation of Timp1 and PTX3 cloning into pTR-UF5**: A, pTR-UF5 vector map showing the original hGFP gene in green color, a neomycin resistant gene in red color, these genes were substituted by the therapeutical genes, B, pAAV-hTimp1 vector map showing restriction enzyme cloning sites *Xba*I and *BamH*I and in red color the cloned gene , C, pAAV-PTX3 showing human long pentraxin 3 gene in blue and the same restriction sites were used to clone PTX3 (long-pentraxin 3) into pTR-UF5.

2.1.2 Production of rAAV vectors

Infectious AAV2 vector particles were generated in 293 cells, cultured in 150-mm-diameter petri dishes, by co-transfecting each plate with 15 μg of vector plasmid (pTR-UF5, pAAV-LacZ, pAAV-Timp1 or pAAV-PTX3) together with an equimolar amount of packagin/helper plasmid pDG (kindly provided by J A Kleinschmidt) [281], containing AAV and adenovirus helper functions. After 48 hours of transfection, cells were harvested and pelleted. To release rAAV virions, cell pellets were lysated in HEPES solution by three to four freeze/thawed cycles and purified by ammonium sulphate fractionation. Afterwards a $CsCl_2$ equilibrium gradient centrifugation was performed during 48 hrs at 39,000 rpm. After centrifugation the gradient was fractionated and the collected fractions were subjected to microdialisis in PBS and pooled. rAAVs band at a CsCl2 density of 1.41g/cm3. The AAV titers were determined from pooled fractions by a quantitative PCR procedure [282]. For this purpose, 20-bp primers were selected in a region of AAV genome corresponding to the cytomegalovirus (CMV) promoter, common

to all the vectors used in this study, and amplyfying a segment of 243 bp (CMV1 5'-ACGGTAAACTGCCCACTTGG-3', and CMV2 5'-CTTGGAAACCCCGTGAGTC-3'). A competitor DNA fragment, with the same sequence as the target of the amplification but containing a 20-bp internal deletion, was amplified in scalar amounts of molecules together with target sequences. A detailed description of the competitive PCR technique is provided elsewhere [282]. The viral preparations used in this thesis had titers of $1x10^{11}$ to $1x10^{12}$ viral genome particles per ml.

2.2 Evaluation of VSMCs transduction *in vitro* by AAV

AAV-GFP infection of human coronary VSMCs

To define the permissivity of smooth muscle cells to AAV vectors in vitro, $1x10^8$ genome particles from a preparation of AAV-GFP (obtained from plasmid pTR-UF5) were used to transduce $1x10^5$ coronary artery smooth muscle cells (purchased from Clonetics, BioWhittaker, Walkersville, MD). Cells were cultured in SmGM-2 specific medium (BioWhittaker) supplemented with fetal bovine serum and chemoattractants (hEGF 0.5 ng/ml, Insulin 2.5 μg/ml, hFGF-B 1 ng/ml, FBS 5%). After 5 days, flow cytometric analysis of GFP expressing cells was performed by a FACScalibur instrument (Becton Dickinson, San José, CA) acquiring $1x10^4$ events for each sample.

Detection of Timp1 by immunocytochemistry

$1x10^5$ coronary artery smooth muscle cells (purchased from Clonetics, BioWhittaker, Walkersville, MD) were cultured in four chambers slides (LAB-TEK, Nalgene, Naperville, IL), transduced with 1 x 10^8 genome particles of rAAV-Timp1 and incubated for 5 days. After the period of transduction attached cells were fixed in cold methanol (-20°C) for 20 minutes and incubated in 0.3% H_2O_2 to eliminate endogenous peroxidase activity. Slides were washed in PBS, blocked in 5% horse serum for 30 min, and incubated 30

minutes in a humid chamber at room temperature with anti-hTimp1 (1:500 dilution, NeoMarkers). Detection of primary antibody was performed with the kit VECTASTAIN ABC (Vector Laboratories, Inc) following the manufacturer instructions as described in section 2.7.4. After detection slides were counter stained with hematoxilin and mounted with Eukitt (Sigma), see section 2.7.2.

2.3 *In vitro* effects of AAV-Timp1

2.3.1 Chemoinvasion assay

To assay the ability of SMCs to invade matrix, 1x10^5human coronary artery SMCs were either transduced with AAV-*LacZ* or AAV-Timp1 (1x10^8 genome particles) for 48 hours and then seeded in serum-free medium into the cell culture inserts of 8 M pore size invasion chambers coated with matrigel (BioCoat Matrigel Invasion Chambers, Becton Dickinson, San José, CA). The same medium supplemented with serum and chemoattractants (hEGF 0.5 ng/ml, Insulin 2.5 g/ml, hFGF-B 1 ng/ml, FBS 5%) was placed in the lower chamber. After 24 hr of incubation, cells that migrated to the lower side of the filter were fixed in methanol, stained with Giemsa solution and counted in eight fields per membrane at 400x magnification. Each assay was carried out in triplicate. Results were expressed as the mean number of migrated cells ± standard error of mean (SEM).

2.3.2 Zymography and Reverse Zymography

Source of rat's MMPs

As a source of MMPs we employed injured arteries. Three male Wistar rats were balloon injured as described in section 2.4.2, after 3 days arteries were harvested as described in section 2.7.1, washed in sterile PBS and cultured for 3 days in a specific medium (SmGM-2, BioWhittaker) containing penicillin, streptomycin and fungizone

without supplements in a standar cell culture incubator (humid environment, 37°C and 5% CO_2). At the end of the period of incubation, 500μL of arteries supernatants were concentrated 10 times in microcon Y-10 (Amicon).

Zymography

Concentrated supernatants were mixed 1:1 volume with non-reducing loading buffer and incubated 30 minutes at 55°C in a thermoblock. Samples were loaded in a freshly prepared acrylamide-gelatin gel (7.5% Acrylamide:Bis-acrylamide 40:1, 0.6% Gelatin) and run in a SDS-PAGE electrophoresis. Afterwards the protein gel was incubated for 1 hr in 2.5% Triton X-100 at room temperature. After activation of metalloproteinases, the acrylamide-gelatin gel was incubated over night in collagenase buffer (50mM tris-HCl pH 7.5, 150mM NaCl, 5mM $CaCl_2$, 0.1% TX-100) at 37°C in gentle shaking. Next day the acrylamide-gelatin gel was stained in Coommassie Blue for 15 minutes and destained in a buffer (40% Methanol-20% Acetic acid) until bands were evident.

Reverse Zymography

As a source of human Timp1 we used transfected HEK 293 cells as follows. Two petri dishes with 4-5 X 10^6 HEK 293 cells were cultured in D-MEM (Dulbecco's modified minimum essential medium, GibcoBRL Life Technologies) supplemented with 5% fetal bovine serum and 50 μg/ml Gentamicin. After 50-60% of confluence was achieved, 20 μg of pAAV-Timp1 per petri dish were transfected using the calcium-phosphate method. After an over night incubation, transfection medium was substitute with fresh medium (Serum free D-MEM 1 gr glucose/L). Three days later, 10 ml of supernatant (10ml per petri dish) was concentrated 10 times to 1 ml with centricon Y-10 (Amicon). Concentrated supernatants were mixed 1:1 volume with non-reducing loading buffer and incubated 30 minutes at 55°C in a thermoblock. Samples were loaded in a freshly prepared acrylamide-gelatin gel (11% Acrylamide:Bis-acrylamide 40:1, 0.6% Gelatin) and

run in a SDS-PAGE electrophoresis. Afterwards the protein gel was incubated for 1 hr in 2.5% Triton X-100 at room temperature. After activation of metalloproteinases, the acrylamide-gelatin gel was incubated 2 hrs in a 1:1 mixture of 12 ml of collagenase buffer (50mM tris-HCL pH 7.5, 150mM NaCl, 5mM $CaCl_2$, 0.1% TX-100) and supernatant of injured arteries, as described in the section 2.3.2, at 37°C in gentle shaking. After this period, the acrylamide-gelatin gel was stained in Coommassie Blue for 1 hr and destained in a buffer (40% Methanol-20% Acetic acid) until bands were evident.

2.4 Vessel injury

2.4.1 Ethical issues in animals work

Animal care and treatment was in conformity with institutional guidelines issued in compliance with national and international laws and policies (EEC Council Directive 86/609, OJL 358, December 12th 1987).

2.4.2 Carotid angioplasty in rats

Anaesthesia

Male Wistar rats weighing 300-400 g were hand restrained and anesthetized by intraperitoneal injection of ketamine 100mg/kg (Ketavet, Parker-Davis, Milan) and xylazine 5 mg/kg (Sigma). Once the effect was evident and corroborated by pain and corneal reflexes the surgical field was devoid of hair and we proceeded to artery isolation

Carotid artery isolation

Right carotid artery was exposed and dissected through a middle-neck incision, blood flow was isolated from a 1.5 cm long carotid segment as follows; 1) A Müller vascular clamp of 0.8 N(Aesculap, FE23K) was positioned at the proximal segment of common carotid, 2) A 4-0 prolene (Ethicon) suture was tied at the most distal segment of

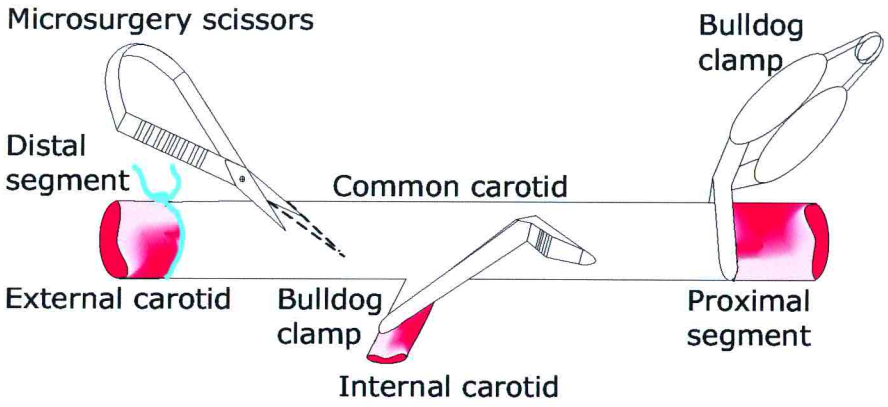

Figure 2.2: Isolation of common carotid and blood flow is represented schematically. Right carotid artery was first dissected completely from neurovascular vaina and blood flow was isolated combining two vascular clamps with permanent ligation of the external carotid branch.

external carotid, 3) A De Bakey-Hess bulldog vascular clamps (Aesculap, BH030R) was positioned at the starting of internal carotid, see Figure 2.2).

Balloon injury in rats

Arteriotomy of external carotid with microsurgery scissors (Aesculap, OC496R) was made at 45 degrees, see Figure 2.2. Blood contained in isolated segment was flushed out with PBS and as soon as possible an intravasular devaricator was introduced in the vessel wound. A 2F Fogarty embolectomy catheter (Baxter-Edwards Health Care, Irvine, CA) was introduced through the distended artetriotomy into the external carotid artery until reaching the distal segment, and then inflated to 1.5-2 atmospheres. Injury was induced by inflating the balloon in two to three adjacent arterial segments covering a total length of 1 cm (duration: 80 seconds per segment). Immediately after balloon removal flash release of the proximal clamp allowed blood flow, this maneuver was to avoid blood clot formation at proximal sites of vessel clamp. The injured segment of the carotid artery was labelled with black ink.

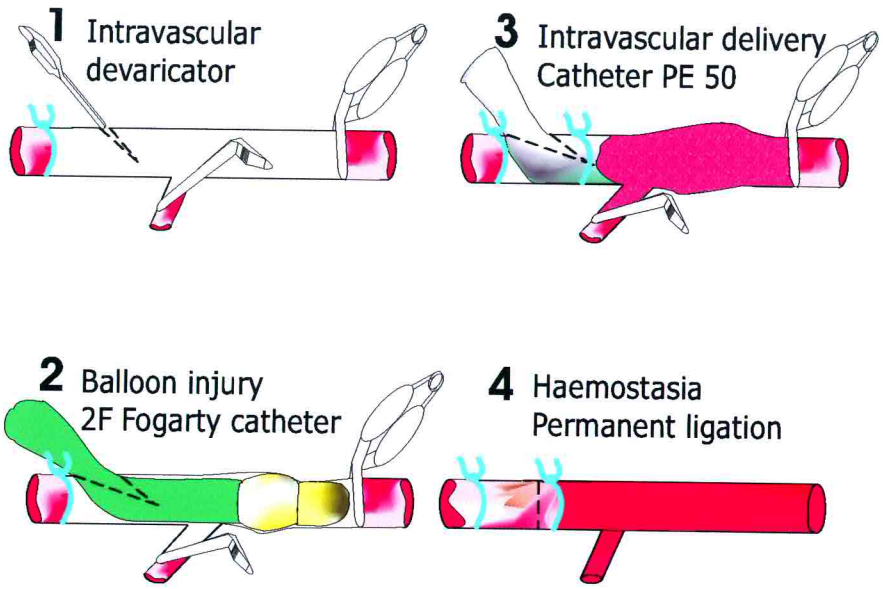

Figure 2.3: Balloon injury and intravasular delivery is represented schematically in four steps. 1, devarication of arteriotomy, 2, Introduction of embolectomy catheter and balloon inflation in three adjacent segments, 3, Introduction of a polyethylene cannula, suture fixation and intraluminal delivery 4, Catheter withdrawn, artery ligation and release of vascular clamps.

2.5 Intravascular delivery

2.5.1 Intravascular delivery in rat's vessel

Intravascular delivery was done as follows; 1) The intravasular devaricator was placed in the vessel wound and the tip of a polyethylene cannula (Intramedic PE50, Becton-Dickinson) was introduced, 2) A 4-0 prolene (Ethicon) suture was tied tightly proximal to the commence of catheter entrance. 3) 100μL of PBS or rAAV vectors were delivered intraluminally slowly with the help of an angioplasty pressure device and kept into the closed artery for 40 min.(artery distention was maintained constant), 4) Afterwards the fixed catheter with solution was withdrawn, 5) A 4-0 prolene (Ethicon) suture was tied tightly proximal to the arteriotomy and distal to internal carotid commence, 6) Blood flow was restored through the common carotid artery by setting free first the internal carotid clamp, making haemostasia in the arteriotomy, second by setting free the common carotid clamp, only once that haemostasia was achieved, see Figure 2.3

and 3.8.

2.6 Experimental design

Twenty-nine animals were subjected to artery injury, followed by treatment with AAV-Timp1, AAV-PTX3 or combination of the two. This group of treated animals was divided as follows: 1) ***Timp1 group***: 10 rats were delivered intravascularly with 100μL of AAV-Timp1 (1 x 10^{12} particles); 2) ***PTX3 group***: 11 rats were delivered intravascularly with 100μL of AAV-PTX3 (1 x 10^{12} particles); 3) ***Timp1/PTX3 group***: 8 rats were delivered intravascularly with 100μL of AAV-Timp1/AAV-PTX3 (1 x 10^{11} equal number of particles).

Seventeen animals were used as control and were divided as follows: 1) 4 rats treated with only balloon injury (BI), 2) 2 rats treated with BI + intravascular delivery with 100μL of PBS; 3) 11 rats treated with BI + intravascular delivery with 100μL of rAAV-LacZ (1 x 10^{10-11} particles).

Animals were sacrificed after 14 and 28 days (***Timp1 group*** n= 5 at each time point, ***PTX3 group*** n= 5, n= 6, control group n=11 and n= 6, respectively and ***Timp1/PTX3 group*** n= 8 at 28 days).

2.7 Histology and immunohistochemistry

2.7.1 Vessel harvesting

For further analysis, carotid arteries were exposed and dissected through a middle-neck incision. Right (injured) and left (control) carotid arteries were ligated distally and proximally, first the right carotid artery (RCA) was harvested, soon after the left artery was also harvested and the animal sacrificed by anesthetic overdose.

2.7.2 Hematoxilin and eosin staining (HE)

After harvesting, arteries were washed briefly in PBS and immediately fixed in buffered formalin solution (2% formaldehyde in PBS pH 7.4) and embedded in paraffin. For each specimen, at least 4 individual sections (at 350μm intervals) 5-μm thick were taken and mounted in lysin coated slides, dried at 65°C, deparaffinized in pure xylene, hydrated in ethanol solutions of decreasing percent (100%, 90%, 70% and 50%), rinsed in tap water and stained 30 seconds in Harris's hematoxilin, after hematoxilin staining slides were differentiated in tap water for 5 minutes and stained in 0.1% eosin for 2 minutes, passed to ethanol 90%, 100% immersed in pure xylene and mounted in resin (Eukitt, Sigma).

2.7.3 Weigert-Van Gieson and Azan-Mallory staining

Collagen and elastin content was assessed by Weigert-Van Gieson and Azan-Mallory staining. For Weigert-Van Gieson staining, sections were first deparaffinized in pure xylene, hydrated in ethanol solutions of decreasing percent (100%, 90%, 70% and 50%), rinsed in tap water and stained for 1 hr in Weigert resorcin fucsin solution at 60°C. Afterwards, cooled at room temperature, differentiated briefly in acid alcohol (95% ethanol, 1% HCl) rinsed in tap water, counterstained in Van Gieson solution for 5 minutes, dehydrated in increasing series of ethanol solutions, immersed in pure xylene and mounted in resin (Eukkit, Sigma).

For Azan Mallory staining rehydrated sections were consecutively stained in Azo-carmin and Azan solutions, using phosphotungstic acid as a mordant and a careful differentiation in anilin.

Collagen and elastin content estimation

For each animal analyzed, at least 3 individual sections (at 350 μm intervals) were stained with Azan Mallory or Weigert-Van Gieson to evaluate collagen (cyan, red) and

elastin (darkblue, black), respectively. Histological quantification was performed by transforming the respective colors into monochrome with a 255-level gray scale (NIH Image J 1.29 software, Maryland, USA), followed by the evaluation of the relative number of pixels after adjustment of the individual thresholds for each color, thus permitting a binary analysis [283]. Results are expressed as the number of pixels per area classified as collagen or elastin divided by total number of pixels in each area.

2.7.4 Immunohistochemical techniques

Immunohistochemistry

After standard paraffin embedding, 5-μm thick tissue sections were deparafinized overnight in xylene, hydrated in decreasing ethanol series and rinsed in tap water. The section were then placed in 3% hydrogen peroxidase for 5 min, rinsed in bi-destilated water, and antigens were unmasked in 10mM sodium citrate buffer, pH 6.0 by heating specimens (HIER: Heat Induced Epitope Retrieval) in a Microwave oven for 7 minutes at 360 Watts (Intellowave LG grill). After cooling at room temperature, the section were washed in PBS, blocked in 5% horse serum for 30 min, and incubated with one of the following antibodies; anti-Timp1 (1:500 dilution, NeoMarkers), anti-CD45 (1:500 dilution, Vector Laboratories, Inc.), anti-α-SMA (1:40 dilution, Sigma Chemical Co., St. Louis, MO) and anti-proliferating cell nuclear antigen (PCNA) (sc-56, Santa Cruz Biotechnology) at room temperature for 1 hour. The section were then washed in a solution of PBS-Tween 20 and incubated with a horse secondary antibody (1:2000 dilution, Vector Laboratories, Inc.) for 30 min at room temperature. After antibody incubation, slides were rinsed in PBS and signal was developed from 1 to 5 minutes using 3,3'-diaminobenzidine (DAB) as substrate for the peroxidase chromogenic reaction (Lab Vision Corporation, Fremont, CA). Next, slides were rinsed in tap water, counter stained in hematoxilin and mounted as above described.

2.8 Beta-galactosidase detection

2.8.1 Detection by X-Gal staining

X-Gal staining

Right and left carotid arteries were harvested as described in section 2.7.2, washed in PBS to remove remaining blood and cut in two pieces. Proximal segments were fixed in 1mL of 0.25% of glutaraldehyde (Sigma) for 2 hrs at room temperature. Arteries were washed in a buffered solution (0.02% NP40-PBS) overnight in constant gentle shaking. Next morning arteries where placed in 2mL of X-Gal staining solution (5mM K_3, 5mM $K_4[Fe(CN)_6]$, 2mM $MgCl_2$, 1mg/mL of X-Gal in PBS) and incubated at 37°C for 4 to 6 hrs. Next, arteries were washed once in PBS, marked with black ink in the surface of interest and fixed in a buffered formalin solution (4% formaldehyde in PBS pH 7.4). Specimens were dehydrated and paraffin embedded according to standard histotechical procedures.

Nuclear fast red counter staining

For each specimen, at least 3 individual sections (at 350μm intervals) 5-μm thick were taken mounted, deparaffinized, and hydrated in ethanol solutions of decreasing percent as described above (100%, 90%, 70% and 50%), rinsed in tap water and stained for 5 to 6 minutes in nuclear fast red (Vector Laboratories). After staining slides were differentiated in tap water for 5 minutes and slides were dehydrated in increasing series of ethanol solutions, immersed in pure xylene and mounted in resin (Eukkit, Sigma).

2.9 Fluorescence *in situ* hybridisation (FISH)

2.9.1 Detection of rAAV-*LacZ* genome in rat carotid arteries

FISH on paraffin embedding tissues

To assess the effectiveness of artery wall infection after an intravascular delivery with rAAV we made use of a DNA probe from pAAV-*LacZ* to visualize the localization of rAAVs in the isolated segment of artery.

DNA probe synthesis

Probe synthesis template was obtained from pAAV-LacZ digestion with *Pst*1, which has restriction sites at each ITR end of vector. A 5.6 kb band was then resolved by agarose gel electrophoresis and recovered by gel extraction. Around 1 μg of material was denatured and labelled by random labelling procedure according to manufacturer instructions (DNA Labelling Kit, Roche). Excess of Dig-dNTPs was removed by LiCl and ethanol precipitation, efficiency labelling was quantified by chemioluminiscence according to manufacturer instructions (Chemioluminiscence Detection Kit, Roche).

Pre-Hybridisation

5μm sections were obtained with microtome blade from carotid arteries embedded in paraffin blocks. Sections were mounted in poly-lysine coated slides and baked at 65°C during 1 hour, deparaffinized twice in pure xylene and hydrated in ethanol solutions of decreasing concentration (100%, 90%, 70% and 50%). Tissue was permeabilized as follows; 1) 20 minutes incubated in 0.2N HCl, 2) Rinsed in destilated water, 3) 20 minutes incubated in Proteinase K (100μg/mL) at 37°C and 3) Rinsed in tap water. Afterwards tissue sections were treated as follows; 1) Fixed during 1 min in buffered formalin solution (10% formaldehyde in phosphate saline (PBS) pH 7.4), 2) Rinsed in tap water, 3) 10 minutes incubation in 0.1M Trietanolamine-0.25% Acetic Anhydride,

4) Rinsed in phosphate saline (PBS) three times and dehydrated in ethanol solutions of increasing concentration (50%, 70%, 90% and 100%) and allowed to air-dry.

Hybridisation

Samples were denatured in 70% formamide diluted in 2X SSC, pre-warmed in the oven and incubated at 75°C for 5 minutes, immediately after dipped in - 20°C pre-cooled ethanol solutions of increasing concentration (50%, 70%, 90% and 100%) 1 minute each one and allowed to air-dry. Simultaneously AAV-*LacZ* probe was diluted at 5ng/μL in 2X hybridisation buffer (4X SSC, 2X Denhardt's solution and 0.2M Sodium phosphate pH 6.5), 50% Dextran Sulfate and 1μg/mL salmon sperm DNA and denatured at 75°C for 10 minutes and chilled in an ice bath. Samples were hybridised in a humid chamber at 42°C for 16 hours.

Detection

After hybridisation slides were washed once in 2X SSC-0.1mM DTT at room temperature during 30 minutes, washed once in 0.1X SSC-0.1mM DTT at 37°C during 30 minutes and rinsed briefly in 0.1X SSC. Preliminary to detection, samples were incubated in blocking buffer (2XSSC, 0.05% Triton X-100, 30% Foetal calf serum heat inactivated) over night at room temperature.

Next day, samples were washed twice in TBS buffer during 10 minutes each. Anti-Dig-Rhodamine antibody was diluted 1:100 in dilution buffer (TBS, 0.5% Triton X-100, 5% FCS) and applied to samples, covered with paraffin and incubated between 45 and 60 minutes in the moist chamber at 37°C. Antibody was washed out twice in TBST buffer(0.1% Tween 20) during 10 minutes each. Sections were dehydrated in ethanol solutions of increasing concentration (70%, 90% and 100%) 1 minute each one, mounted in mounting media (KLP Inc.) 9:1 Hoescht 33258 and sealed with nail polish.

2.10 Confocal laser microscopy (CLM)

Theory of Confocal laser microscopy (CLM)

The Principle of LSM technique is to project the light of a point light source (a laser) through an objective onto a certain object plane of interest as a nearly diffraction-limited focus. However, in order to obtain a single plane image all the light produced outside the object plane, or the fluorescence of fluorescent specimens, should be eliminated to avoid disturbance in the in-focus image of object point of interest, otherwise it would result in a blurred image of poor contrast. To capture only the light coming immediately from the object point in focus, while obstructing the light coming from out-of-focus areas of the specimen. The technical solution to this problem is that the fluorescence light produced, at the focus of the objective is projected onto a variable pinhole diaphragm by the same objective and a tube lens. The focus inside the specimen and the pinhole are situated at optically conjugate points (confocal imaging). In this way essentially no other light than that coming from the object plane of interest can pass the narrow pinhole and be registered by a detector. Most of unwanted light coming from other specimen areas is focused outside the pinhole. The final result is that the image point generated is largely free from blur caused by unwanted light.

In order to obtain an image of the selected object plane as a whole, it is necessary to scan the object plane in a point-by-point, line-by-line raster by means of an XY light deflection system. The detectors -as a rule, photomultipliers - convert the optical information into electric signals. This allows the image of any object plane to be generated and stored within less than a second. By a defined focusing (Z axis) movement it is possible to look at any object plane of interest. By scanning a succession of object planes in a specimen, a stack of slice images can be produced. This way, the LSM technique in conjunction with ICS optics (Infinity Color-Corrected System) brings improvements over conventional microscopy in terms of resolving power and confocal

depth contrast, this goes to the limits of object features in the order of 0.2 μm can be resolved, and height differences of less than 0.1 μm made visible, without the use of interference methods.

Morphometry analysis with Confocal laser microscopy (CLM)

The paraffin blocks were coded as to hide group of origin. Hematoxilin and eosin stained slides were visualized in an optic microscope (Olympus CX40), and at least 3 slides per specimen were selected depending only on architecture integrity of the artery ring. An average of 3 slides per animal were use for analysis under a confocal laser scanning microscope (Zeiss LSM 510). Scanning was made using as excitation source at channel 1 light transmision and at channel 2 Argon laser 543nm. The acquired images showed nuclei and elastic laminas stained in fluorescent red, internal and external elastic laminas are easily evidenced as red lines due to the autofluorescence of elastin. Employing the LSM510 software 5.0 arterial layers (media and neointima) were manually outlined and perimeter and area calculation function were used to assess and record the following parameters, external elastic lamina (EEL) area (μm^2), internal elastic lamina (IEL) area (μm^2) and lumen area (μm^2), medial area was calculated by subtracting EEL area to IEL area, neointimal area was calculated by subtracting IEL area to lumen area. The three different slides were taken at 200 to 350μm intervals.

2.11 Coronary stents for stent-based gene delivery

Binding of rAAV-*LacZ* to PC-coated stents

Stainless steel disks and stents coated with synthetic phosphorilcolin (PC) were a kind gift from Biocompatibles UK, Inc. Coating material was designed to be immunologically well tolerated and to adsorb and release molecules by ionic interactions. There are two types of coating design, one for molecules bigger than 30 kD called MatrixHi and other

for molecules smaller than 30kD called MatrixLo.

Preliminary studies to optimize the rAAV binding conditions were done using stainless steel PC-Disks MatrixHi. After optimization, the rAAV binding to PC-stents MatrixHi was done as follows. First rAAV-*LacZ* was diluted at $5x10^9$ particles/ml in 10mM Tris-HCl pH 8.3 just before its use, PC-stents MatrixHi were prewashed in 10mM Tris pH 8.3 and then incubated in 1 ml of solution with rAAV for 45 minutes in gentle circular agitation. The efficiency of binding to PC-stents was either evaluated by the level of transduction on plated cells or by the number of genome particles recovered from treated stents. In a parallel experiment, the attachment of rAAV vectors was visualized directly by electron microscopy scanning (EMS) after the optimized rAAV binding protocol.

To evaluate the *in vitro* infection and expression of rAAV-*LacZ* loaded PC-stents, sarcoma kaposi cells (KS) [284] were plated in a 12-well petri dish at a density of 2 x 10^4 cells per well in D-MEM (Dulbecco's modified minimum essential medium, GibcoBRL Life Technologies) complemented with 10% FCS and 3.5μg/ml of Gentamycin. rAAV-*LacZ* loaded PC-stents were incubated during 48 hrs with cells, then cells were fixed in a buffered formalin solution (2% formaldehyde in PBS pH 7.4) during 15 minutes, stained with X-Gal as described in section 2.8 and analyzed by light microscopy to count β-galactosidase positive cells.

To evaluate the binding efficiency of rAAV-*LacZ* to PC-stents we estimated number of genome particles recovered from treated stents by quantitative polymerase chain reaction (Q-PCR). To remove unbound virons stents were taking out of 12-well petri dish immediately after the 45 minutes rAAV-*LacZ* incubation period and extensively washed in PBS. In order to obtain ss-DNA samples to be analyzed by Q-PCR from stents we digested viron's capsid as follows. Washed rAAV-*LacZ* loaded PC-stents were incubated at 56°C during 1 hour in a buffer containing 100μg/ml proteinase K (PK), 10mM Tris-EDTA pH 8.0 and 25mM $MgCl_2$. The material obtained from vi-

ron's capsid digestion was collected and PK inactivated at 95°C during 10 minutes. This material was used as template at different dilution for quantitative polymerase chain reaction (Q-PCR). We made use of oligonucleotides that flank a cytomegalovirus (CMV) promoter region of 243 bp located upstream of *LacZ* gene in the AAV-*LacZ* and as competitor a template of plasmid DNA containing the same region that lacks 20 bp, this template is of a known number of molecules and can be easily distinguished in acrylamide gel electrophoresis. After ethidium bromide staining of acrylamide gels, bands intensity and ratios between template and competitor were calculated with the Kodak 1D 3.0 software.

To visualize directly virion's capsid binding to PC-coated stents, two stents were treated as described above, the mock treated stent was incubated in the same solutions as the rAAV treated one, omitting only the rAAV vectors. Immediately after either rAAV or mock incubation and extensive washing, the stents were placed in an vaccum chamber and visualized under an Electron scanning microscope.

Aorta infection with rAAV-*LacZ*-PC-Stents: Organ culture

A single stent was re-used and treated as in section 2.11, immediately after AAV-*LacZ* binding to PC-stent, stents were extensively washed and mounted in a Maverick 2.0 catheter (Boston Scientific). The abdominal aorta of an anaesthetized wistar rat was dissected in its abdominal portion below the renal arteries. Blood flow was isolated with proximal and distal bulldog vascular clamps and an arteriotomy was made in the most distal part of the isolated segment, before its bifurcation in to illiac arteries. The pre-mounted AAV-*LacZ*-PC-stent/Maverick 2.0 catheter was inserted through the arteriotomy and dilated at 6 atm for 1 minute, to allow complete expansion of stent. The segment of artery containing the stent was excised and maintained in organ culture in SmGM-2 medium (Biowhittaker) supplemented as described in section 2.2 during 2 weeks. A portion of the specimen was taken at day 10th for X-Gal staining and

processed as described in section 2.8 and other piece of artery was taken at day 14 for the same procedure.

2.12 Statistical analysis

For statistical calculations the Microsoft Excel and SigmaPlot 8.0 were used. Data were averaged for observation and expressed as means± SEM or ± SD. Analysis of variance (ANOVA) was use to compare more than one group and Student's t test was used to compare between two groups. A probability value of less than 0.05 ($P<0.05$) was considered as statistically significant in both tests.

Chapter 3

Results

3.1 *In vitro* characterization of AAV-Timp1

3.1.1 Expression of Timp1 by pAAV and rAAV

The rAAV vectors described in this chapter, AAV-LacZ, AAV-Timp1 and AAV-PTX3, were produced from pAAV-LacZ, pAAV-Timp1 and pAAV-PTX3 plasmids, constructed by N. Arsic and S. Zacchigna, by subcloning the *E.Coli LacZ* gene, the human Timp1 and the human long pentraxin 3 (PTX3) cDNAs into pTR-UF5 backbone. The results of cloning and production of the rAAV-Timp1 can be found in detail in S. Zacchigna's degree thesis [280].

As a first step of our study, we tested how efficiently the recombinant hTimp1 protein was produced by the plasmid pAAV-Timp1 and, subsequently, by its cognate recombinant vector, AAV-Timp1. The characterization of the pAAV-Timp1 was performed as a prerequisite for the production of a fully active rAAV-Timp1 vector.

Total cell lysates and supernatants of CHO cells transfected with pAAV-Timp1 were analyzed by Western Blotting using an anti-Timp1 antibody. The presence of a 23 kDa polypeptide band in the total cell lysate, corresponding to non-glycosylated Timp1, and a 28 kDa polypeptide band, only in concentrated supernatant from pAAV-

Timp1 transfected cells, indicates that a properly glycosylated Timp1 was produced, processed and secreted, see Figure 3.1A. This plasmid was then used to obtain a high titer preparation of a corresponding AAV viral vector, according to the procedure described in the chapter 2, section 2.1.2.

This vector (rAAV-Timp1) was used to assess the *in vitro* Timp1 gene expression. rAAV-Timp1 was used to transduce CHO cells. To facilitate permissivity, cells were pretreated with Hidroxyurea (HU) [259]. Total cell lysates and supernatants were analyzed by western blotting using an anti-Timp1 antibody, as described above. The results were reproducible and comparable to those obtained with pAAV-Timp1. A 23 kDa and a 28 kDa polypeptide bands were respectively found in total cell lysate and in concentrated supernatant from rAAV-Timp1 transduced cells. These data demonstrated that rAAV-Timp1 expression levels were adequate and that a Timp1 protein was properly glycosylated, processed and secreted, see Figure 3.1B.

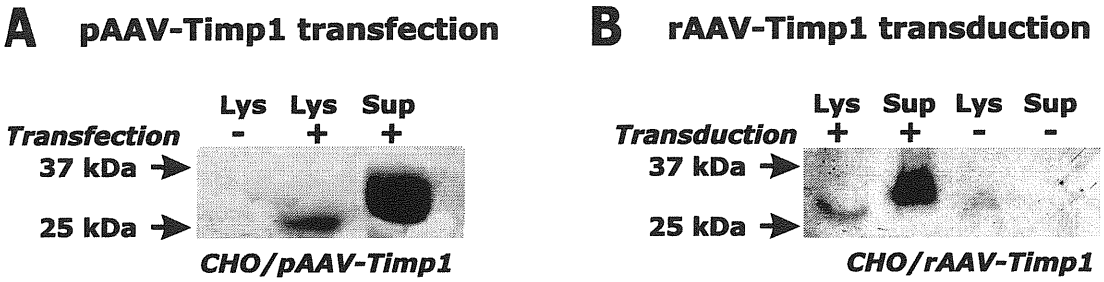

Figure 3.1: **Expression of Timp1 by pAAV and rAAV**: A and B, Expression of Timp1 by transiently transfected and transduced CHO cells by pAAV and rAAV, respectively.

3.1.2 Permissivity of human coronary VSMCs to rAAV vectors

Since the final goal of the present research was to target VSMCs of the artery wall in order to prevent the restenotic process, we checked the actual permissivity of coronary human vascular SMCs to rAAV vectors infection. To this end we generated an AAV vector expressing the GFP reporter gene (rAAV-GFP), starting form the pTR-UF5 plasmid. *In vitro* cultured vascular SMCs were infected with this vector at an MOI

between 100 to 1000, without pretreatment with HU or other DNA damaging agent (usually used in order to increase the transduction efficiency, see section 1.6.2). After 5 days from transduction, cells positive for GFP expression were quantified by cytofluorometric analysis. The results obtained are illustrated in the Figure 3.2. As it can be observed form the cytometry profile in panel B, ~20% of the infected cells express GFP. This level of transduction is expected to have a therapeutic value *in vivo* in an injured artery, considering that the expressed secreted proteins could exert their effect on the surrounding non-transduced cells.

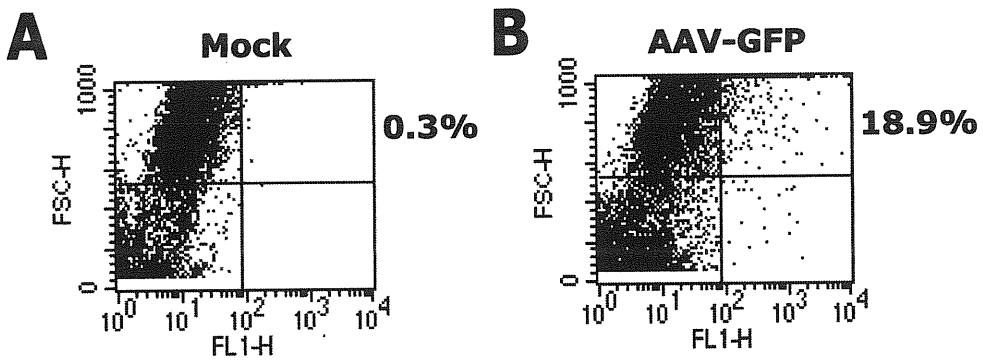

Figure 3.2: **FACS analysis of human coronary VSMCs transduced with AAV-GFP**: A, Shows mock infected VMSCs cells, notice the low background fluorescence, B, Transduction of vascular VSMCs from human coronary artery with high titer AAV-GFP. Cell fluorescence was analyzed by flow cytometry, showing 18.9% of positive cells 5 days after infection (counts in the upper right panel).

Next, the ability of rAAV-Timp1 to transduce human VSMCs *in vitro* was also evaluated by immunocytochemistry with an antibody against Timp1. The treated cells showed intense cytoplasmic positivity, as seen Figure 3.3B,D. The mock transduced SMCs showed a very low reactivity background, since they were human cells with a low level of expression of hTimp1. The finding of Timp1 gene expression at day 5 post-infection is in concordance with the results from rAAV-GFP and FACS analysis. The strong staining pattern could be related to high levels of expression achieved under the influence of a CMV promoter.

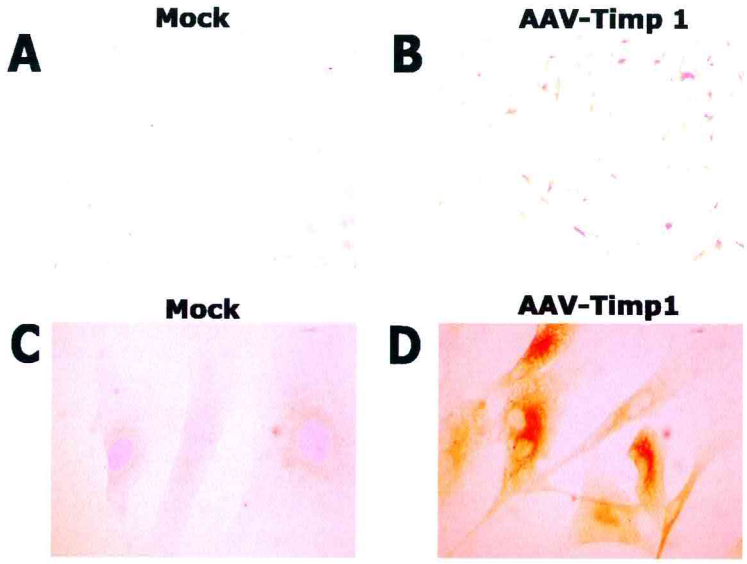

Figure 3.3: **Timp1 overexpression in human coronary VSMCs visualized by immunohistochemistry**: **A** and **B**, The microphotographs at low power filed (10X) show mock infected VSMCs cells (notice the low background staining) and transduction of vascular VSMCs from human coronary artery with high titer AAV-Timp1, respectively. Positivity was evident 5 days after infection. C and D, photographs at 40X. **C**, shows mock infected VSMCs. Again, notice the low background staining, **D**, immunoreactivity on transduced vascular VSMCs showing strong and uniform cytoplasmic expression of Timp1.

3.1.3 Effects of rAAV-Timp1 on migration of VSMCs

The biological functions of Timp1 is the inhibition of MMPs, which are required for cell migration; consequently, overexpression of Timp1 is expected to inhibit the migration of transduced cells. To this end the effect of Timp1 expression in VSMCs was assessed by a chemoinvasion assay, which measures the capacity of cells to degrade a matrigel membrane and to migrate in response to chemoattraction. As shown in Figure 3.4A, SMCs transduced with AAV-Timp1 were significantly inhibited in their ability to invade the matrigel barrier; Timp1 gene transfer induced a 46% reduction in the number of migrated cells (23.5±2.55 *vs.* 41±4.24, P <0.001, n=3). This inhibitory effect on VSMCs migration was previously reported in a similar *in vitro* system using adenoviral vector and rat VMSCs, they showed a reduction of 27% in cell migration [124]. The degree of inhibition obtained in this experiment, despite we expected that only ~20% of cells would be transduced, is in favor of a paracrine effect exerted by the secreted

Timp1.

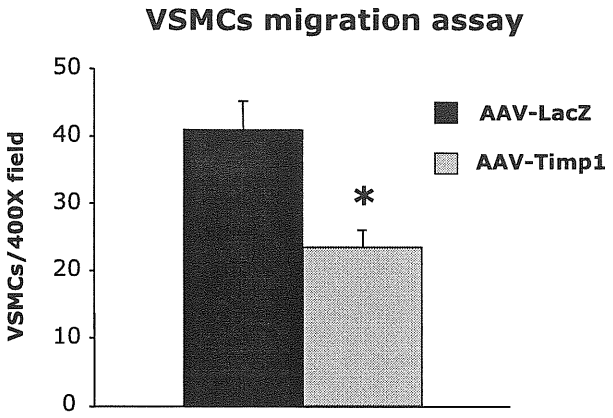

Figure 3.4: **Effect of Timp1 overexpression on SMC migration across a matrigel barrier**: A suspension of VSMCs, transduced with either AAV-*LacZ* or AAV-Timp1, was placed in the upper chamber and medium with chemoattractants was placed in the lower compartment. The bars show the number of cells migrated in response to chemo-attraction. The invasion activity is expressed as the mean number of cells that had migrated per microscopic field (400X) ± SEM for triplicate determinations. The asterisk denotes statistical significance (P=0.0005) in the Student *t*-test.

In vitro inhibition of rat MMPs enzymatic activity

A possible concern for the validity of our experimental strategy was that Timp 1 from human origin could not efficiently inhibit rat MMPs. This consideration prompted us to test the *in vitro* effects of the interaction of these two species. Normal rat arteries were subjected to balloon injury, harvested at day 3 post-injury and kept in organ culture for 3 days. Supernatants from these cultures contained activated MMP-9, as evidenced by a gelatinolytic band at 72kDa in a zymography assay. At the same time pro-MMP9 and activated MMP-2 were observed, see Figure 3.5A. The organ culture supernatants were used for the reverse zymography in which human Timp1 overexpressed by pAAV-Timp1 in HEK 293 cells was loaded. The inhibition of the gelatinolytic activity of MMPs could be appreciated here; all the gelatin of acrylamide-gelatin gel (7.5%/0.6% Gelatin) was digested with the exception of the zone where human Timp1 was present, see Figure 3.5B.

These data demonstrate that Timp1 of human origin displays a full biological activity in a rat animal model.

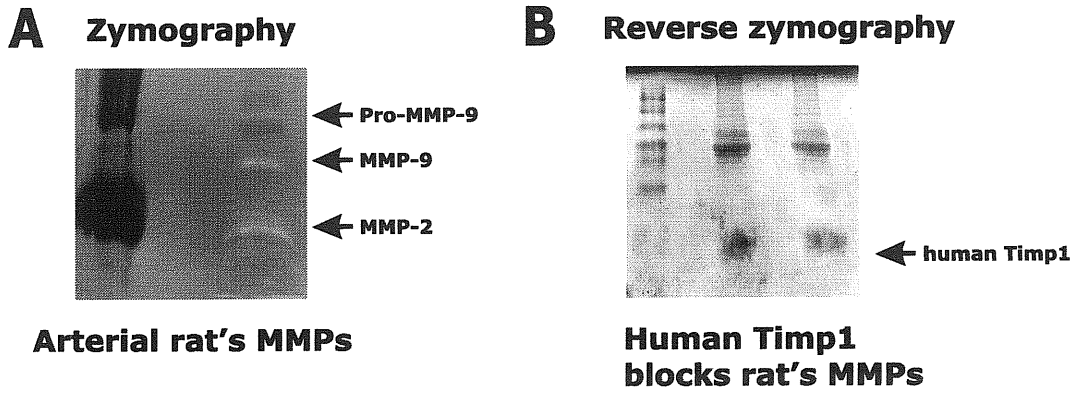

Figure 3.5: **Rat MMPs inhibition by human Timp1**: A, Shows Pro-MMP-9 band at 92kDa, gelatinolytic activity of MMP-9 at 72kDa and MMP-2 at 32kDa identified by apparent molecular weight, B, Overexpression of Timp1 by HEK 293 cells was corroborated and in reverse zymography and it the lack of gelatinolytic activity is evident in the surroundings of human Timp1 migration at 28kDa. The acrylamide-gelatin gel (11% acrylamide:bis-acrylamide 40:1, 0.6% gelatin) was run in a SDS-PAGE electrophoresis.

3.2 *In vitro* characterization of AAV-PTX3

3.2.1 Effects of rAAV-PTX3 on VSMCs proliferation

As an additional therapeutic gene for the prevention of restenosis, we decided to study the role of the human long-pentraxin PTX3 as a fibroblast growth factor 2 (FGF-2) inhibitor in the vascular system. Unpublished results from our collaborators have demonstrated that the addition of recombinant PTX3 to human VSMCs inhibited FGF-2-dependent proliferation. Since FGF-2 is seminal to the pathogenesis of restenosis(1.4.3) and of atherosclerosis(1.3.2) a pAAV-PTX3 and a rAAV-PTX3 vector were constructed. The working hypothesis is that overexpression of PTX3 in the vascular system could target FGF-2 proliferative signals and decrease the proliferation of VSMCs.

3.2.2 Expression of PTX3 by pAAV and rAAV

As we did for Timp1, vector plasmid coding for PTX3 was initially tested for its ability to efficiently produce the recombinant protein. CHO cells were transfected with pAAV-PTX3; total cell lysates were analyzed by Western Blotting using an anti-PTX3 antibody. As expected the presence of a specific PTX3 49 kDa polypeptide band was found only in lysates from pAAV-PTX3 transfected cells. These results indicated that cDNA of PTX3 was cloned in the right frame and that expression levels of pAAV-PTX3 were detectable, see Figure 3.6A.

rAAV-PTX3 was used to transduce CHO cells, after which the total cell lysates and supernatants were analyzed also by western blotting using an anti-Timp1 antibody. The presence of a 49 kDa polypeptide band was found in both total cell lysate and concentrated supernatant from rAAV-PTX3 transduced cells. These results demonstrated that rAAV-Timp1 gave origin to a PTX3 protein that was properly produced, processed and secreted, see Figure 3.6B.

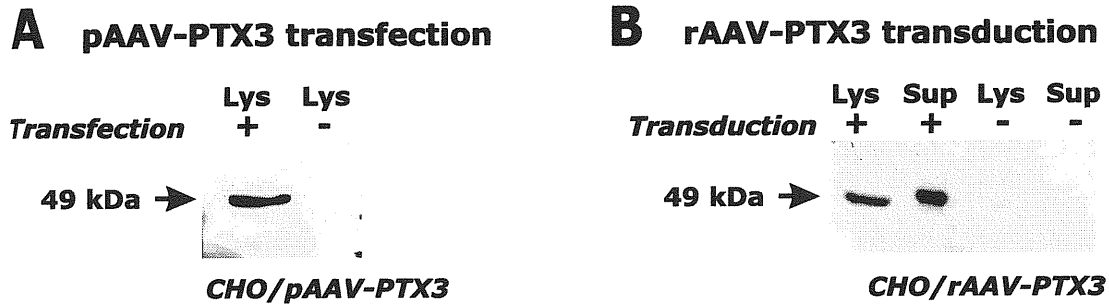

Figure 3.6: **Expression of PTX3 by pAAV and rAAV**: A and B, Expression of PTX3 by transiently transfected and transduced CHO cells.

3.3 *In vivo* characterization of AAV vectors

In the second part of this work the efficiency of the rAAV vectors produced was assessed *in vivo*. We decided to test the efficacy of Timp1 and PTX3 genes in a well-established animal model for restenosis, which is based on the balloon injury in rat carotid. There-

fore, the first steps of our experimental framework were the set-up of the restenosis model and the intravascular delivery using Wistar rats.

3.3.1 Effects of balloon injury

In order to induce a restenotic response, the right carotid artery from an anesthetized Wistar rats was surgically exposed, blood flow was isolated with vascular clamps, balloon catheter was introduced in common carotid and injury was applied at 1.5 to 2 atm for 80 seconds with a PTCA device. In these rat carotid arteries the induction of a remarkable neointimal hyperplasia was reproducibly observed at both 14 and 28 days after balloon injury. Morphometry examination of the cross-section arterial areas of balloon injured and non ballooned revealed a hyperplastic response only in the arteries damaged with the balloon, this neointimal hyperplasia could be quantified by measuring the neointimal area. The neointimal area from 14 to 28 days was increased by 35.17% ($p=0.025$), see Figure 3.7A. The increase in neointimal area was correlated with the increase of intima-to-media ratio in both groups, 14 and 28 days post-angioplasty ($r^2=0.86$ and $r^2=0.7$, respectively, $p<0.0001$), see Figure 3.7C,D. This correlation indicates that there is an enlargement of the vessel size as an outward remodelling in response to injury, see section 1.4.2 and Figure 1.5.

3.3.2 Intravascular delivery

Subsequently, we set up the conditions for the delivery of rAAV vectors to the vessel wall after carotid balloon injury. The carotid artery from Wistar rats was subjected to a balloon injury, following the procedure described above, and then to an intravascular delivery. The intravascular delivery consisted in the intraluminal insertion of a polyethylene cannula tip through the external carotid, loaded with 100μL of either saline solution (PBS) or rAAV-LacZ. This was followed by fixation of catheter tip at the vessel entrance, injection of the loaded solution maintaining the pressure for 40 min-

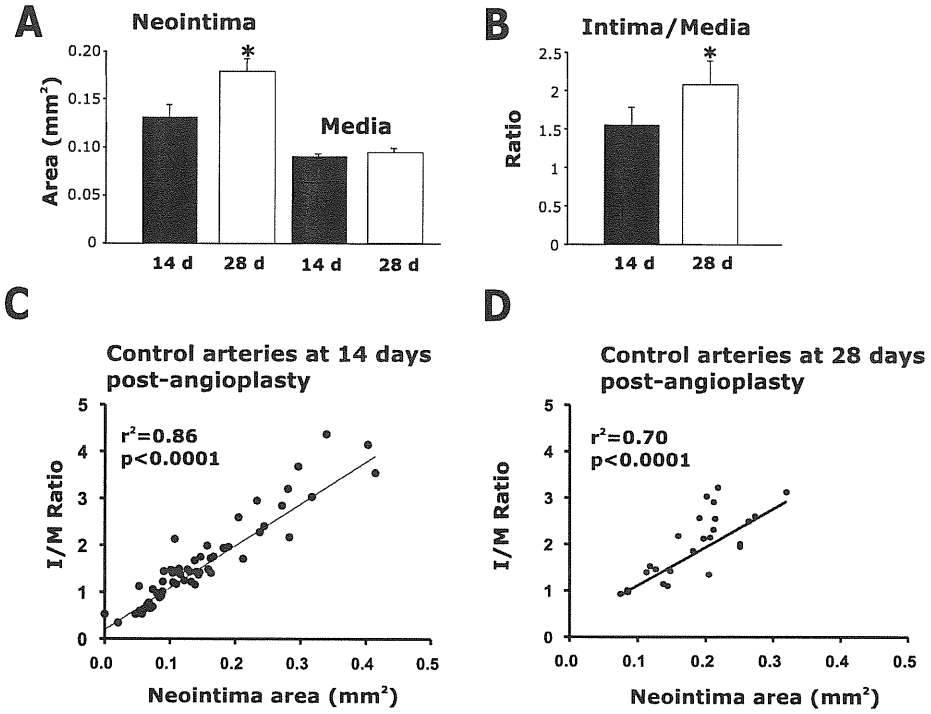

Figure 3.7: **Effects of balloon injury**: **A**, Shows cross-sectional area of neointimal and medial layers at 14 and 28 days, black and white bars, respectively. The neointimal area was increased by 35.17% from 14 to 28 days ($P<0.05$). **B**, The overall changes in the vessel are demonstrated by the Intima/media ratio, the larger is the ratio the more is the restenosis of the vessel, 14 and 28 days after balloon injury (angioplasty), black and white bars, respectively. The intima-to-media ratio was increased by 83% from 14 to 28 days ($P<0.05$). **C,D**, Correlation analysis of intima-to-media ratio *vs* neointimal area at 2(C) and 4(D) weeks post-angioplasty. The larger is the neointimal area the larger is the ratio, this is true only if there are not changes in the vessel size.

utes. The intravascular delivery technique was reproducible and this can be observed in Figure 3.8A, B.

We observed that the reproducibility of the intravascular delivery depended on several critical factors such as the trauma applied to the vessel at the moment of polyethylene cannula insertion, the strength of fixation of catheter tip at vessel entrance and on the equilibration of the pressure applied by a PTCA device connected to a

polyethylene catheter. In rats, a 1.5 cm long segment of carotid artery was isolated and a volume around 10 to 15μL was injected.

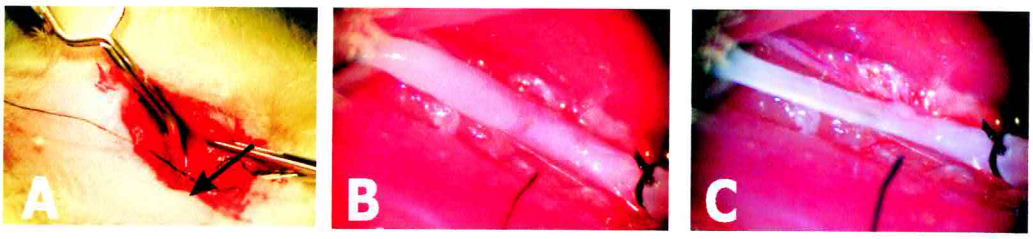

Figure 3.8: **AAV intravascular delivery in rat carotid artery**: A, Delivery at a panoramic view when rat carotid is distended, B, An enlargement of the same procedure to show rat carotid distention under intraluminal pressure, C, show a rat carotid artery empty after 40 minutes of intravascular delivery. Black arrow show the position of the transparent catheter tip with respect to the surgical field.

3.3.3 Efficacy of AAV-*LacZ* infection and transduction after balloon injury

Next, to assess the infectivity and expression of rAAV-*LacZ* in the vessel wall *in vivo*, rat carotid arteries were balloon-injured and exposed to either PBS or AAV-*LacZ* ($1x10^{11}$ viral particles), following the procedure described above. Control and AAV-*LacZ* transduced arteries were harvested at 14 and 28 days after treatment and the carotid segments were divided in proximal and distal segments. Proximal segments were fixed in 0.25% glutaraldehyde, permeabilised, stained in X-gal and embedded in paraffin. Transgene expression was identified by cytoplasmic blue precipitates generated after the X-Gal staining.

Distal segments were fixed in buffered 4% formalin and embedded in paraffin to be further analyzed by fluorescence *in situ* hybridization (FISH). In control and AAV-*LacZ* transduced arteries the presence of rAAV-*LacZ* genomes was analyzed using fluoresence *in situ* hybridization (FISH) using a probe generated from pAAV-*LacZ*. FISH analysis in the rAAV-*LacZ* treated arteries demonstrated strong positive signals in most of the cells of the injured vessel wall, 28 days after injury and delivery, see Figure 3.9A and

C. This observation indicates that rAAV is able to infect neointima and media layers of the vessel wall. The high rate of penetration of rAAVs through the vessel wall could be explained by its small size, ~25 nm, and by the conditions of the vessel at the moment of the delivery. These results suggest that rAAVs have a high rate of infection in an injured artery.

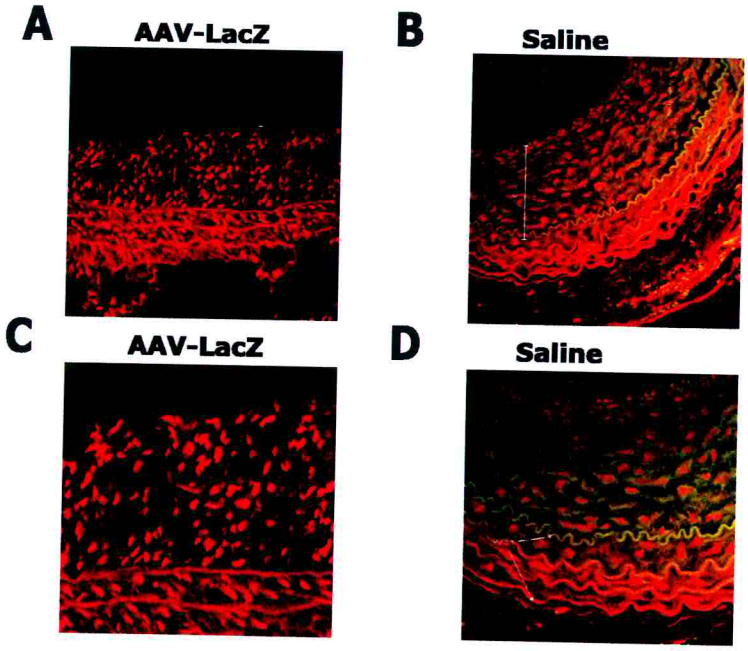

Figure 3.9: **Visualization of rAAV genomes in an artery wall**: **A**, and **C**, Show representative positive signals after FISH for rAAV-LacZ with a ds-DNA digoxigenin labelled probe of 5kb. Intravascular deliveries were performed as described in section 2.5 during 40 minutes. Digoxigenin presence was detected by an anti-Dig antibody labelled with rhodamine. Positive signals appear as red dots in the nuclei. **B** and **D**, show representative photos of negative controls for signals after *in situ* hybridization with the same probe.

In parallel, X-gal staining detected beta-gal expression at 14 and 28 days after treatment. Marker gene expression was found to be already detectable at 14 days after vector delivery and to persist later on, see Figure 3.10A. The expression of the beta-galactosidase transgene was visualized throughout all the arterial wall, with greater intensity of staining in the cells of the neointima, followed by those of the media and the adventitia; see Figure 3.10B and D. The blue staining was specific, since PBS exposed arteries, also fixed and stained by X-gal in the same way, showed no positive

signals.

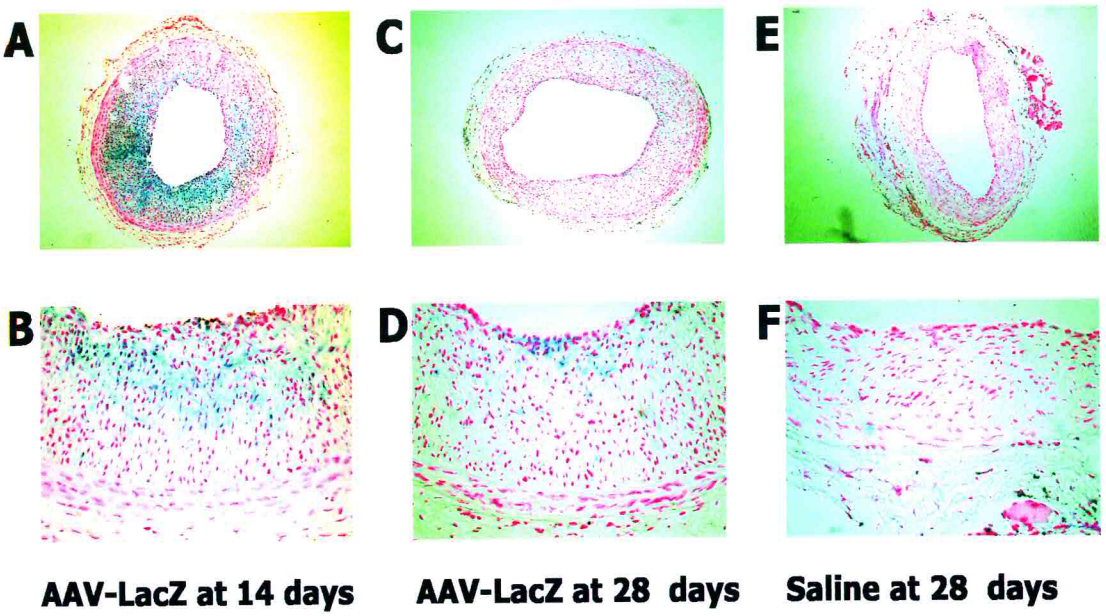

Figure 3.10: ***In vivo* permissivity of AAV vectors:** **A** and **B**, Show strong positivity for X-gal staining demonstrating transducion of rAAV-*LacZ* at day 14 post-injury-delivery, **C** and **D**, show positive signals for X-gal staining in samples taken at day 28 post-injury-delivery. **E** and **F** show controls arteries that were injured, PBS exposed and stained with X-Gal.

Cells populating the neointima were positive for *alpha*-smooth actin indicating their SMC-like phenotype. The same population of cells was also *beta*-gal positive as seen in Figure 3.11A and C. This could be better appreciated in an uninjured artery that was exposed to AAV-*LacZ* and analyzed 14 days post-delivery. In this case X-gal staining was followed by immunohistochemistry for *alpha*-smooth actin and it was possible to observe some cells in the medial layer that are double positives (see Figure 3.11B).

The levels of *beta*-gal staining were much lower than signals obtained from the FISH data. FISH experiments were performed in condition that can not discriminate between ss-DNA and ds-DNA. Therefore, the strong signals observed in infected arteries were most probably secondary to ss-DNA of the AAV-LacZ vector genomes, thus reinforcing the notion that despite the high rate of *in vivo* infections only a small proportion of viral genome becomes transcriptionally active inside transduced cells(1.6.2).

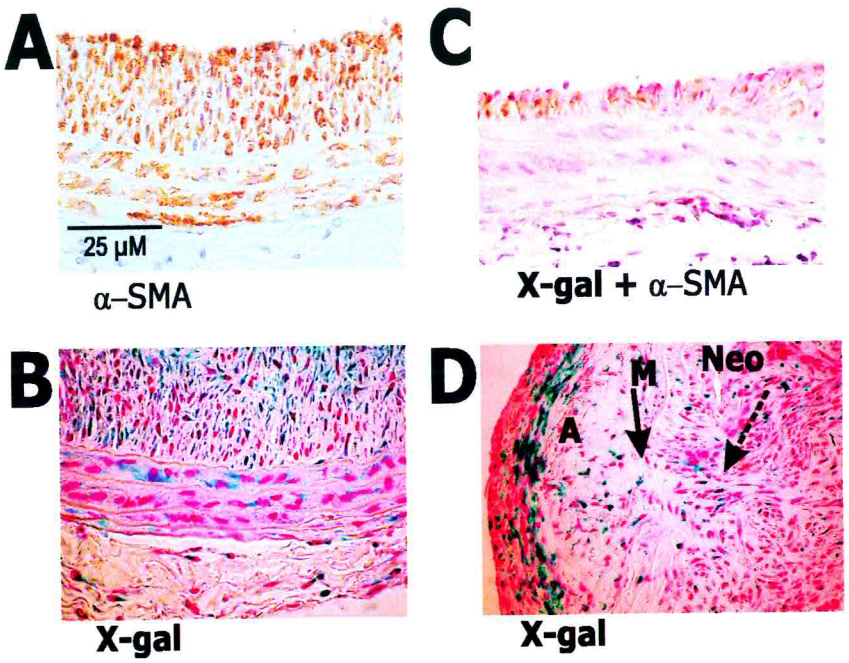

Figure 3.11: **Expression pattern of *beta*-gal**: **A**, Shows a strong positivity for *alpha*-smooth actin in neointima and medial layer, **B**, cells populating the neointima are also positive for X-gal staining, **C**, shows positive signals for X-gal staining and *alpha*-smooth actin in an uninjured artery 14 days post-delivery, **D**, shows strong positive signals in adventitia (A), (M) complete medial rupture (arrow) and a pattern of stellate cells suggestive of migration (dashed arrow) to neointima (Neo).

3.4 Effects of gene therapy

This section presents the results of *in vivo* gene transfer of AAV-Timp1 and AAV-PTX3 to the artery wall. As previously shown in the *in vitro* experiments, AAV-Timp1 was active in inhibiting VSMCs migration and rat MMPs, while AAV-PTX3 also inhibits FGF-2-dependent proliferation in human VSMCs (Rusnati et al., in preparation).

3.4.1 Effects of AAV-Timp1 transduction after balloon injury

The ability of AAV-Timp1 vector to express Timp1 in the damaged arterial wall was assessed *in vivo*. Rat carotid arteries were balloon-injured and exposed to either AAV-*LacZ*, PBS or AAV-Timp1 ($1x10^{11}$ viral particles) for 40 minutes, as above described. In the control rat carotid arteries (AAV-*LacZ* and PBS) the induction of a remarkable

neointimal hyperplasia was reproducibly observed at both 14 and 28 days after balloon injury. Morphometry examination of the cross-section arterial areas revealed that the hyperplastic response was similar between non-transduced arteries (saline) and arteries treated with AAV-*LacZ* (17 animals in total), see Figure 3.13.

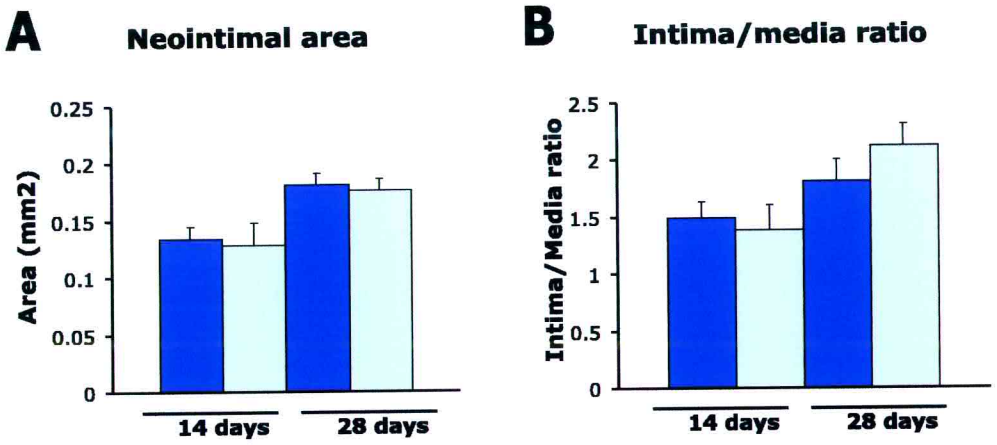

Figure 3.12: **Homogeneous vessel changes in control arteries**: **A**, A similar hyperplastic response after balloon injury in the AAV-*LacZ* treated arteries *versus* the saline treated, light blue and grey bars, respectively. **B**, The similar overall changes in the vessel were demonstrated by similar Intima/media ratios. There was no statistical difference between AAV-*LacZ* and saline treated according to the Student *t*-test

Subsequently, AAV-*LacZ* and AAV-Timp1 transduced arteries were analyzed for the presence of Timp1 expression using a polyclonal anti-Timp1 antibody. The over-expression of human Timp1 after AAV-Timp1 transduction was shown by a strong positivity after immunohistochemistry; no positive signals were present in the rAAV-*LacZ* treated arteries, see Figure 3.9A and B.

The efficacy of Timp1 to prevent neointima formation was then studied in 10 rats that were treated with AAV-Timp1 immediately after balloon injury. The stenotic response was quantified by measuring the intima and media areas of at least four sections per animal. Medial area of injured rat carotids was similar when comparing the control *vs* AAV-Timp1-treated groups at both time points and when comparing the

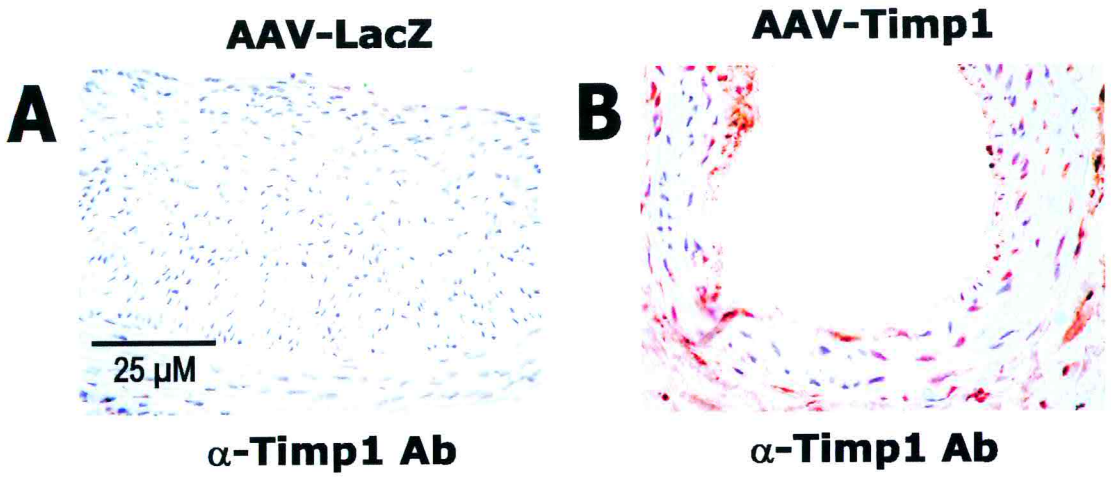

Figure 3.13: **Expression of Timp1 in arteries**: **A**, A hyperplastic response 14 days after balloon injury in AAV-*LacZ* treated arteries with no immunoreactivity, **B**, Shows Timp1 immunoreactivity at 14 days post-injury-delivery, notice the signals throughout the vessel wall.

the control at 14 days vs control at 28 days. However, in the AAV-Timp1 groups medial area was a decrease by 15% (0.114±0.005 *vs* 0.0974± 0.004 mm^2, $P < 0.05$) from 14 to 28 days when compared within the same group (Figure 3.14B). The neointimal area of the AAV-Timp1-treated group was reduced by 55.3% and by 51.9% at 14 and 28 days when compared to controls, respectively (0.132±0.01 *vs* 0.059± 0.006 mm^2, $P < 0.0001$ and 0.179± 0.012 vs 0.086± 0.013 mm^2, $P < 0.0001$; Figure 3.14A). The intima-to-media ratio, which is a more sensitive parameter for assessing relative restenotic changes, is reported in Figure 3.14C. This ratio was significantly lower in the Timp1-treated group at both 14 days (0.46±0.16 *vs.* 1.56±0.22; P= 0.0001) and 28 days (0.86±0.22 *vs.* 1.97±0.24; P=0.003) after treatment. These values correspond to 70.5% and 58.5% reduction of intima-to-media ratio, respectively. Representative images of AAV-Timp1 treated arteries can be seen in Figure 3.15. In the AAV-Timp1-treated groups neointimal area was not significantly increased (0.0861± 0.013 mm^2*vs* 0.059± 0.006 mm^2, P=NS) from 14 to 28 days. However, in the same group the inhibition of intima-to-media ratio dropped 12% (70.5% vs 58.5%), the difference in the intima-to-media ratio was significant (P=0.01).

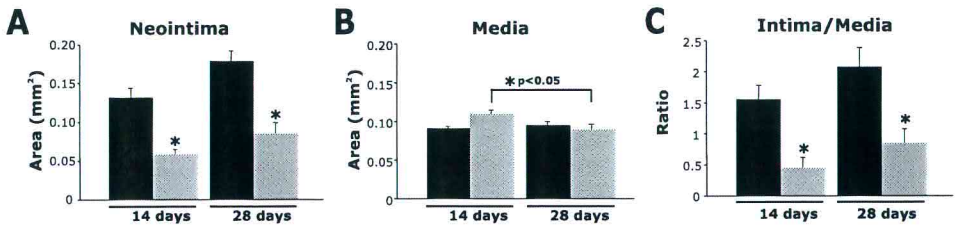

Figure 3.14: **Inhibition of intimal hyperplasia by AAV-Timp1**: **A**, Inhibition of neointima formation by AAV-Timp1 at 14 and 28 days after injury. Arterial morphometrical analysis was performed in 11 and 6 animals (treated with AAV-LacZ/saline) at 14 and 28 days (black bars), respectively, and in 5 animals per group at 14 and 28 days in animals treated with AAV-Timp1 (white bars), respectively. **B**, Shows the average of medial layer cross-sectional area, no differences were observed between controls, whereas within the AAV-Timp1 groups medial area was a decrease by 15%, **C**, Shows the reduction of the intima/media ratio by 70.5% and 58.5% in the AAV-Timp1-treated groups at both 14 and 28 days, when compared to controls, whereas within the same group the inhibition of the intima-to-media ratio dropped 12%. The values are showed as means ± standar error measurement(SEM) . Medial areas and intima/media ratios were evaluated at least in three sections per animal. The asterisk denotes statistical significance ($P<0.05$) after using an unpaired Student t-test.

Modulation of extracellular matrix composition by AAV-Timp1 transduction

It is known that MMPs inhibition by non-specific inhibitors have effects on collagen synthesis and degradation [285] and that Timp1 overexpression affects at a postranslational level elastin metabolism [128]. Therefore we explored the extracellular matrix composition in the AAV-Timp1 treated and control animals. For this purpose, cross-sections of rat carotid arteries at 14 and 28 days after injury were stained with the Azan-Mallory and Weigert-Van Gieson techniques, which reveal collagen and elastin content, respectively. The content of the matrix was evaluated in a semi-quantitative way by software image analysis (ImageJ NIH). Representative images of Azan-Mallory and Weigert-Van Gieson staining can be seen in Figures 3.16 and 3.17.

It was found that in AAV-*LacZ*-treated animals, collagen occupied 83.5% ±1.28 of the neointimal layer at 14 days after transduction. Collagen deposition did not

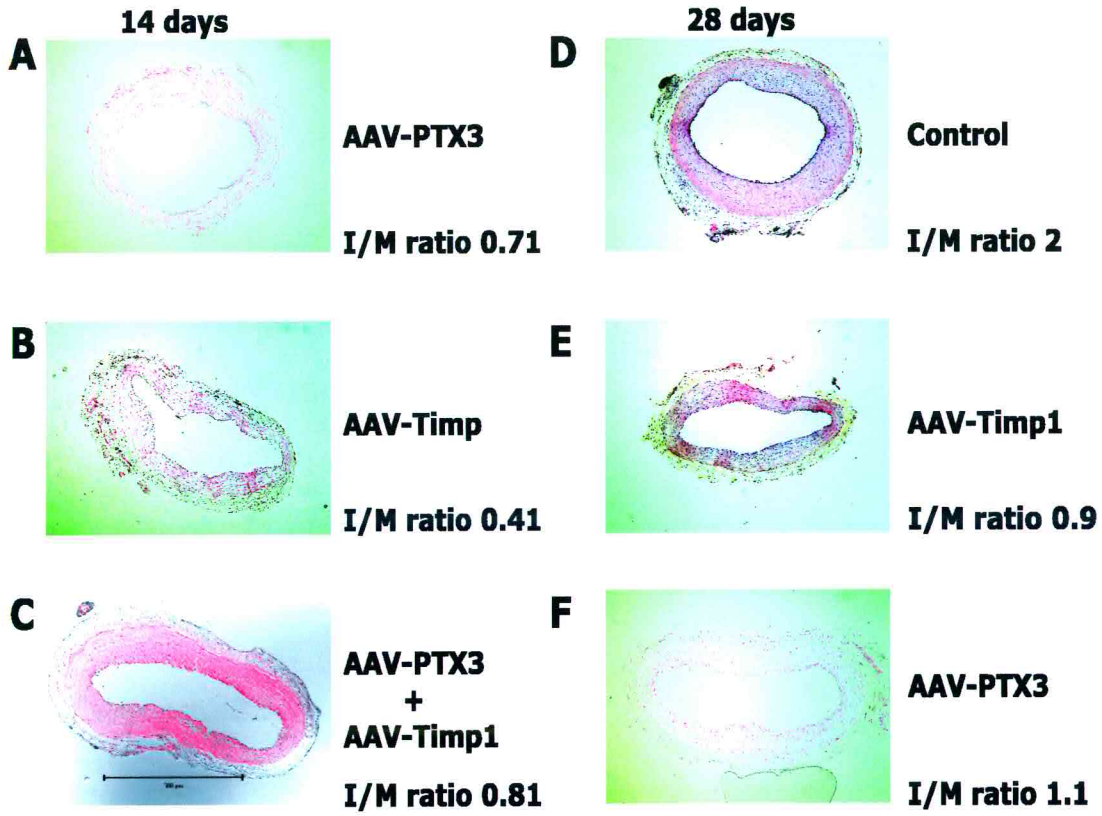

Figure 3.15: **Representative images of AAV-Timp1 and AAV-PTX3 treated arteries:** **A**, A representative image of the effect achieved by AAV-PTX3, **B**, A representative image of the effects achieved by AAV-Timp1, **C**, A representative image of the effect obtained by AAV-PTX3 and AAV-Timp1. All the images are from treated arteries at day 14 and beside each image the I/M ratio of the image that corresponds with the average of each respective group is shown. **D**, Shows a representative image of the hyperplastic response obtained in a control artery, **E** and **F**, show images of AAV-Timp1 and AAV-PTX3, respectively, from treated arteries at day 28. In this case the I/M ratio that corresponds with the average of each respective group are also described. Scale bar corresponds to 500μm

change significantly over a 2-week period in this control group (73.7%±6.49 at day 28; P= NS). In contrast, collagen content in the AAV-Timp1-transduced arteries was decreased by 22.9% and 42.6% at 14 and 28 days, respectively (83.5%±1.28 *vs.* 64.8% ±3.92; P= 0.009 and 73.7% ±6.49 *vs.* 42.2% ±7.64; P= 0.03; the decrease between 14 and 28 days in the AAV-Timp1 group is also statistically significant; P<0.01). These results demonstrate an important effect in modulation of collagen deposition by AAV-Timp1 transduction, see Figure 3.18C. No significant differences were found in collagen content in medial layers, see Figures 3.18A.

In contrast to collagen, elastin fibers, as evaluated after staining with Weigert-

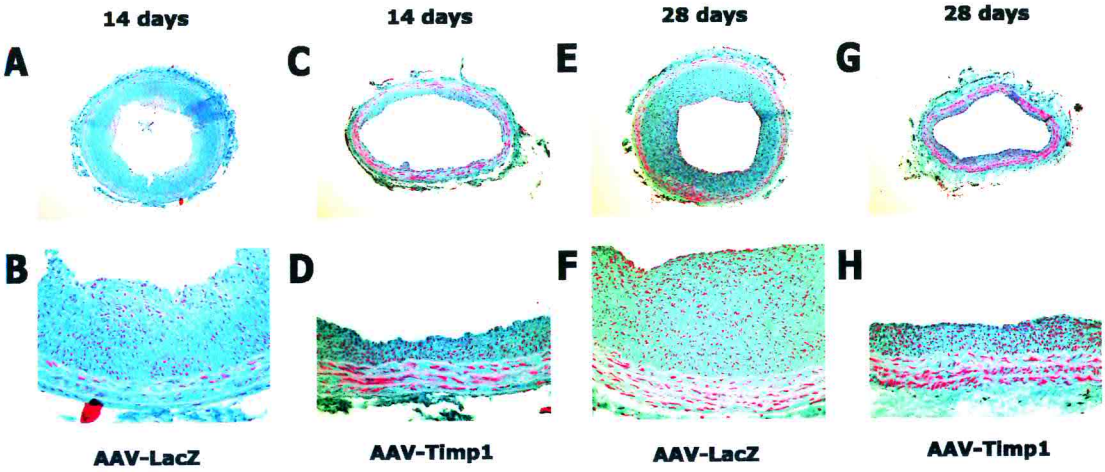

Figure 3.16: **Azan-Mallory stainings for AAV-Timp1 treated and control arteries:** **A**, and **B**, Show representative stainings for Azan-Mallory of AAV-*LacZ* treated arteries to be compared with **C** and **D** that are representative of AAV-Timp1 treated arteries, at 14 days after injury. **E** and **F**, show representative stainings for AAV-*LacZ* treated arteries to be compared with **G** and **H** that are representative of AAV-Timp1 treated arteries at 28 days. Microscope enlargement is 10X for the upper and 40X for the lower panels. In this staining, collagen appears in blue and nuclei and elastin in cyan.

Van Gieson, were found to be more abundant in the neointimal areas of the AAV-Timp1 transduced arteries with respect to those treated with AAV-*LacZ* at both 14 (16.5%± 1.36 *vs.* 26.9% ±4.46 of neointima; P= 0.01) and 28 days (23% ±4.4 *vs.* 42.3% ±10.59; P= 0.04, this difference represents an increase by 63.1% and by 84%, respectively), see Figure 3.18D. As for collagen, the elastin content within the media was similar at both time points in both treated and control arteries Figure 3.18B. Taken together, these observations suggest that the reduction of neointimal thickness determined by MMP inhibition after AAV-Timp1 transduction is paralleled by the inhibition of extensive collagen accumulation and the promotion of elastin deposition in the neontimal lesion.

3.4.2 Effects of AAV-PTX3 transduction after balloon injury

As a next step of this study we evaluated the efficacy of rAAV-PTX3 in 10 rats, 5 rats were sacrificed at both 14 days and 28 days post-injury and delivery. Moreover, we also explored the additive and/or synergistic effects of AAV-Timp1 and AAV-PTX3 in

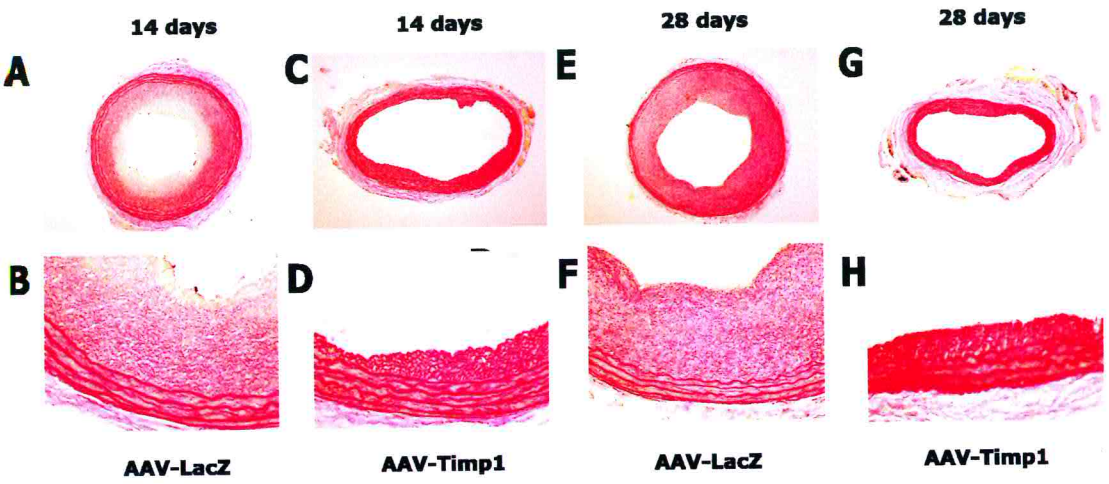

Figure 3.17: **Weigert-Van Gieson stainings for AAV-Timp1 treated and control arteries:** **A**, and **B**, Show representative stainings for Weigert-Van Gieson of AAV-*LacZ* treated arteries to be compared with **C** and **D** that are representative of AAV-Timp1 treated arteries, at 14 days, **E** and **F**, show representative stainings for AAV-*LacZ* to be compared with **G** and **H** that are representative of AAV-Timp1 treated arteries at 28 days. Microscope enlargement is 10X for the upper and 40X for the lower panels. In this staining the collagen appears in red and elastin in dark blue.

8 rats, all sacrificed at 14 days post-injury and delivery.

Immediately after balloon injury, rAAV-PTX3 or an equimolar mixture of the two vectors (rAAV-PTX3 and rAAV-Timp1) was delivered into the injured arteries. The rationale of this experimental strategy would be to block at the same time the two most important axes of restenosis, the migration (MMPs-dependent) and the proliferation (FGF-2 dependent) of SMCs. Two rAAV vectors are able to transduce the same cell at a high MOI and to persist as circular episomes [270, 286] after intermolecular concatamerization, by head-to-tail recombination. These properties allow the delivery of multiple recombinant vectors *in vivo* and transgene expression of more than one therapeutic gene product by the same cell.

The hyperplastic and stenotic response were quantified in the same manner as for AAV-Timp1. To compare the effects of PTX3 with those of AAV-Timp1 the same controls were used, composed of AAV-*LacZ* and saline treated animals.

Medial area of injured rat carotids was similar when comparing between controls

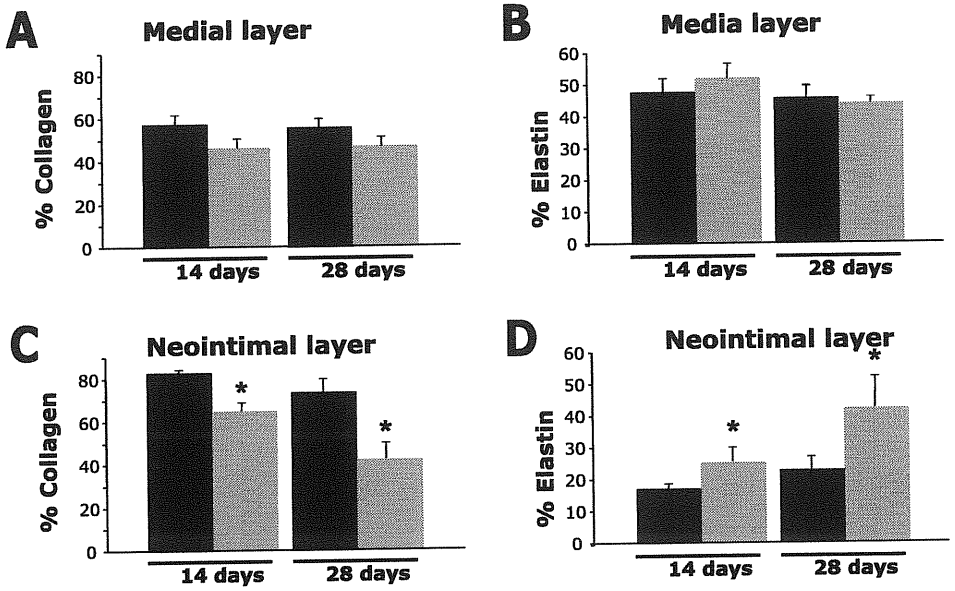

Figure 3.18: **Collagen and elastin quantification**: **A**, and **B**, Show the relative amount of collagen and elastin in the medial layers, respectively, expressed as percentage of the layer. **C**, shows the quantification of collagen content in the neointimal layer in AAV-LacZ treated arteries and AAV-Timp1 treated arteries, **D**, shows elastin content in the neointimal layer of same groups, % of content is expressed as mean values and SEM. The asterisk denotes statistical significance between AAV-Timp1 and AAV-*LacZ* treated arteries (P<0.01) according to the Student *t*-test.

(14 days *vs* 28 days), as reported above. On the contrary, medial areas of AAV-PTX3-treated group and AAV-Timp1/AAV-PTX3-treated group at 14 days were increased by 29.4% and 24% when comparing their the control, respectively (0.1174±0.005 and 0.1133±0.004 *vs* 0.0907± 0.002 mm^2, $P < 0.0001$), medial area of AAV-PTX3-treated group at 28 days increased by 19.8% when compared with the control (0.1141±0.003 *vs* 0.0952± 0.004mm^2, $P < 0.0001$)(Figure 3.19B). The neointimal area of the treated groups was reduced by 36.5% and 34% at 14 days (AAV-PTX3 and AAV-Timp1/AAV-PTX3) and by 31.2% at 28 days in AAV-PTX3 group (0.132±0.01 *vs* 0.084± 0.02 mm^2 and 0.087± 0.02 mm^2, $P < 0.0001$ and 0.179± 0.012 vs 0.123± 0.02 mm^2, P<0.05; Figure 3.19A). The intima-to-media ratio, which is a sensitive parameter to assess relative changes in the overall vessel, is reported in Figure 3.19C. This ratio was significantly lower in the PTX3 group at both 14 days (0.66±0.09 *vs.* 1.56±0.22; P= 0.0001) and 28

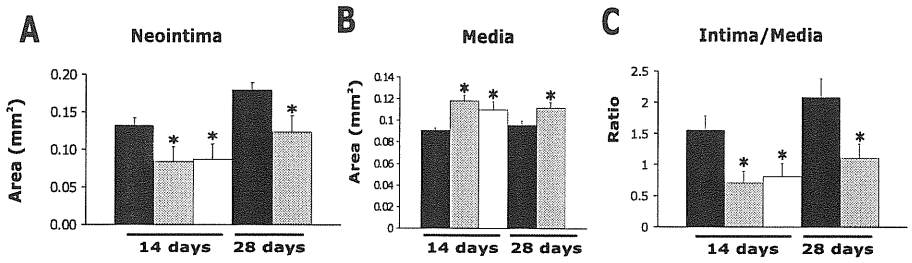

Figure 3.19: **Inhibition of restenosis by AAV-PTX3**: **A**, Arterial morphometry analysis was performed in 11 and 6 control animals (treated with AAV-*LacZ*/saline) at 14 and 28 days respectively (black bars), and in 5 animals per AAV-PTX3 group at 14 and 28 days (grey bars), and 8 animals per AAV-Timp1/AAV-PTX3 at 14 days (white bar). A reduction of neointima formation by 36.5% and 34% can be observed in AAV-PTX3 and AAV-Timp1/AAV-PTX3 groups at 14 days after injury, AAV-PTX3 reduced neointima area by 31.2% at 28 days post-injury. **B**, Shows the average of medial layer cross-sectional area, at 14 days medial areas increased by 29.4% and 24% in AAV-Timp1 and AAV-Timp1/AAV-PTX3 groups, respectively, whereas at 28 days medial areas increased by 19.8%. **C**, Shows the reduction of the intima/media ratio by 57.7% and 43.6% in the AAV-PTX3 treated groups at both 14 and 28 days, respectively, and by 48.07% in the AAV-Timp1/AAV-PTX3 treated group. The values are showed as means ± standar error measurement(SEM) . Medial areas and intima/media ratios were evaluated at least in three sections per animal. The asterisk denotes statistical significance ($P<0.05$) after using a Student *t*-test.

days (1.11±0.32 *vs.* 1.97±0.24; P=0.003) after treatment. These values correspond to 57.7% and 43.6% inhibition of stenosis, respectively. In the AAV-Timp1/AAV-PTX3 group at 14 days (0.81±0.21 *vs.* 1.56±0.22; P< 0.0001) this value corresponds to a 48.07% inhibition of stenosis. Representative cross-sections of AAV-PTX3 at 28 days and AVV-PTX3 or AAV-Timp1/AAV-PTX3 treated arteries at 14 days after transduction are shown in Figure 3.15.

Chapter 4

Discussion and Conclusions

4.1 AAV-Timp1 and AAV-PTX3 modulate VSMCs behavior

The experimental work presented in this thesis demonstrates the feasibility of the use of recombinant AAV vectors for the delivery of therapeutic genes to vascular SMCs and undelines the effectiveness of the overexpression of Timp1 and PTX3 genes for the prevention of restenosis.

Adeno-associated viral vectors are currently the most useful gene therapy vectors for *in vivo* gene therapy. The appealing features that render them so attractive include the broad host range infectivity, the efficiency in transducing many cell types *in vivo*, including muscle, liver and brain [227, 228, 229, 230, 231, 232], and the absence of induction of inflammatory reaction [219] since vectors keep less than 10% of the viral genome and do not code for viral proteins. These advantages over other vectors such as Adenovirus are highly appreciated when stable and long-term expression is aimed. AAV vectors have been able to sustain expression of the transduced gene for long periods of time up to more than 4 years [220]. Given all these considerations we decided to exploit AAV vectors for gene delivery to the arterial wall aiming at the prevention of restenosis

using an experimental rat model. As a strategy to counteract the development of neointima following balloon injury, we targeted two pathways known to be important for restenosis, SMCs migration and proliferation.

We have tested the overexpression of Timp1 and PTX3 proteins *in vitro*, as a preliminary part of this strategy to treat restenosis in an experimental model. Data from collaboration demonstrated that AAV-PTX3 transduce human coronary VSMCs and impairs FGF2-dependent proliferation. Timp1 and PTX3 have the advantage that both proteins are actively secreted and thus harbor paracrine properties. The paracrine property of the gene products is desirable in a complex system such as in an animal experimental model. Any model harbors intrinsic variabilities, first in the rate of transduction between animals and second in the technique of intravascular delivery. The principal advantage is that even in conditions where optimal transduction can not be achieved, neighboring cells, that were not transduced, would still be exposed to the therapeutic protein.

Here we show for the first time the effects of a rAAV-Timp1 on migration of human VSMCs. Our experiments have showed the *in vitro* efficacy of recombinant AAV vectors to transduce primary human coronary vascular smooth muscle cells as was clearly demonstrated by FACS analysis and immunohistochemistry. When we tested the for the prevention of VSMCs migration we found different levels to those reported in the literature (46% vs 27%) [124]. This means that the ability of rAAV-Timp1 on preventing VSMCs migration was 19% better than the one found using adenoviral vectors overexpressing Timp1 on rat VSMCs.

We believe that the differences observed with the results reported by Dollery et al could be related to a different efficiency on cell transduction ($\sim$20%) and to a difference in the cell system employed, rat VSMCs vs human coronary VSMCs. Recently it has been shown that SMCs isolated from the aortic arch (ASMCs) displayed a greater capacity for inducible proliferation and migration than paired cultures of femoral artery

SMCs from the same animal, and this difference was secondary to a distinct regulation of mitogen-activated protein kinases and p27Kip1 [287].

The paracrine property exerted by Timp1 *in vitro* can be exemplified by the case of migration experiments where transduction efficiency of ~20% of cells was not proportional to cells that were prevented from migration.

In parallel to the studies of rAAV-Timp1 effects on migration, the *in vitro* inhibition of the gelatinolytic activity of MMPs produced by injured rat carotids was also demonstrated. This result is in concordance with other reports using human Timp1 to block rat VSMCs migration *in vitro* and *in vivo* [124]. The present results support the use of the rat model of restenosis to further investigate the *in vivo* effects of AAV-Timp1.

We conclude that our results indicate that primary human vascular SMCs are permissive to AAV transduction *in vitro*, rAAV-Timp1 vector is highly active in preventing cell migration-invasion, human Timp1 is able to inhibit rat MMPs and that rAAV-PTX3 vectors is highly active in preventive FGF2-dependent proliferation.

4.2 Arteries are permissive to rAAV infection and transduction

AAV has been successfully used to transduce cells of the cardiovascular system *in vitro* and *in vivo*, including rat myocardial cells in culture, rat and pig myocardium [274], human umbilical vein endothelial cells (HUVEC) *in vitro*, and endothelial (EC) and vascular smooth muscle cells (VSMCs) *in vivo* in non-injured rat carotid arteries [275, 276], and in medial and adventitial cells in injured rat carotid arteries [277]. Additionally, rAAV has also been able to transduce adventitial microvessels of non-human primate atherosclerotic arteries [278].

The reproducibility of the models of arterial injury and of intravascular delivery

used in this work were ensured before exploring the efficiency of rAAVs on infection and transduction. The advantages of the rat angioplasty model include the easy access to common carotid, since the diameter of this vessel in rat is sufficiently large to perform an intravascular delivery without the aid of a stereomicroscope. After the balloon injury there is a rapid formation of a neointimal lesion, this lesion is highly reproducible and readily observed by routine histology as soon as 14 days after injury. This model is optimal to study targets that modulate cellular proliferation and migration. However, as in other animal models the rat model of restenosis presents also limitations. The vessel used for the study is initially healthy, and even after experimental induction of hyperlipidemia there is no change in the evolution of the lesion [43]. Indeed, the use of an atherosclerotic small animal model would facilitate the study of the effects of angioplasty and experimental therapies in more realistic conditions. The proliferative response in the rat arteries after injury is much higher than that observed in human vessel lesions, where VSMCs proliferation does not represent the dominant mechanism of restenosis.

The results obtained in this thesis suggested that under optimal conditions of intravascular delivery, recombinant AAV vectors are able to efficiently infect the cells of the vessel wall after balloon injury. The critical parameters to be maintained for a successful AAV intravascular delivery include; the induction of minimal trauma when the polyethylene cannula is inserted into the vessel, avoidance of excessive strength in the suture knot used for the fixation of the catheter tip at the vessel entrance and on the equilibration of the pressure applied by a PTCA device.

We used a vector encoding for the *LacZ* reporter to demonstrate the extent of infection with AAV and the efficiency of the trangene expression. *In situ* hybridization for vector genome sequence allows the identification of specific AAV genome sequences, these signals were widely distributed through the wall of treated arteries.

In parallel, also the expression of the beta-galactosidase could be visualized

throughout the arterial wall, with the greatest intensity of staining in the cells of the neointima. This finding was in contrast with what reported by other studies, were the expression of the transgene was reported to be restricted only to certain areas of the vessel wall [275, 276, 277, 278, 279].

However, in our hands the overall efficiency of transduction varied widely, from 10% to 50% of the entire vascular wall, which is in agreement with a recent study which reported 58% of transduction in optimal conditions [279]. This variability may be secondary to differences in the conditions of the intravascular delivery, the extent of balloon injury and the cell types infected at the moment of injury when neointimal cells are not present.

The level of transduction efficiency, judged by the level of X-gal staining, was lower than the infection efficiency, judged by the level of FISH signals. This difference was not surprisingly since is known that despite the high rate of *in vivo* infections only a small proportion of viral genome becomes transcriptionally active inside transduced cells (see 1.6.2).

In our samples, the pattern of localization of β-gal corresponded with the sites of maximal damage, in agreement with a recent study [277]. Since neointima is in part generated by migration and proliferation of SMCs in response to injury, it seems that the high concentration of the vector genome and transgene expression in this layer of vessel wall could be explained by the infection of a progenitor cell during the injury. The hypothesis of the existence of a resident (local) progenitor/stem cell that migrates and give rise to a cell population that differentiates into neointimal cells is supported by reports that describe myofibroblast-like cells resident in the adventitia [54]. These cells harbor characteristics of stem cells and are able to migrate even from distant sites and to form part of the neointima after an injury [54]. It is probable that we infected also these myofibroblast-like cells, since we demonstrated a strong beta-gal positivity in the adventitial layer. Injury caused damage in the endothelium and abolished the first

anatomical barrier for vector diffusion. Thanks to the small size of AAVs ($\sim$ 25nm,), to the disruption of layers such as internal elastica lamina (IEL) and to the good internal pressure to which damaged carotids were exposed, rAAVs could reach the adventitia.

In conclusion, we set up an efficient method to deliver intravascularly the AAV vectors in rats and we were able to evaluate the infectivity and expression of AAV-*LacZ* by X-gal and FISH techniques. From our *in vivo* AAV permissivity experiments we can support the notion that AAV vectors are efficient tools to deliver genes to the arterial wall by single intraluminal bolus. The efficiency of AAV vectors for gene transfer to the damaged arterial wall was lower than that obtained by using first generation adenoviral vectors, but this is largely outweighed by the lack of undesirable inflammatory effects and the long-term expression of the therapeutic genes [219, 288]. Additionally, we conclude that the rate of *in vivo* transduction observed was satisfactory, especially when the transferred gene encodes a secreted protein (such as Timp1 and PTX3), which exerts effects not only on transduced cells, but also on neighboring cells that might not have undergone gene transduction.

Thus, AAV vectors are not only of interest for their potential therapeutic applications, but also represent valuable tools to assess the *in vivo* effects of gene overexpression. The possibility to deliver and express a suitable gene within the arterial wall for prolonged periods of time might facilitate the molecular understanding of the disease process and the implementation of new therapeutic strategies without systemic side effects.

4.3 AAV-Timp1 and AAV-PTX3 exert beneficial effects on injured vessels

Since AAV vectors can infect cells at high MOI it is feasible to design therapeutic strategies for the simultaneous delivey of multiple therapeutic genes in the same cell.

The main goal of the work presented in this thesis was the evaluation of the potency of two different strategies used to counteract the development of restenosis following angioplasty. To this end, we targeted two fundamental steps in the progress of the restenotic phenomenon, namely the migration and the proliferation of smooth muscle cells of the arterial wall. We selected two genes, Timp1 and PTX3, which act by inhibiting MMPs activity and FGF2-mediated proliferation and their individual or synergistic effect was evaluated *in vitro* and *in vivo*, respectively.

The morphometry results obtained from injured arteries, at 14 or 28 days after delivery of AAV-Timp1 showed a significant reduction on neointimal hyperplasia with respect to controls (-55.3% and -51.9%) and a clear reduction of the neointima to media ratio (-70.5% and -58.5%), respectively. The reduction of neointimal hyperplasia in comparison with controls was similar at both time points (14 and 28 days) whereas the total area of the neointimal layer was not significantly increased from 14 to 28 days in the AAV-Timp1 treated group. However, Timp1-mediated reduction of the intima-to-media ratio was not preserved at 28 days, where the inhibition decreased by 12% (p=0.01). The unfavorable values of intima-to-media ratio at our experimental later time point is explained by the significant decrease in medial area from 14 to 28 days (15%), in contrast the neointimal area remained unchanged.

Our data suggest that although the presence of Timp1 overexpression reduced neointima formation to a great extent, the sole reduction of neointima over the time is not sufficient to compensate the lack of proper outward remodelling. The decrease of medial area could be secondary to vessel shrinkage or in other words inward remodelling. The poor effect at 28 days is probably secondary to Timp1 inability to modified other relevant mechanisms that are involved in proper geometrical remodelling.

In this context, the inhibition of intimal hyperplasia in injured rat carotid arteries by AAV-Timp1 underscores the importance of extracellular matrix remodelling in the pathogenesis of this process (reviewed in refs [289, 21]). This result is consistent

with biochemical studies that have revealed MMP overexpression after coronary angioplasty [290] or other procedures that have damaged the vascular endothelium [291, 292]. Recent genetic studies have also highlighted the role of MMP2 and MMP9 polymorphisms on the rate of restenosis [293]. Moreover studies performed in MMP9-knock out animals have demonstrated that MMP9 is essential for adequate geometrical remodelling and SMCs replication [19, 18]. The therapeutic role of pharmacological inhibition of MMP activity on the stenotic process further underlines a critical involvement of MMPs in restenosis [133, 294, 295].

In contrast to systemic therapy with unspecific inhibitors of MMP activity in the minipig model, which were shown to affect constrictive arterial remodelling but not neointima formation [133], we observed that the local overexpression of Timp1 in the arterial wall markedly reduced neointimal fromation. This effect might be related to the advantages of local gene delivery and expression as compared to systemic treatment, as well as to inhibition of MMP9 by Timp1. What is the actual molecular mechanism by which local overexpression of Timp1 in the arterial wall reduces neointimal formation? Timp1 could exert its effects through other MMP-independent mechanism. Baker et al [106] has proposed that in some cell types, Timp1 and Timp2 may have receptors directly linked to intracellular signalling pathways regulating cell behavior. In fact, recently Timp2 has shown anti-angiogenic effects non related with MMPs inhibiton [296] and Timp3 has shown to inhibit angiogenesis through the blocking the binding of VEGF to its receptor VEGFR2 [297]. These findings open the possibility that Timp1 could also modulate cell behavior through unknown survival/death signals [106]. However, the understanding of the exact mechanism by which Timp1 leads to the reduction of restenosis has not been clarified yet.

Other experimental evidences indicates that MMPs are overexpressed in the early phases of the stenotic process and that their activity is essential for neointima formation [298, 133, 118]. Up-regulation of MMP expression - especially of MMP2 and

MMP9 - was shown to be even higher after stent implantation than after balloon angioplasty [298]. In this respect it is worth noting that restenosis and constrictive remodelling are positively correlated with endothelial dysfunction and collagen accumulation, whereas elastin density is inversely correlated with neointimal growth [283]. Consistent with these findings, Strauss et al. have also observed that collagen synthesis and degradation was altered in a double-balloon injury model in normo-lipemic rabbits, and that pharmacological inhibition of MMPs resulted in diminished collagen accumulation [285].

We observed that AAV-Timp1 treatment altered the normal turnover of collagen and elastin, this modulation of the extracellular matrix metabolism (ECM) was towards a decreased of collagen deposition and an increase in elastin content at 14 and 28 days after AAV-mediated Timp1 gene transfer. This is in agreement with the observations, as well as with the conclusions of the work of Forough et al., who have shown that local overexpression of Timp1 increases elastin accumulation through a modification of post-translational processing mechanisms [128]. Most likely, the overall outcome of the modifications induced by Timp1 overexpression is the reduction of passive tensile strength (less collagen) and the maintenance of the elastic properties of the arterial wall (more elastin). The activity of MMPs is essential to permit the SMC migration and invasion of the neointima, which is also confirmed by the results of the *in vitro* chemoinvasion assay. In addition, MMPs might also bear a direct impact on the extent of replication of SMCs, as was recently shown by studying the proliferation of these cells in MMP9 - knock out mice at day 8 post-injury [18]. In our *in vivo* experiments we observed that Timp-1 gene transfer did not modify the the fraction of proliferating cells, as inferred by reactivity to PCNA immunostaining (data not shown). This finding was probably influenced by the time points (14 and 28 days) at which the proliferative status was studied. The overall result of the earlier organization of the neointimal matrix and the inhibition of SMC migration and proliferation, at early time points, is

the reduction of neointimal thickness. This conclusion could be consistent with Timp1 expression in the early phases after injury, i.e. in the first seven days when MMPs are overexpressed [118]. This is later reflected as a higher efficacy in blocking the stenotic response (day 14 as compared to day 28). Taken together, the results described in this thesis support the notion that MMPs contribute to the restenosis process favoring SMC migration from the media to the intima and that MMPs inhibition induced extensive remodelling of extracellular matrix, which in turn might be essential for SMC survival signals within the neointima.

Proliferation of VSMCs plays a key role in the development of pathological processes characterized by neointimal thickening, such as atherosclerosis, restenosis after angioplasty and stent placement [6, 55]. In the rat model of angioplasty medial VSMCs begin to proliferate within hours after injury [299]. VSMCs then multiply three to five fold over the next 2 weeks, accounting for 90% of the intimal population [300]. It is known that FGF-2 can initiate VSMCs proliferation [301]. PDGF and FGF-2 work as "competence factors" initiating transcription of immediate early genes *fos* and *myc* that allow cell cycle entry [302]. The consequence of PDGF and FGF-2 stimulus is the activation of cdk1/cdk2 and overexpression of cyclinE/A and PCNA in the intima and medial layers within the first 14 days after vessel injury [303].

PTX3 was overexpressed in the arterial wall with the aim to block VSMCs proliferation and the downstream signaling of FGF-2. The results obtained indicate that PTX3 gene transfer decreased the neointmal development and intima-to-media ratio in similar extent as Timp1 at 14 days. Additionally, also at 14 days, PTX3 gene transfer increased the total medial area by 29.4% with respect to their control arteries and Timp1/PTX3 gene transfer increased the total medial area by 24%. There were no differences in medial areas when PTX3 and Timp1/PTX3 gene transfer were compared with AAV-Timp1-treated group at 14 days. When AAV-PTX3 was combined with AAV-Timp1 for the gene transfer the effect on reducing neointimal development

was surprisingly 21.3% ($p<0.05$) less effective than AAV-Timp1 alone, and the effect on reducing the intima-to-media ratio was 22.43% ($p<0.05$) less effective than AAV-Timp1 alone, always at 14 days. When comparing the effects of AAV-PTX3 with AAV-Timp1/AAV-PTX3 there was no difference on the reduction of neointma development nor in the reduction of the intima-to-media ratio. These data suggest that opposite to the expected outcome, no synergistic, nor additive effects were found in the group treated with AAV-Timp1/AAV-PTX3. The co-infection of the vessel wall with AAV-Timp1 did not alter the effect of AAV-PTX3 gene transfer, the effect achieved when AAV-Timp1/AAV-PTX3 were injected together was probably dependent only on AAV-PTX3 properties.

The time point at which this effects are observed fits with an early interference on FGF-2 dependent proliferation, where an increased levels of cell cycle proteins (such as PCNA and cyclins) and their activation occurs during the first two weeks of lesion formation in the vessel wall [303].

Later on, at day 28, the results obtained indicate that PTX3 gene transfer exerted a clear benefit on neointima development, as neointimal hyperplasia was reduced by 31.2% and intima-to-media ratio was reduced by 43.5%. The level of decrease of neointimal development and intima-to-media ratio was of similar extent as the level observed in AAV-Timp1 treated group at 28 days. Additionally, as for the AAV-PTX3 and AAV-Timp1/AAV-PTX3 treated groups at 14 days, medial area of AAV-PTX3-treated group was increased by 19.8% at day 28 . If we compare the medial area of AAV-Timp1-treated group *vs* the medial area of AAV-PTX3-treated group, we can observe an increase of 17.1% ($P=0.007$) in the later, this difference can be interpreted as a change in the vessel size.

These data suggest that PTX3 gene transfer beyond modulating the neointima development, increased also the medial area, thus favoring a better intima-to-media ratio which reflects a better outward remodelling of the vessel. In the case of AAV-

Timp1 gene transfer it seems that inhibition of neointima was strong and sufficient at 14 days, to show a good intima-to-media ratio, whereas at 28 days the decrease of medial area was interpreted as a decrease of vessel size and this effect was responsible for the drop in the inhibition of the intima-to-media ratio. However, intima-to-media ratios between AAV-Timp1 and AAV-PTX3 gene transfer groups were not significantly different at 28 days and through different morphologic changes both treatments improved the restenotic changes as inferred by intima-to-media ratios.

Exploring the possible role of PTX3 in humans disesaes, it has been suggested recently that PTX3 contribute to the pathogenesis of human atherosclerosis, the authors drew this conclusion after they found specific PTX3 immunoreactivity in human atheromata specimens [139]. This is a relevant issue for the proposed therapeutical potential of PTX3 in restenosis. Atherosclerosis and restenosis have similar underlying processes leading to neointimal thickening, therefore PTX3 gene transfer could have divergent effects on vessel homeostasis.

One possibility could be that PTX3 overexpression inhibits FGF-2-dependent proliferation of VSMCs and this is later traduced as less neointima. However, the proliferative signals of FGF-2 are later needed by EC to achieve endothelial regrowth [304], hence re-establishing vessel homeostasis. Thus, PTX3 overexpression could potentially interfere by delaying endothelial recovery at later phases.

Alternatively, PTX3 overexpression in the vessel wall modulates the thrombogenesis and complement cascade [305], since PTX3 induces tissue factor (TF) expression [306] and binds to C1q. Tissue factor (TF) is a low-molecular-weight glycoprotein that initiates the extrinsic clotting cascade and is considered a major regulator of arterial thrombogenicity [307]. Inhibition of TF by overexpressing its natural inhibitor TF pathway inhibitor (TFPI) decreases thrombogenicity and neointima formation in the mice model [307]. These data suggest that TF/TFPI imbalance by PTX3-induced TF expression could have potential deleterious effects for the vessel, contrasting the PTX3

inhibition of proliferation.

On the other hand, multimeric PTX3 binds to C1q in a specific and saturable manner [137] and PTX3 can inhibit the classical complement pathway by sequestering C1q from immune complexes. Inhibition of complement in the vessel wall could be beneficial, since activation of the complement systems plays a key role in the pathogenesis of atherosclerosis [308]. Complement cascade modulation could have therapeutic potential not only in atheroscelrosis, but also in restenosis and myocardial ischemia/reperfusion injury [309]. C1q contributes to the development of atherosclerosis by down-regulating the expression of an enzyme required to maintain cholesterol hemostasis in the artery wall [310]. C1q also binds to endothelial receptors up-regulating adhesion molecules on the endothelium surface, such as E-selectin and intercellular and vascular cell adhesion molecules 1 (ICAM-1 and VCAM-1) [311], thus affecting the recruitment of circulating inflammatory cells. If PTX3 blocks the complement cascade, it reduces the availability of downstream complement components that trigger pro-inflammatory cytokines: IL-6 or IL-8 and monocyte chemoattractant protein-1 (MCP-1) [312]. Thus, sequestering C1q by PTX3 could down-regulate an inflammatory response that has been correlated with neointima progression.

In conclusion, the results demonstrate that rAAV-Timp1 vector is highly active in preventing cell migration-invasion and that human Timp1 is able to inhibit rat MMPs *in vitro*. AAV vectors are efficient tools to delivery genes to the arterial wall by single intraluminal bolus and the MMPs:Timps balance is seminal for the generation of intimal hyperplasia. Finally, the long-pentraxin 3(PTX3) gene transfer reduces restenosis as well as Timp1 overexpression although probably acts mainly interfering with the natural geometrical remodelling that leads to stenosis after balloon injury.

AAV-Timp1 gene delivery might find an application in an approach that aims to avoid neointima formation in the process of in-stent (IR) restenosis, which depends mostly on intimal hyperplasia. The development of a stent-based AAV gene delivery

strategy for this condition might be of great interest as an alternative approach to the implantation of drug-coated stents. AAV-PTX3 could find better applications aiming to block inward remodelling after balloon injury or aiming to down-regulate vessel wall inflammation in chronic states. PTX3 gene transfer to atherosclerotic blood vessel might also be of great value to study PTX3 potential to decrease atherosclerosis progression.

Chapter 5

Corollary: Coronary stents for stent-based gene delivery

5.1 Background

A stent is a device placed in a body structure (usually tubular) to provide support and keep the structure open. An intraluminal coronary artery stent is a small, self-expanding, stainless steel mesh tube that is placed within a coronary artery to keep the vessel open.

Biocompatibles UK, Inc., has developed in 1984 innovative polymers to coat stainless-steel stents, in order to increase their efficiency and tolerability as implantable medical products. These polymers contain phosphorylcoline (PC), as substance present in the human inner and outer cell membrane. Due to its neutral electrical nature, PC is an ideal coating component that decreases the adhesion of proteins or cells to stents surface, and counteracts the promotion of clot formation. In addition, PC technology has demonstrated to be immunologically well tolerated and to be suitable as a platform for localized drug delivery, adsorbing and releasing molecules by ionic interactions. There are two different designs for PC-coating, one is designed for molecules bigger

than 30 kD called MatrixHi and other is designed for molecules smaller than 30kD called MatrixLo, see Figure 5.1. Phorsphorylcoline (PC) coated stents are commercially available in Europe, have a good penetration in the market and are adapted to delivery drugs and DNA in a sustained way.

Gene therapy approaches for "in-stent" restenosis have held back due to a lack of effective gene delivery systems that could couple stenting with gene delivery [313]. We hypothesized that site-specific delivery of Adeno-associate viral (AAV) vectors from a PC-stent could be achieved through a mechanism involving ionic interactions. This section presents results obtained during the development of a protocol to attach rAAVs to PC-coated stents.

5.2 Results

5.2.1 Attachment of rAAV-*LacZ*

In order to develop a strategy to attach rAAV vectors to PC-coated stents, a variety of biochemical conditions were preliminary explored, including pre-coating stents with heparin, and using different solvents at variable ionic strength to dilute the vector. None of the tested conditions gave satisfactory results and prompt us to develop the following rationale model. Since the most abundant AAV capsid protein (VP1) has a pKa of 6.4, it was predicted that diluting the virions in solvents with high pH values could be sufficient to shift the net charge of the amine groups present on virion capsid from predominantly positive to predominantly negative. In this way, the chances of favorable ionic interactions between the viral particles and the stents surface could be increased. A predominantly negatively charged AAV capsid should bind to the positively charged phosphorylcoline (PC) group of PC-coated stents, without the need of a negatively charged molecule (such as heparin) acting as an interphase, as we originally proposed.

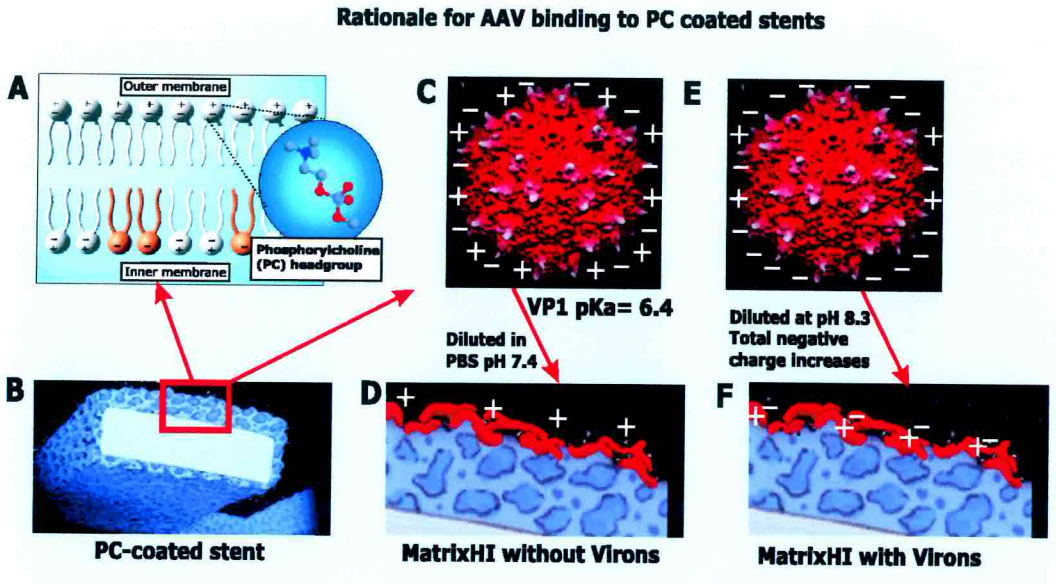

Figure 5.1: **Rationale model for AAV binding to PC coated stents**: A, Schematic representation of ionic charge and composition of coating material, B, Representation of PC coated stent cross section to show coating disposition, C, The capsid charge at neutral pH, D, Represents the lack of interaction between virions in the state showed in C and a positively charged PC MatrixHI, E, Shows the negative capsid charge at pH 8.3, F, Shows the predicted increase of favorable ionic interactions between virions in the state showed in E and a positively charged PC MatrixHI.

The aim of this work was to demonstrate that under the above described conditions rAAVs were able to be bound to stents. In this experiment rAAV-LacZ was diluted at 1 x 10^9 particles/ml in 10mM Tris pH 8.3 just before its use. Four PC-stents MatrixHi (ST2, ST3, ST4 and ST5) were prewashed two times for 5 minutes in 10mM Tris pH 8.3 in circular agitation, in a 12-well sterile petri dish and then incubated in 1 ml of solution with rAAV for 45 minutes in gentle circular agitation. Unbound virons were removed from stents, immediately after the incubation period by extensive washes (5 times) with sterile PBS under fast circular agitation. For stents ST2 and ST3 the binding incubation procedure was repeated twice by addition of fresh amount of rAAV vector at the same concentration as before. After the last wash in PBS, stents ST2 and ST5 were used to infect attached growing cells, see Figure 5.3 and section 5.2.2, while stents ST3 and ST4 were analyzed for the presence of bound AAV virions, see

Figure 5.2.

After treatment with proteinase K that removes attached virions and digests viral capsid proteins, the amount of viral genomes was quantified by competitive PCR, see section Figure 5.2. Stent ST3 (loaded twice with AAV) bound 5 x 10^7 total genome particles, while ST4 bound 5 x 10^6, see 2.1.2 and Figure 5.2A. These values were inferred by the dilutions of the material recovered form proteinase K digestions and by the ratio of band intensity between competitor/template, see Figure 5.2B. The best result obtained was equivalent to recovery of ~10% of virion genome particles with respect to input virus. Altogether these results suggest that rAAV indeed binds to the stent surface, as genome particles can be recovered after proteinase K digestion. This follows the supposition that if rAAV are bound to the stent surface after capsid digestion, ss-DNA genome is released and detectable by polymerase chain reaction. Although this is not informative of the ability of the bounded virions to be released or to be infective, it clearly demonstrates that rAAV binds in a reproducible manner to PC coated stents.

5.2.2 AAV-*LacZ*-PC-STENTS: *In vitro* infection and expression

After demonstrating that rAAVs can be bound to stents, we next assessed the ability of AAV-coated stents to release infective virons. The stents ST2 and ST5 were incubated on chamber slides containing equal numbers of plated Kaposi sarcoma (KS) cells. In order to evaluate their AAV release ability, a positive control for rAAV-LacZ infection was included, which consisted in cells exposed directly to 1 x 10^9 total genome particles, see Figure 5.3A. In this way infectivity of the released AAV-LacZ virons could be evaluated by X-Gal staining of KS cells and compared. The transduction efficiency of stents ST2 was significantly greater than ST5, (59%±10 *vs* 11%±3.1, P=0.003), which means that the stent AAV loaded twice (ST2) was able to transduce 4.3-fold more cells than the stent AAV loaded only once (ST5), see Figure 5.3B and D, and Figure 5.4.

A

Semiquantitative PCR

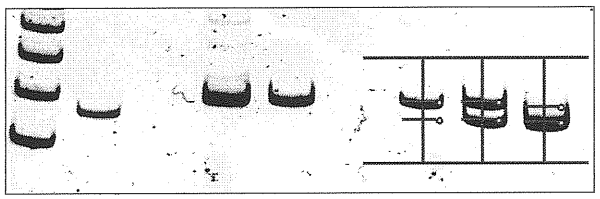

B

Band intensity analysis

Competitor	10^4/µl	10^5/µl	10^6/µl
Template	240,476.7	245,285	68,424.3
Competitor	21,403.2	216,508.1	389,691.7

Ratio Template/competitor

11.2 **1.1** **0.17**

Figure 5.2: **Binding efficiency of rAAV-*LacZ* to PC-stents**: Competitive PCR for a CMV promoter region in adeno-associate viral vectors genome (AAV). rAAV-LacZ (10^9 genome particles/ml) were incubated for 45 minutes together with PC-Stents. A, PCR products corresponding to a CMV region (230bp) demonstrates the viral particles were attached and then recovered by capsid digestion, B) Band analysis of semi-quantitative PCR gives the ratio between the signal of CMV region and a 20 bp smaller competitor of a known number of molecules [282, 314].

The KS cells infected with rAAV-*LacZ* 10^9 genome particles/ml as positive control of viral preparation showed a transduction efficiency of 71%±13.1. The efficiency in transduction achieved by the ST2 was 83% of that of the positive control (59%±10 *vs* 71%±13.1, P=NS), whereas the ST5 was 15% of that of the positive control (11%±3.1 *vs* 71%±13.1, P=0.0003), see Figure 5.4.

5.2.3 Visualization of AAV-*LacZ*-PC-STENTS by EMS

In order to directly visualize morphological changes at the surface of PC stents incubated (treated) with rAAVs, a different technique was used to visualize the rAAVs binding. Under sterile conditions two new stents were subjected to either rAAVs or

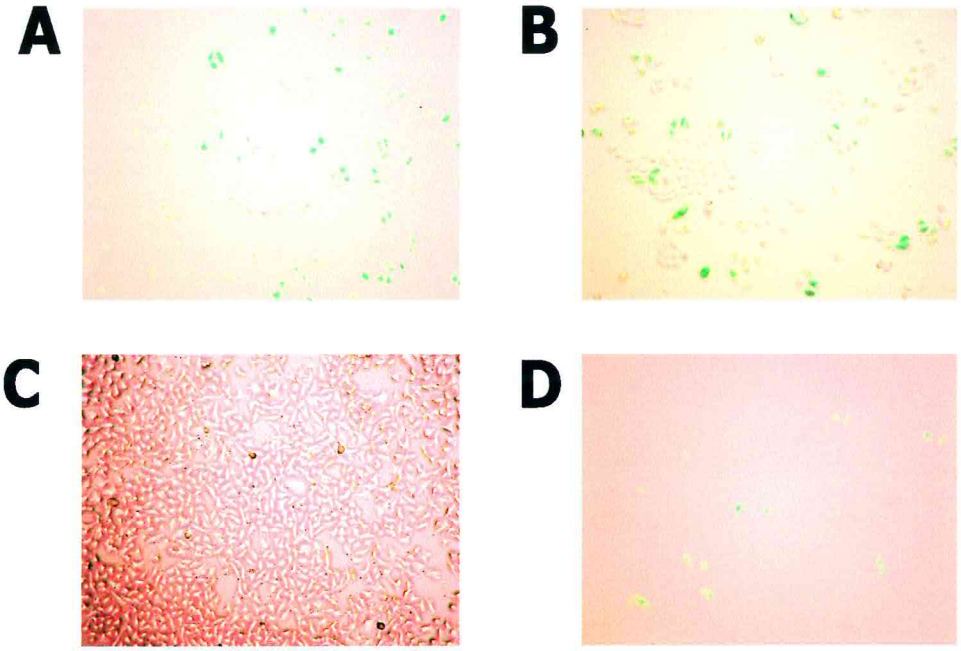

Figure 5.3: ***In vitro* transduction of rAAV-*LacZ*-PC-stents**: X-Gal staining of KS cells infected with AAV-*LacZ* attached to PC stents. Kaposi sarcoma (KS) cells were plated in 2 chamber-slides and incubated for 48 hrs with A, rAAV-*LacZ* 10^9 genome particles/ml, B, AAV-*LacZ*-PC-Stent coated for the second time (ST2) C, a non treated PC-Stent, or D, an AAV-*LacZ*-PC-Stent coated for the first time (ST5), *E. Coli beta*-galactosidase transgene expression was evidenced by X-Gal staining.

0.01M Tris-HCl pH 8.3 in identical conditions and after extensive washings AAV treated and Mock treated stents were visualized under the electron microscope scanning. Microphotographs were taken at several amplification power in order to establish at which magnification it was possible to identify changes on stent surfaces. It was found that mock treated stents presented a very homogenous surface without any particles despposition, see Figure 5.5A and B. In contrast, the AAV loaded stent presented clusters of particles deposition of various sizes present through all the surface of the stent. Representative images can be seen in Figure 5.5D, E and F.

It was not possible to define a specific aggregation pattern of these rAAV clusters. However, hundreds of different rAAV clusters could occupy the area of a single cell.

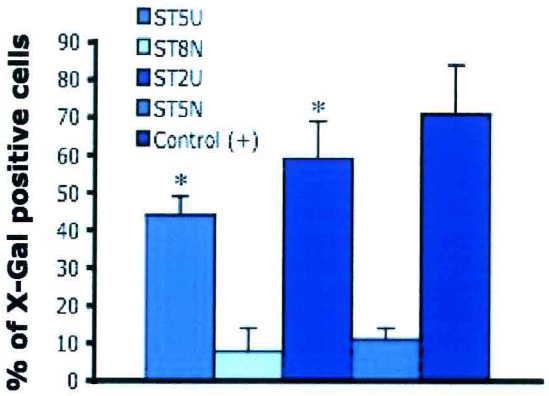

Figure 5.4: **Quantification of X-Gal stained KS cells infected by AAV-*LacZ* attached to PC stents**: Percentage of positive cells was evaluated by counting five low power fields for each case. Fields were randomly chosen, positive control (+) were cells infected with rAAV-*LacZ* 10^{9} genome particles/ml. Data are represented as % of positive cells ±SD. The asterisk denotes statistical significance ($P < 0.05$) after a Student *t*-test.

According to the observed results it could be plausible to think that the observed particle depositions, organized as clusters, correspond to rAAV aggregation particles, as in the non treated stent such signals were not present. Signals were considered specific and dependent on the presence of rAAV, due to the fact that both stents were exposed to the same solvents and salt concentrations.

5.2.4 Aorta transduction by AAV-*LacZ*-PC-STENTS: expression in organ culture

The encouraging results obtained from the preliminary experiments indicated that rAAVs were indeed able to bind to PC stents and to infect cells growing *in vitro*. However, it was still possible that the efficiencies of binding, release and transduction observed *in vitro* could not be sufficient to achieve transduction *in vivo* when inserted into the artery wall of an animal. In order to investigate the *in vivo* transduction efficiency of AAV treated stents, a model of aorta organ culture was set up, the model is explained in detail in the section 2.11. rAAVs were bound to PC stents using the designed protocol and immediately after the stents were extensively washed. When un-

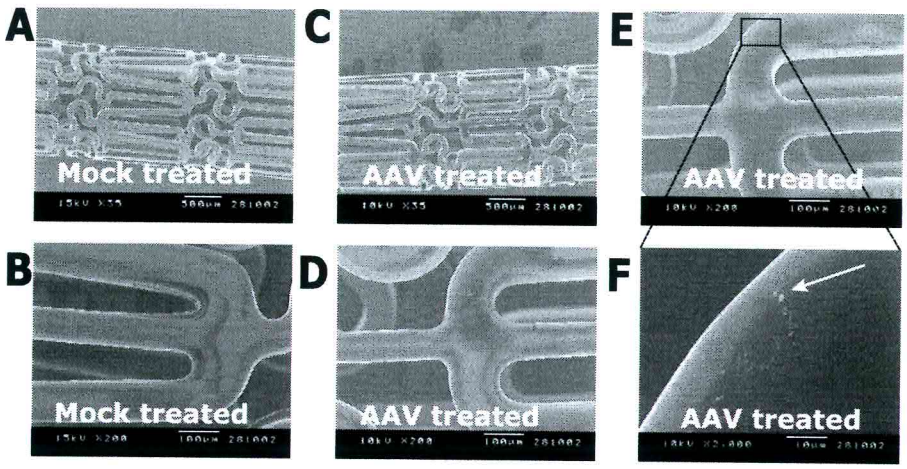

Figure 5.5: **Visualization of the attachment of rAAV-*LacZ* virons to PC-Stents by electron microscopy scanning (EMS)**: Binding of rAAVs on PC coated stents was performed as described in section 2.11. Two PC-stents were treated in identical conditions with either 0.01 M Tris-HCl pH 8.3(Mock treated)A and B, or rAAV-*LacZ* (AAV treated) C to F. A, Scanning electron micrograph (SEM) showing the surface of an untreated arterial PC-stent (SEM 35X). B, PC-stent surface demonstrating uniform coating of the stent struts (SEM 35X). C, The surface of an AAV treated arterial PC-stent (SEM 35X).D, PC-stent surface demonstrating retention of aggregated particles of various sizes (white arrow) on the stent struts of PC coating across all stent structure, D and E (SEM 200X) and F (SEM 2000X). The conditions and titers of rAAV loading were similar to those used for *in vitro* assays (10^9 genome particles/ml).

bound rAAVs were removed the PC-stent-AAV was mounted in a Maverick 2.0 catheter (Boston Scientific), inserted in the abdominal aorta of an anesthetized Wistar rat and finally inflated to 6 atm for 1 minute. After the expansion of the catheter in the abdominal aorta the animal was sacrificed and the stented aorta segment excised, see Figure 5.6, and maintained in organ culture.

After 10 days of incubation on the specific supplemented SmGM-2 medium (Biowhittaker), a portion of the stented aorta segment was excised from stent and stained with X-Gal. Positive blue signals corresponding to marker gene expression revealed proof of principle for successful delivery of rAAV by the engineered rAAV-*LacZ*-PC-stent. Although, beta galactosidase expression was weak, it was localized in relevant target tissues (media and adventitia layer), see Figure 5.7C. The presence of marker gene expression at this point by rAAV-*LacZ*-PC-stent was considered to be a good indicator of the efficiencies of binding, release and transduction observed *in vitro*,

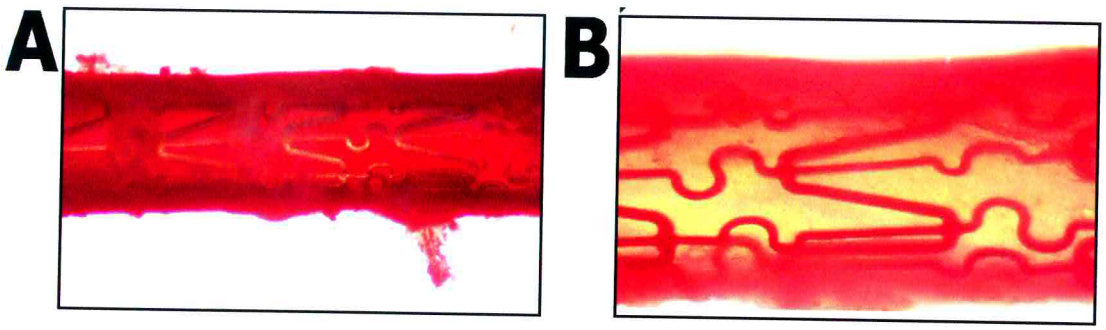

Figure 5.6: **Visualization of intra-aortic rAAV-*LacZ*-PC-stent**: The segment of artery containing the stent was excised and maintained in organ culture in SmGM-2 medium (Biowhittaker) supplemented as described in section 2.2 for 2 weeks. A and B, Stereo microscope photographs showing intra-aortic stent at low and high magnification, respectively.

which could in turn be relevant for *in vivo* gene transfer.

The expression of the LacZ gene on the aorta artery wall with the implanted AAV-coated stent was then confirmed at 14 days, as revealed by X-Gal staining. The pattern of expression was very similar to the one observed in the specimen at 10 days, but with stronger signals, see Figure 5.7D. Altogether these results suggest that the binding efficiency, the rate of release and transduction of rAAVs are sufficient to achieve transduction in cell culture and in the rat aorta organ culture.

5.3 Discussion

In conclusion the results of this chapter suggest that rAAV not only binds to PC stents but is also able to be released from the stent surface and infect the neighboring cells. This observation is supported by the data of competitive PCR and *in vitro* transduction experiments. It is likely that rAAVs, which were released from PC-stents surface at an unknown rate in the cell culture medium, resulted infective also for cells distant with respect to the stent surface contact points. In summary, these results demonstrate that rAAV binds to PC coated stents, is released both *in vitro* and *in vivo*, preserving infective and transduction properties. Also, in this context it was observed that stents

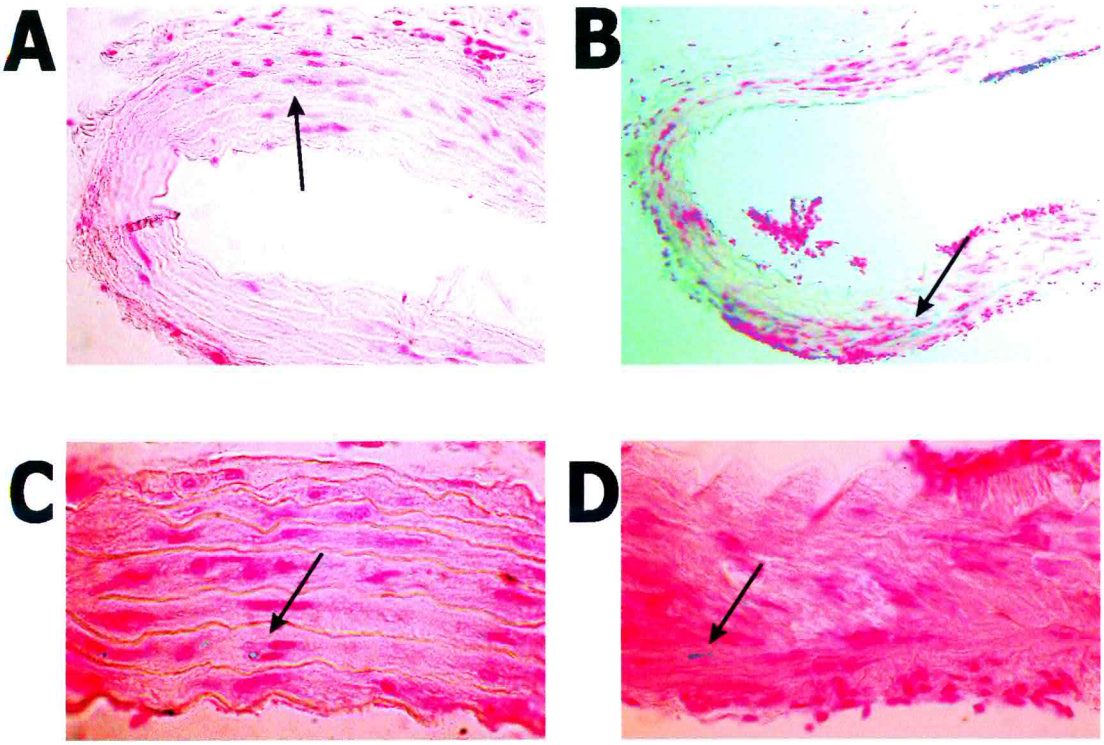

Figure 5.7: **Infection and expression in organ culture by AAV-*LacZ*-PC-STENT**: The artery was injured *in vivo* with simultaneous AAV-LacZ-PC stent placement, maintained in organ culture for 10 and 14 days. *E. Coli beta*-galactosidase expression was evidenced by X-Gal staining. A and B, arteries harvested at day 10th and 14th post-stent placement. C and D, the same arteries at higher magnification (60x). Arrows denote regions where blue cells can be seen.

loaded with AAVs more than one time could transduce cells around 4 times more than stents loaded with rAAVs only once, suggesting that at least two rounds of rAAV binding to PC-stents are needed to achieve optimal functionality.

Intravascular gene therapy has been widely explored as an alternative therapy for many diseases, such as endothelial dysfunction [315], pulmonary and systemic hypertension [316, 317], arterial thrombosis [318], saphenous vein graft disease [319], atherosclerosis [320] and post-angioplasty restenosis [152, 155, 158]. This strategy harbors some inconveniences such as limited time exposure to vector, limited site specific gene delivery and risk of systemic vector spreading [321]. These difficulties can be easily overcome by a stent-based gene delivery device as demonstrated earlier. Klugherz

et al reported successful stent based gene delivery, from a plasmid DNA-controlled release stent using the pig coronary arteries [313]. Although plasmid DNA is safe and easy to prepare for clinical grade applications, it exhibits low levels of transduction and transient expression. The same group reported later successful stent based gene delivery using antibody-tethered adenovirus [321]. They achieved high levels of transduction reaching 17% in neointima and around 6% in the overall artery, but this was analyzed only at day 7 post-implantation. Also, it would have been ideal to explore the inflammatory reaction and endothelial dysfunction [144, 145] often associated to adenoviral gene transfer. The impairment of endothelium-dependent relaxation after adenoviral vectors infection reported by Channon et al. [145] has important implications due to the association of endothelial dysfunctions as a cause of cardiovascular events. On the contrary, adeno-associate viral vectors (AAV) have gained increasing popularity in the gene therapy community due to a number of appealing features. These vectors can be purified and produced at high titers, are not immunogenic, do not induce an inflammatory reaction, can be safely injected in vivo, and maintain transgene expression for very long periods of time [219]. In addition, AAV delivery to the vascular systems has never been associated to adverse effects such as endothelial dysfunction [277, 276, 275, 278, 322, 279].

Many experimental studies and large prevention trials (LTR, APPLE, PREDICT), have tried to evaluate the role of systemic administration of statins (HMG-CoA reductase inhibitors) on the prevention or delay of restenosis after conventional PTCA, however statins role remains unclear [73, 74]. Interestingly, Walter et al. have shown promising results about the role of statins on preventing restenosis after coronary stenting [75]. To date, the interventions with administration of systemic drugs have not demonstrated definitive positive results on preventing In-stent restenosis.

The only two interventions that have shown a true benefit on preventing In-stent restenosis have been paclitaxel and rapamycin drug eluting stents. However, this strate-

gies have been associated to late acute thrombosis [90], impaired re-endothelialization [89, 91] and inhibition of endothelial cells proliferation [92], respectively. Many other drugs are under evaluation, including other immunosuppressants, antineoplastic agents, vascular endothelial growth factor (VEGF) and 17-β-oestradiol [26].

Gene therapy could be an attractive strategy to hamper In-stent restenosis in alternative to the available therapies. Secondary to the development of a proper scaffold for a localizable vector delivery in the blood vessels, a stent based gene delivery system could transfer genes to artery wall with protective properties. Instead of solely blocking cell proliferation indiscriminately, gene therapy could aim to introduce a therapeutic gene for long-term expression of a more physiological and protective molecule such as VEGF.

Recently Hedman and colleagues [180] suggested that catheter-mediated intracoronary gene transfer approach is feasible, safe and tolerable in humans. Although VEGF gene therapy to prevent restenosis after coronary stenting did not influence the incidence of post-PTCA angioplasty (around 6%), it did improve myocardial perfusion in the VEGF-Adv treated group. The results from this anti-restenosis clinical trials suggest that the next target in preventing restenosis could be endothelial recovery [181].

5.4 Conclusions

A successful stent-based gene delivery system in an *in vitro* and in a organ culture model is reported, this system uses AAV-*LacZ* bound to biocompatible PC-stents via electrostatic interactions. We also demonstrated efficient and highly localized gene delivery to KS cells in culture and to arterial smooth muscle cells in rat aorta organ culture. Therefore it was concluded that a vascular PC-stent is a suitable scaffold for a localizable AAV vector delivery system that could be potentially used to prevent systemic spread of vector. Therefore, gene transfer using PC-stent-based AAV gene

delivery represents a powerful new approach for site-specific expression of genes aiming to block in-stent (IR) restenosis.

Appendix A

Features of human TIMPs

Here, the distinguishing characteristics of human TIMPs with respect to MMP inhibitory activity and phenotypic modulation of cells both in vitro and in vivo are summarised in a table. Data are taken from Baker [106].

	TIMP-1	TIMP-2	TIMP-3	TIMP-4
Protein [kDa]	28	21	24-27	22
N-glycosylation sites	2	0	1	0
Protein localization	Soluble	Soluble-cell surface	ECM	Soluble-cell surface
Pro-MMP association	pro-MMP-9	pro-MMP-2	pro-MMP-2/9	pro-MMP-9
MMPs poorly inhibited	MT1 to MT3-MMP MT5-MMP MMP-19	None	None	None
ADAM inhibition	ADAM 10	None	ADAM 12, 17, 19, 10 ADAMTS-4, TS-5	None
Cell proliferation	↑ Erythroid precursors ↑ Tumoral cells	↑ Erythroid precursors ↑ Tumoral cells ↑ Fibroblast ↑ SMCs ↓ Endothelial cells	↑ SMC and cancer cells	↑ Mammary tumor cells ↑ Wilm's tumour cells
Apoptosis	↓ Burkitt's Lymphoma cells	↑ Colorectal cancer cells ↓ Melanoma	↑ SMCs ↑ Tumoral cells ↑ Retinal pigmented epithelial cells	↑ Cardiac firboblast
Tumor angiogenesis	↑ Mammary	↓ Melanoma	↓ Melanoma	
Angiogenesis	No effect	Inhibits	Inhibits	Inhibits
Tumourigenesis	Inhibits	Inhibits	Inhibits	Inhibits
Metastasis	Stimulates			Stimulates

Bibliography

[1] R. S. Cotran, V. Kumar, and T. Collins. *Robbin's Pathologic basis of disease.* W.B. Saunders, Philadelphia, PA.

[2] B. C. Berk. Vascular smooth muscle growth: autocrine growth mechanisms. *Physiol. Rev.*, 81(3):999–1030, 2001.

[3] G. R. Campbell and J. H. Campbell. The phenotypes of smooth muscle expressed in human atheroma. *Ann. N. Y. Acad. Sci.*, 598:143–158, 1990.

[4] M. G. Frid, A. A. Aldashev, E. C. Dempsey, and K. R. Stenmark. Smooth muscle cells isolated from discrete compartments of the mature vascular media exhibit unique phenotypes and distinct growth capabilities. *Circ. Res.*, 81(6):940–952, 1997.

[5] R. Ross. Atherosclerosis - an inflammatory disease. *N. Engl. J. Med.*, 340(2):115–126, 1999.

[6] R. Ross. The pathogenesis of atherosclerosis: a perspective for the 1990s. *Nature*, 362(6423):801–809, 1993.

[7] A. J. Lusis. Atherosclerosis. *Nature*, 407(6801):233–241, 2000.

[8] S. M. Lessner, H. L. Prado, E. K. Waller, and Z. S. Galis. Atherosclerotic lesions grow through recruitment and proliferation of circulating monocytes in a murine model. *Am J Pathol*, 160(6):2145–55, 2002. 22052265 0002-9440 Journal Article.

[9] M. Sata, A. Saiura, A. Kunisato, A. Tojo, S. Okada, T. Tokuhisa, H. Hirai, M. Makuuchi, Y. Hirata, and R. Nagai. Hematopoietic stem cells differentiate into vascular cells that participate in the pathogenesis of atherosclerosis. *Nat. Med.*, 8(4):403–409, 2002.

[10] Y. Hu, M. Mayr, B. Metzler, M. Erdel, F. Davison, and Q. Xu. Both donor and recipient origins of smooth muscle cells in vein graft atherosclerotic lesions. *Circ. Res.*, 91(7):e13–20, 2002.

[11] Y. Shi, J. E. O'Brien, A. Fard, J. D. Mannion, D. Wang, and A. Zalewski. Adventitial myofibroblasts contribute to neointimal formation in injured porcine coronary arteries. *Circulation*, 94(7):1655–1664, 1996.

[12] D. H. Walter, K. Rittig, F. H. Bahlmann, R. Kirchmair, M. Silver, T. Murayama, H. Nishimura, D. W. Losordo, T. Asahara, and J. M. Isner. Statin therapy accelerates reendothelialization: a novel effect involving mobilization and incorporation of bone marrow-derived endothelial progenitor cells. *Circulation*, 105(25):3017–3024, 2002.

[13] K. Shimizu, S. Sugiyama, M. Aikawa, Y. Fukumoto, E. Rabkin, P. Libby, and R. N. Mitchell. Host bone-marrow cells are a source of donor intimal smooth- muscle-like cells in murine aortic transplant arteriopathy. *Nat. Med.*, 7(6):738–741, 2001.

[14] J. L. Hillebrands, F. A. Klatter, and J. Rozing. Origin of vascular smooth muscle cells and the role of circulating stem cells in transplant arteriosclerosis. *Arterioscler. Thromb. Vasc. Biol.*, 23(3):380–387, 2003.

[15] Y. Hu, F. Davison, B. Ludewig, M. Erdel, M. Mayr, M. Url, H. Dietrich, and Q. Xu. Smooth muscle cells in transplant atherosclerotic lesions are originated from recipients, but not bone marrow progenitor cells. *Circulation*, 106(14):1834–1839, 2002.

[16] J. L. Hillebrands, F. A. Klatter, B. M. van den Hurk, E. R. Popa, P. Nieuwenhuis, and J. Rozing. Origin of neointimal endothelium and alpha-actin-positive smooth muscle cells in transplant arteriosclerosis. *J. Clin. Invest.*, 107(11):1411–1422, 2001.

[17] C. I. Han, G. R. Campbell, and J. H. Campbell. Circulating bone marrow cells can contribute to neointimal formation. *J. Vasc. Res.*, 38(2):113–9, 2001.

[18] A. Cho and M. A. Reidy. Matrix metalloproteinase-9 is necessary for the regulation of smooth muscle cell replication and migration after arterial injury. *Circ. Res.*, 91(9):845–851, 2002.

[19] Z. S. Galis, C. Johnson, D. Godin, R. Magid, J. M. Shipley, R. M. Senior, and E. Ivan. Targeted disruption of the matrix metalloproteinase-9 gene impairs smooth muscle cell migration and geometrical arterial remodeling. *Circ. Res.*, 91(9):852–859, 2002.

[20] American Heart Association. 2003 heart and stroke statistical update. Technical report, American Heart Association, Dallas, 2003.

[21] Z. S. Galis and J. J. Khatri. Matrix metalloproteinases in vascular remodeling and atherogenesis: the good, the bad, and the ugly. *Circ. Res.*, 90(3):251–262, 2002.

[22] C. T. Dotter and M. P. Judkins. Transluminal treatment of arteriosclerotic obstruction. Description of a new technic and a preliminary report of its application. *Radiology*, 172:904–920, 1989.

[23] A. Gruntzig. Transluminal dilatation of coronary-artery stenosis. *Lancet*, 1(8058):263, 1978.

[24] C. Landau, R. A. Lange, and L. D. Hillis. Percutaneous transluminal coronary angioplasty. *N. Engl. J. Med.*, 330(14):981–993, 1994.

[25] U. Sigwart, J. Puel, V. Mirkovitch, F. Joffre, and L. Kappenberger. Intravascular stents to prevent occlusion and restenosis after transluminal angioplasty. *N. Engl. J. Med.*, 316(12):701–706, 1987.

[26] R. Fattori and T. Piva. Drug-eluting stents in vascular intervention. *Lancet*, 361(9353):247–249, 2003.

[27] M. Nobuyoshi, T. Kimura, H. Nosaka, S. Mioka, K. Ueno, H. Yokoi, N. Hamasaki, H. Horiuchi, and H. Ohishi. Restenosis after successful percutaneous transluminal coronary angioplasty: serial angiographic follow-up of 229 patients. *J. Am. Coll. Cardiol.*, 12(3):616–623, 1988.

[28] M. R. Bennett and S. M. Schwartz. Antisense therapy for angioplasty restenosis. *Circulation*, 92(7):1981–1993, 1995.

[29] D. R. Holmes, M. J. Van Raden, G. S. Reeder, R. E. Vlietstra, G. C. Jang, K. M. Kent, G. W. Vetrovec, M. J. Cowley, G. Dorros, S. F. Kelsey, and et al. Return to work after coronary angioplasty: a report from the National Heart, Lung, and Blood Institute Percutaneous Transluminal Coronary Angioplasty Registry. *Am. J. Cardiol.*, 53(12):48C–51C, 1984.

[30] S. C. Smith, J. T. Dove, A. K. Jacobs, J. W. Kennedy, D. Kereiakes, M. J. Kern, R. E. Kuntz, J. J. Popma, H. V. Schaff, D. O. Williams, R. J. Gibbons, J. P. Alpert, K. A. Eagle, D. P. Faxon, V. Fuster, T. J. Gardner, G. Gregoratos, and R. O. Russell. ACC/AHA guidelines for percutaneous coronary intervention-executive summary: a report of the American College of Cardiology/American Heart Association task force on practice guidelines. *Circulation*, 103(24):3019–3041, 2001.

[31] Jr. Holmes, D. R. State of the art in coronary intervention. *Am. J. Cardiol.*, 91(3A):50A–53A, 2003.

[32] R. S. Schwartz and T. D. Henry. Pathophysiology of coronary artery restenosis. *Rev. Cardiovasc. Med.*, 3 Suppl 5:S4–9, 2002.

[33] G. S. Mintz, K. M. Kent, A. D. Pichard, L. F. Satler, J. J. Popma, and M. B. Leon. Contribution of inadequate arterial remodeling to the development of focal coronary artery stenoses. an intravascular ultrasound study. *Circulation*, 95(7):1791–1798, 1997.

[34] R. S. Schwartz, E. J. Topol, P. W. Serruys, G. Sangiorgi, and Jr. Holmes, D. R. Artery size, neointima, and remodeling: time for some standards. *J. Am. Coll. Cardiol.*, 32(7):2087–2094, 1998.

[35] G. Sangiorgi, A. J. Taylor, A. Farb, A. J. Carter, W. D. Edwards, D. R. Holmes, R. S. Schwartz, and R. Virmani. Histopathology of postpercutaneous transluminal coronary angioplasty remodeling in human coronary arteries. *Am. Heart. J.*, 138(4 Pt 1):681–687, 1999.

[36] R. Mehran, G. S. Mintz, J. J. Popma, A. D. Pichard, L. F. Satler, K. M. Kent, J. Griffin, and M. B. Leon. Mechanisms and results of balloon angioplasty for the treatment of in-stent restenosis. *Am. J. Cardiol.*, 78(6):618–622, 1996.

[37] G. S. Mintz, K. M. Kent, A. D. Pichard, J. J. Popma, L. F. Satler, and M. B. Leon. Intravascular ultrasound insights into mechanisms of stenosis formation and restenosis. *Cardiol. Clin.*, 15(1):17–29, 1997.

[38] A. Farb, D. K. Weber, F. D. Kolodgie, A. P. Burke, and R. Virmani. Morphological predictors of restenosis after coronary stenting in humans. *Circulation*, 105(25):2974–2980, 2002.

[39] R. Virmani and A. Farb. Pathology of in-stent restenosis. *Curr. Opin. Lipidol.*, 10(6):499–506, 1999.

[40] Z. Zhou, K. Wang, M. S. Penn, S. P. Marso, M. A. Lauer, F. Forudi, X. Zhou, W. Qu, Y. Lu, D. M. Stern, A. M. Schmidt, A. M. Lincoff, and E. J. Topol. Receptor for AGE (RAGE) mediates neointimal formation in response to arterial injury. *Circulation*, 107(17):2238–2243, 2003.

[41] P. Libby, D. Schwartz, E. Brogi, H. Tanaka, and S. K. Clinton. A cascade model for restenosis. a special case of atherosclerosis progression. *Circulation*, 86(6 Suppl):III47–52, 1992.

[42] D. Kritchevsky, S. A. Tepper, D. A. Scott, D. M. Klurfeld, D. Vesselinovitch, and R. W. Wissler. Cholesterol vehicle in experimental atherosclerosis. part 18. comparison of north american, african and south american peanut oils. *Atherosclerosis*, 38(3-4):291–299, 1981.

[43] D. Mehta, G. D. Angelini, and A. J. Bryan. Experimental models of accelerated atherosclerosis syndromes. *Int. J. Cardiol.*, 56(3):235–257, 1996.

[44] A. W. Clowes, M. A. Reidy, and M. M. Clowes. Mechanisms of stenosis after arterial injury. *Lab. Invest.*, 49(2):208–215, 1983.

[45] A. W. Clowes, M. M. Clowes, J. Fingerle, and M. A. Reidy. Regulation of smooth muscle cell growth in injured artery. *J. Cardiovasc. Pharmacol.*, 14 Suppl 6:S12–15, 1989.

[46] J. Fingerle, R. Johnson, A. W. Clowes, M. W. Majesky, and M. A. Reidy. Role of platelets in smooth muscle cell proliferation and migration after vascular injury in rat carotid artery. *Proc. Natl. Acad. Sci. USA*, 86(21):8412–8416, 1989.

[47] C. Indolfi, G. Esposito, E. Stabile, L. Cavuto, A. Pisani, C. Coppola, D. Torella, C. Perrino, E. Di Lorenzo, A. Curcio, L. Palombini, and M. Chiariello. A new rat model of small vessel stenting. *Basic Res. Cardiol.*, 95(3):179–185, 2000.

[48] C. J. Robinson and S. E. Stringer. The splice variants of vascular endothelial growth factor (VEGF) and their receptors. *J. Cell. Sci.*, 114(Pt 5):853–865, 2001.

[49] A. Vink, A. H. Schoneveld, J. J. van der Meer, B. J. van Middelaar, J. P. Sluijter, M. B. Smeets, P. H. Quax, S. K. Lim, C. Borst, G. Pasterkamp, and D. P. de Kleijn. In vivo evidence for a role of toll-like receptor 4 in the development of intimal lesions. *Circulation*, 106(15):1985–1990, 2002.

[50] M. A. Reddy, P. R. Thimmalapura, L. Lanting, J. L. Nadler, S. Fatima, and R. Natarajan. The oxidized lipid and lipoxygenase product 12(S)-hydroxyeicosatetraenoic acid induces hypertrophy and fibronectin transcription in vascular smooth muscle cells via p38 MAPK and cAMP response element-binding protein activation. mediation of angiotensin II effects. *J. Biol. Chem.*, 277(12):9920–9928, 2002.

[51] J. Ruef, Z. Y. Hu, L. Y. Yin, Y. Wu, S. R. Hanson, A. B. Kelly, L. A. Harker, G. N. Rao, M. S. Runge, and C. Patterson. Induction of vascular endothelial growth factor in balloon-injured baboon arteries. a novel role for reactive oxygen species in atherosclerosis. *Circ. Res.*, 81(1):24–33, 1997.

[52] G. Barillari, L. Albonici, S. Incerpi, L. Bogetto, G. Pistritto, A. Volpi, B. Ensoli, and V. Manzari. Inflammatory cytokines stimulate vascular smooth muscle cells locomotion and growth by enhancing alpha-5-beta-1 integrin expression and function. *Atherosclerosis*, 154(2):377–385, 2001.

[53] Y. Okamura, M. Watari, E. S. Jerud, D. W. Young, S. T. Ishizaka, J. Rose, J. C. Chow, and 3rd Strauss, J. F. The extra domain a of fibronectin activates toll-like receptor 4. *J. Biol. Chem.*, 276(13):10229–10233, 2001.

[54] J. N. Wilcox, E. I. Okamoto, K. I. Nakahara, and J. Vinten-Johansen. Perivascular responses after angioplasty which may contribute to postangioplasty restenosis: a role for circulating myofibroblast precursors? *Ann. N. Y. Acad. Sci.*, 947:68–90, 2001.

[55] S. M. Schwartz, D. deBlois, and E. R. O'Brien. The intima- soil for atherosclerosis and restenosis. *Circ. Res.*, 77(3):445–465, 1995.

[56] M. Haude, R. Erbel, G. Hafner, B. Heublein, H. W. Hoepp, D. Franzen, W. Prellwitz, P. Lichtlen, H. H. Hilger, and J. Meyer. Multicenter results of coronary implantation of balloon expandable palmaz-schatz vascular stents. *Z. Kardiol.*, 82(2):77–86, 1993.

[57] J. S. Powell, J. P. Clozel, R. K. Muller, H. Kuhn, F. Hefti, M. Hosang, and H. R. Baumgartner. Inhibitors of angiotensin-converting enzyme prevent myointimal proliferation after vascular injury. *Science*, 245(4914):186–188, 1989.

[58] A. W. Clowes and M. M. Clowes. Kinetics of cellular proliferation after arterial injury. II. inhibition of smooth muscle growth by heparin. *Lab. Invest.*, 52(6):611–616, 1985.

[59] C. L. Jackson, R. C. Bush, and D. E. Bowyer. Mechanism of antiatherogenic action of calcium antagonists. *Atherosclerosis*, 80(1):17–26, 1989.

[60] W. Volker and V. Faber. Aspirin reduces the growth of medial and neointimal thickenings in balloon-injured rat carotid arteries. *Stroke*, 21(12 Suppl):IV44–5, 1990.

[61] M. W. Webster, J. H. Chesebro, and V. Fuster. Platelet inhibitor therapy. Agents and clinical implications. *Hematol. Oncol. Clin. North. Am.*, 4(1):265–289, 1990.

[62] C. J. Pepine, J. W. Hirshfeld, R. G. Macdonald, M. A. Henderson, T. A. Bass, S. Goldberg, M. P. Savage, G. Vetrovec, M. Cowley, A. S. Taussig, and et al. A controlled trial of corticosteroids to prevent restenosis after coronary angioplasty, M-HEART group. *Circulation*, 81(6):1753–1761, 1990.

[63] P. W. Serruys, D. P. Foley, G. Jackson, H. Bonnier, C. Macaya, M. Vrolix, A. Branzi, J. Shepherd, H. Suryapranata, P. J. de Feyter, R. Melkert, G. A. van Es, and P. J. Pfister. A randomized placebo-controlled trial of fluvastatin for prevention of restenosis after successful coronary balloon angioplasty; final results of the fluvastatin angiographic restenosis (FLARE) trial. *Eur. Heart. J.*, 20(1):58–69, 1999.

[64] T. Corcos, P. R. David, P. G. Val, J. Renkin, V. Dangoisse, H. G. Rapold, and M. G. Bourassa. Failure of diltiazem to prevent restenosis after percutaneous transluminal coronary angioplasty. *Am. Heart. J.*, 109(5 Pt 1):926–31, 1985.

[65] D. Holmes, P. Fitzgerald, S. Goldberg, J. LaBlanche, A. M. Lincoff, M. Savage, P. W. Serruys, J. Willerson, J. R. Granett, R. Chan, N. H. Shusterman, and M. Poland. The presto (prevention of restenosis with tranilast and its outcomes) protocol: a double-blind, placebo-controlled trial. *Am. Heart. J.*, 139(1 Pt 1):23–31, 2000.

[66] R. Gopalan and S. Goldberg. Tranilast in the therapy of coronary artery disease. *Curr. Interv. Cardiol. Rep.*, 2(2):149–156, 2000.

[67] F. M. Sacks, M. A. Pfeffer, L. A. Moye, J. L. Rouleau, J. D. Rutherford, T. G. Cole, L. Brown, J. W. Warnica, J. M. Arnold, C. C. Wun, B. R. Davis, and E. Braunwald. The effect of pravastatin on coronary events after myocardial infarction in patients with average cholesterol levels. *N. Engl. J. Med.*, 335(14):1001–1009, 1996.

[68] F. M. Sacks, R. C. Pasternak, C. M. Gibson, B. Rosner, and P. H. Stone. Effect on coronary atherosclerosis of decrease in plasma cholesterol concentrations in normocholesterolaemic patients. Harvard Atherosclerosis Reversibility Project (HARP). *Lancet*, 344(8931):1182–1186, 1994.

[69] F. M. Sacks, J. L. Rouleau, L. A. Moye, M. A. Pfeffer, J. W. Warnica, J. M. Arnold, D. T. Nash, L. E. Brown, F. Sestier, J. Rutherford, and et al. Baseline characteristics in the cholesterol and recurrent events (CARE) trial of secondary prevention in patients with average serum cholesterol levels. *Am. J. Cardiol.*, 75(8):621–623, 1995.

[70] H. Eckardt and I. Filipovic. Calcium antagonists increase the amount of mrna for the low-density lipoprotein receptor in skin fibroblasts. *Artery*, 18(4):168–183, 1991.

[71] J. Gellman, M. D. Ezekowitz, I. J. Sarembock, M. A. Azrin, L. E. Nochomowitz, E. Lerner, and C. C. Haudenschild. Effect of lovastatin on intimal hyperplasia after balloon angioplasty: a study in an atherosclerotic hypercholesterolemic rabbit. *J. Am. Coll. Cardiol.*, 17(1):251–259, 1991.

[72] M. R. Soma, E. Donetti, C. Parolini, G. Mazzini, C. Ferrari, R. Fumagalli, and R. Paoletti. Hmg coa reductase inhibitors. in vivo effects on carotid intimal thickening in normocholesterolemic rabbits. *Arterioscler. Thromb.*, 13(4):571–578, 1993.

[73] Jr. O'Keefe, J. H., G. W. Stone, Jr. McCallister, B. D., C. Maddex, R. Ligon, R. L. Kacich, J. Kahn, P. G. Cavero, G. O. Hartzler, and B. D. McCallister. Lovastatin plus probucol for prevention of restenosis after percutaneous transluminal coronary angioplasty. *Am. J. Cardiol.*, 77(8):649–652, 1996.

[74] M. E. Bertrand, E. P. McFadden, J. C. Fruchart, E. Van Belle, P. Commeau, G. Grollier, J. P. Bassand, J. Machecourt, J. Cassagnes, J. M. Mossard, A. Vacheron, A. Castaigne, N. Danchin, and J. M. Lablanche. Effect of pravastatin on angiographic restenosis after coronary balloon angioplasty. the predict trial investigators. prevention of restenosis by elisor after transluminal coronary angioplasty. *J. Am. Coll. Cardiol.*, 30(4):863–869, 1997.

[75] D. H. Walter, V. Schachinger, M. Elsner, S. Mach, W. Auch-Schwelk, and A. M. Zeiher. Effect of statin therapy on restenosis after coronary stent implantation. *Am. J. Cardiol.*, 85(8):962–968, 2000.

[76] G. Schnyder, M. Roffi, R. Pin, Y. Flammer, H. Lange, F. R. Eberli, B. Meier, Z. G. Turi, and O. M. Hess. Decreased rate of coronary restenosis after lowering of plasma homocysteine levels. *N. Engl. J. Med.*, 345(22):1593–1600, 2001.

[77] Erbel R., Verin V., Popowski Y., and et. al. Intracoronary beta-irradiation to reduce restenosis after balloon angioplasty: results of a multicenter european dose-finding study. *Circulation*, 100 (suppl I)(I-154), 1999.

[78] Raizner A.E., Oesterle S.N., Waksman R., and et. al. Inhibition of restenosis with beta-emitting radiation (32P): the final report of the PREVENT trial. *Circulation*, 100 (suppl I)(I-75), 1999.

[79] P. S. Teirstein, V. Massullo, S. Jani, J. J. Popma, G. S. Mintz, R. J. Russo, R. A. Schatz, E. M. Guarneri, S. Steuterman, N. B. Morris, M. B. Leon, and P. Tripuraneni. Catheter-based radiotherapy to inhibit restenosis after coronary stenting. *N. Engl. J. Med.*, 336(24):1697–1703, 1997.

[80] P. S. Teirstein, V. Massullo, S. Jani, J. J. Popma, R. J. Russo, R. A. Schatz, E. M. Guarneri, S. Steuterman, K. Sirkin, D. A. Cloutier, M. B. Leon, and P. Tripuraneni. Three-year clinical and angiographic follow-up after intracoronary radiation : results of a randomized clinical trial. *Circulation*, 101(4):360–365, 2000.

[81] R. Waksman, R. L. White, R. C. Chan, B. G. Bass, L. Geirlach, G. S. Mintz, L. F. Satler, R. Mehran, P. W. Serruys, A. J. Lansky, P. Fitzgerald, B. Bhargava, K. M. Kent, A. D. Pichard, and M. B. Leon. Intracoronary gamma-radiation therapy after angioplasty inhibits recurrence in patients with in-stent restenosis. *Circulation*, 101(18):2165–2171, 2000.

[82] M. B. Leon, P. S. Teirstein, A. J. Lansky, and et al. Intracoronary gamma radiation to reduce in-stent restenosis: the multicenter gamma I randomized clinical trial. *J. Am. Coll. Cardiol.*, (33) suppl A(19A), 2001.

[83] M. C. Morice, P. W. Serruys, J. E. Sousa, J. Fajadet, E. Ban Hayashi, M. Perin, A. Colombo, G. Schuler, P. Barragan, G. Guagliumi, F. Molnar, and R. Falotico. A randomized comparison of a sirolimus-eluting stent with a standard stent for coronary revascularization. *N. Engl. J. Med.*, 346(23):1773–1780, 2002.

[84] M. Degertekin, P. W. Serruys, D. P. Foley, K. Tanabe, E. Regar, J. Vos, P. C. Smits, W. J. van der Giessen, M. van den Brand, P. de Feyter, and J. J. Popma. Persistent inhibition of neointimal hyperplasia after sirolimus-eluting stent implantation: long-term (up to 2 years) clinical, angiographic, and intravascular ultrasound follow-up. *Circulation*, 106(13):1610–1613, 2002.

[85] A. Colombo, J. Drzewiecki, A. Banning, E. Grube, K. Hauptmann, S. Silber, D. Dudek, S. Fort, F. Schiele, K. Zmudka, G. Guagliumi, and M. E. Russell. Randomized study to assess the effectiveness of slow- and moderate-release polymer-based paclitaxel-eluting stents for coronary artery lesions. *Circulation*, 108(7):788–794, 2003.

[86] S. J. Park, W. H. Shim, D. S. Ho, A. E. Raizner, S. W. Park, M. K. Hong, C. W. Lee, D. Choi, Y. Jang, R. Lam, N. J. Weissman, and G. S. Mintz. A paclitaxel-eluting stent for the prevention of coronary restenosis. *N Engl J Med*, 348(16):1537–1545, 2003.

[87] M. A. Costa, M. Sabat, W. J. van der Giessen, I. P. Kay, P. Cervinka, J. M. Ligthart, P. Serrano, V. L. Coen, P. C. Levendag, and P. W. Serruys. Late coronary occlusion after intracoronary brachytherapy. *Circulation*, 100(8):789–792, 1999.

[88] R. Waksman. Late thrombosis after radiation. sitting on a time bomb. *Circulation*, 100(8):780–782, 1999.

[89] A. Farb, S. Shroff, M. John, W. Sweet, and R. Virmani. Late arterial responses (6 and 12 months) after (32)P beta-emitting stent placement: sustained intimal suppression with incomplete healing. *Circulation*, 103(14):1912–1919, 2001.

[90] F. Liistro and A. Colombo. Late acute thrombosis after paclitaxel eluting stent implantation. *Heart*, 86(3):262–264, 2001.

[91] A. Farb, P. F. Heller, S. Shroff, L. Cheng, F. D. Kolodgie, A. J. Carter, D. S. Scott, J. Froehlich, and R. Virmani. Pathological analysis of local delivery of paclitaxel via a polymer-coated stent. *Circulation*, 104(4):473–479, 2001.

[92] M. Guba, P. von Breitenbuch, M. Steinbauer, G. Koehl, S. Flegel, M. Hornung, C. J. Bruns, C. Zuelke, S. Farkas, M. Anthuber, K. W. Jauch, and E. K. Geissler. Rapamycin inhibits primary and metastatic tumor growth by antiangiogenesis: involvement of vascular endothelial growth factor. *Nat. Med.*, 8(2):128–135, 2002.

[93] F. Liistro, G. Stankovic, C. Di Mario, T. Takagi, A. Chieffo, S. Moshiri, M. Montorfano, M. Carlino, C. Briguori, P. Pagnotta, R. Albiero, N. Corvaja, and A. Colombo. First clinical experience with a paclitaxel derivate-eluting polymer stent system implantation for in-stent restenosis: immediate and long-term clinical and angiographic outcome. *Circulation*, 105(16):1883–1886, 2002.

[94] R. Virmani, F. Liistro, G. Stankovic, C. Di Mario, M. Montorfano, A. Farb, F. D. Kolodgie, and A. Colombo. Mechanism of late in-stent restenosis after implantation of a paclitaxel derivate-eluting polymer stent system in humans. *Circulation*, 106(21):2649–2651, 2002.

[95] J. Gross and C. M. Lapiere.

[96] J. J. Jeffrey and J. Gross. Collagenase from rat uterus. isolation and partial characterization. *Biochemistry*, 9(2):268–273, 1970.

[97] R. P. Somerville, S. A. Oblander, and S. S. Apte. Matrix metalloproteinases: old dogs with new tricks. *Genome Biol.*, 4(6):216, 2003.

[98] R. H. Gross, L. A. Sheldon, C. F. Fletcher, and C. E. Brinckerhoff. Isolation of a collagenase cDNA clone and measurement of changing collagenase mRNA levels during induction in rabbit synovial fibroblasts. *Proc. Natl. Acad. Sci. USA*, 81(7):1981–1985, 1984.

[99] A. M. Pendas, M. Balbin, E. Llano, M. G. Jimenez, and C. Lopez-Otin. Structural analysis and promoter characterization of the human collagenase-3 gene (MMP13). *Genomics*, 40(2):222–233, 1997.

[100] S. D. Shapiro. Matrix metalloproteinase degradation of extracellular matrix: biological consequences. *Curr. Opin. Cell. Biol.*, 10(5):602–608, 1998.

[101] I. Massova, L. P. Kotra, R. Fridman, and S. Mobashery. Matrix metalloproteinases: structures, evolution, and diversification. *Faseb J.*, 12(12):1075–1095, 1998.

[102] I. E. Collier, G. A. Bruns, G. I. Goldberg, and D. S. Gerhard. On the structure and chromosome location of the 72- and 92-kDa human type IV collagenase genes. *Genomics*, 9(3):429–434, 1991.

[103] C. E. Brinckerhoff and L. M. Matrisian. Matrix metalloproteinases: a tail of a frog that became a prince. *Nat. Rev. Mol. Cell. Biol.*, 3(3):207–214, 2002.

[104] H. E. Van Wart and H. Birkedal-Hansen. The cysteine switch: a principle of regulation of metalloproteinase activity with potential applicability to the entire matrix metalloproteinase gene family. *Proc. Natl. Acad. Sci USA*, 87(14):5578–5582, 1990.

[105] K. Brew, D. Dinakarpandian, and H. Nagase. Tissue inhibitors of metalloproteinases: evolution, structure and function. *Biochim. Biophys. Acta*, 1477(1-2):267–283, 2000.

[106] A. H. Baker, D. R. Edwards, and G. Murphy. Metalloproteinase inhibitors: biological actions and therapeutic opportunities. *J. Cell Sci.*, 115(Pt 19):3719–3727, 2002.

[107] Z. Werb. Ecm and cell surface proteolysis: regulating cellular ecology. *Cell*, 91(4):439–442, 1997.

[108] A. J. Gearing, P. Beckett, M. Christodoulou, M. Churchill, J. Clements, A. H. Davidson, A. H. Drummond, W. A. Galloway, R. Gilbert, J. L. Gordon, and et al. Processing of tumour necrosis factor-alpha precursor by metalloproteinases. *Nature*, 370(6490):555–557, 1994.

[109] E. Levi, R. Fridman, H. Q. Miao, Y. S. Ma, A. Yayon, and I. Vlodavsky. Matrix metalloproteinase 2 releases active soluble ectodomain of fibroblast growth factor receptor 1. *Proc. Natl. Acad. Sci. USA*, 93(14):7069–7074, 1996.

[110] H. R. Lijnen, F. Ugwu, A. Bini, and D. Collen. Generation of an angiostatin-like fragment from plasminogen by stromelysin-1 (MMP-3). *Biochemistry*, 37(14):4699–4702, 1998.

[111] F. Ugwu, B. Van Hoef, A. Bini, D. Collen, and H. R. Lijnen. Proteolytic cleavage of urokinase-type plasminogen activator by stromelysin-1 (MMP-3). *Biochemistry*, 37(20):7231–7236, 1998.

[112] C. Fernandez-Patron, M. W. Radomski, and S. T. Davidge. Vascular matrix metalloproteinase-2 cleaves big endothelin-1 yielding a novel vasoconstrictor. *Circ. Res.*, 85(10):906–911, 1999.

[113] H. G. Welgus, G. P. Stricklin, A. Z. Eisen, E. A. Bauer, R. V. Cooney, and J. J. Jeffrey. A specific inhibitor of vertebrate collagenase produced by human skin fibroblasts. *J. Biol. Chem.*, 254(6):1938–1943, 1979.

[114] A. J. Docherty, A. Lyons, B. J. Smith, E. M. Wright, P. E. Stephens, T. J. Harris, G. Murphy, and J. J. Reynolds. Sequence of human tissue inhibitor of metalloproteinases and its identity to erythroid-potentiating activity. *Nature*, 318(6041):66–69, 1985.

[115] S. J. George. Tissue inhibitors of metalloproteinases and metalloproteinases in atherosclerosis. *Curr Opin Lipidol*, 9(5):413–423, 1998.

[116] E. E. Creemers, J. P. Cleutjens, J. F. Smits, and M. J. Daemen. Matrix metalloproteinase inhibition after myocardial infarction: a new approach to prevent heart failure? *Circ. Res.*, 89(3):201–210, 2001.

[117] R. Pyo, J. K. Lee, J. M. Shipley, J. A. Curci, D. Mao, S. J. Ziporin, T. L. Ennis, S. D. Shapiro, R. M. Senior, and R. W. Thompson. Targeted gene disruption of matrix metalloproteinase-9 (gelatinase B) suppresses development of experimental abdominal aortic aneurysms. *J. Clin. Invest.*, 105(11):1641–1649, 2000.

[118] M. P. Bendeck, N. Zempo, A. W. Clowes, R. E. Galardy, and M. A. Reidy. Smooth muscle cell migration and matrix metalloproteinase expression after arterial injury in the rat. *Circ. Res.*, 75(3):539–545, 1994.

[119] N. Zempo, R. D. Kenagy, Y. P. Au, M. Bendeck, M. M. Clowes, M. A. Reidy, and A. W. Clowes. Matrix metalloproteinases of vascular wall cells are increased in balloon-injured rat carotid artery. *J. Vasc. Surg.*, 20(2):209–217, 1994.

[120] S. J. George, A. B. Zaltsman, and A. C. Newby. Surgical preparative injury and neointima formation increase MMP-9 expression and MMP-2 activation in human saphenous vein. *Cardiovasc. Res.*, 33(2):447–459, 1997.

[121] M. Rouis, C. Adamy, N. Duverger, P. Lesnik, P. Horellou, M. Moreau, F. Emmanuel, J. M. Caillaud, P. M. Laplaud, C. Dachet, and M. J. Chapman. Adenovirus-mediated overexpression of tissue inhibitor of metalloproteinase-1 reduces atherosclerotic lesions in apolipoprotein E-deficient mice. *Circulation*, 100(5):533–540, 1999.

[122] C. Furman, Z. Luo, K. Walsh, N. Duverger, C. Copin, J. C. Fruchart, and M. Rouis. Systemic tissue inhibitor of metalloproteinase-1 gene delivery reduces neointimal hyperplasia in balloon-injured rat carotid artery. *FEBS Lett.*, 531(2):122–126, 2002.

[123] L. Cheng, G. Mantile, R. Pauly, C. Nater, A. Felici, R. Monticone, C. Bilato, Y. A. Gluzband, M. T. Crow, W. Stetler-Stevenson, and M. C. Capogrossi. Adenovirus-mediated gene transfer of the human tissue inhibitor of metalloproteinase-2 blocks vascular smooth muscle cell invasiveness in vitro and modulates neointimal development in vivo. *Circulation*, 98(20):2195–2201, 1998.

[124] C. M. Dollery, S. E. Humphries, A. McClelland, D. S. Latchman, and J. R. McEwan. Expression of tissue inhibitor of matrix metalloproteinases 1 by use of an adenoviral vector inhibits smooth muscle cell migration and reduces neointimal hyperplasia in the rat model of vascular balloon injury. *Circulation*, 99(24):3199–3205, 1999.

[125] S. J. George, J. L. Johnson, G. D. Angelini, A. C. Newby, and A. H. Baker. Adenovirus-mediated gene transfer of the human timp-1 gene inhibits smooth muscle cell migration and neointimal formation in human saphenous vein. *Hum. Gene Ther.*, 9(6):867–877, 1998.

[126] S. J. George, A. H. Baker, G. D. Angelini, and A. C. Newby. Gene transfer of tissue inhibitor of metalloproteinase-2 inhibits metalloproteinase activity and neointima formation in human saphenous veins. *Gene Ther.*, 5(11):1552–1560, 1998.

[127] S. J. George, C. T. Lloyd, G. D. Angelini, A. C. Newby, and A. H. Baker. Inhibition of late vein graft neointima formation in human and porcine models by adenovirus-mediated overexpression of tissue inhibitor of metalloproteinase-3. *Circulation*, 101(3):296–304, 2000.

[128] R. Forough, N. Koyama, D. Hasenstab, H. Lea, M. Clowes, S. T. Nikkari, and A. W. Clowes. Overexpression of tissue inhibitor of matrix metalloproteinase-1 inhibits vascular smooth muscle cell functions in vitro and in vivo. *Circ. Res.*, 79(4):812–820, 1996.

[129] E. Marshall. Gene therapy death prompts review of adenovirus vector. *Science*, 286(5448):2244–2245, 1999.

[130] J. Silence, D. Collen, and H. R. Lijnen. Reduced atherosclerotic plaque but enhanced aneurysm formation in mice with inactivation of the tissue inhibitor of metalloproteinase-1 (TIMP-1) gene. *Circ. Res.*, 90(8):897–903, 2002.

[131] V. Lemaitre, P. D. Soloway, and J. D'Armiento. Increased medial degradation with pseudo-aneurysm formation in apolipoprotein E-knockout mice deficient in tissue inhibitor of metalloproteinases-1. *Circulation*, 107(2):333–338, 2003.

[132] M. P. Bendeck, C. Irvin, and M. A. Reidy. Inhibition of matrix metalloproteinase activity inhibits smooth muscle cell migration but not neointimal thickening after arterial injury. *Circ. Res.*, 78(1):38–43, 1996.

[133] B. J. de Smet, D. de Kleijn, R. Hanemaaijer, J. H. Verheijen, L. Robertus, Y. J. van Der Helm, C. Borst, and M. J. Post. Metalloproteinase inhibition reduces constrictive arterial remodeling after balloon angioplasty: a study in the atherosclerotic yucatan micropig. *Circulation*, 101(25):2962–2967, 2000.

[134] T. H. Lee, G. W. Lee, E. B. Ziff, and J. Vilcek. Isolation and characterization of eight tumor necrosis factor-induced gene sequences from human fibroblasts. *Mol. Cell. Biol.*, 10(5):1982–1988, 1990.

[135] F. Breviario, E. M. d'Aniello, J. Golay, G. Peri, B. Bottazzi, A. Bairoch, S. Saccone, R. Marzella, V. Predazzi, M. Rocchi, and et al. Interleukin-1-inducible genes in endothelial cells. cloning of a new gene related to C-reactive protein and serum amyloid P component. *J. Biol. Chem.*, 267(31):22190–22197, 1992.

[136] A. Basile, A. Sica, E. d'Aniello, F. Breviario, G. Garrido, M. Castellano, A. Mantovani, and M. Introna. Characterization of the promoter for the human long pentraxin PTX3. role of NF-kappa-B in tumor necrosis factor-alpha and interleukin-1-beta regulation. *J. Biol. Chem.*, 272(13):8172–8178, 1997.

[137] B. Bottazzi, V. Vouret-Craviari, A. Bastone, L. De Gioia, C. Matteucci, G. Peri, F. Spreafico, M. Pausa, C. D'Ettorre, E. Gianazza, A. Tagliabue, M. Salmona, F. Tedesco, M. Introna, and A. Mantovani. Multimer formation and ligand recognition by the long pentraxin PTX3. similarities and differences with the short pentraxins C-reactive protein and serum amyloid P component. *J. Biol. Chem.*, 272(52):32817–32823, 1997.

[138] C. Garlanda, E. Hirsch, S. Bozza, A. Salustri, M. De Acetis, R. Nota, A. Maccagno, F. Riva, B. Bottazzi, G. Peri, A. Doni, L. Vago, M. Botto, R. De Santis, P. Carminati, G. Siracusa, F. Altruda, A. Vecchi, L. Romani, and A. Mantovani. Non-redundant role of the long pentraxin PTX3 in anti-fungal innate immune response. *Nature*, 420(6912):182–186, 2002.

[139] M. S. Rolph, S. Zimmer, B. Bottazzi, C. Garlanda, A. Mantovani, and G. K. Hansson. Production of the long pentraxin PTX3 in advanced atherosclerotic plaques. *Arterioscler. Thromb. Vasc. Biol.*, 22(5):e10–14, 2002.

[140] G. Peri, M. Introna, D. Corradi, G. Iacuitti, S. Signorini, F. Avanzini, F. Pizzetti, A. P. Maggioni, T. Moccetti, M. Metra, L. D. Cas, P. Ghezzi, J. D. Sipe, G. Re, G. Olivetti, A. Mantovani, and R. Latini. PTX3, a prototypical long pentraxin, is an early indicator of acute myocardial infarction in humans. *Circulation*, 102(6):636–641, 2000.

[141] E. G. Nabel, G. Plautz, F. M. Boyce, J. C. Stanley, and G. J. Nabel. Recombinant gene expression in vivo within endothelial cells of the arterial wall. *Science*, 244(4910):1342–1344, 1989.

[142] M. J. Mann, G. H. Gibbons, P. S. Tsao, H. E. von der Leyen, J. P. Cooke, R. Buitrago, R. Kernoff, and V. J. Dzau. Cell cycle inhibition preserves endothelial function in genetically engineered rabbit vein grafts. *J. Clin. Invest.*, 99(6):1295–1301, 1997.

[143] R. Morishita. Lessons from human arteries: how to design a gene therapy strategy for treatment of cardiovascular disease. *Circ. Res.*, 82(12):1349–1351, 1998.

[144] A. Lafont, G. Loirand, P. Pacaud, F. Vilde, P. Lemarchand, and D. Escande. Vasomotor dysfunction early after exposure of normal rabbit arteries to an adenoviral vector. *Hum. Gene Ther.*, 8(9):1033–1040, 1997.

[145] K. M. Channon, H. S. Qian, S. A. Youngblood, E. Olmez, G. A. Shetty, V. Nepliouéva, M. A. Blazing, and S. E. George. Acute host-mediated endothelial injury after adenoviral gene transfer in normal rabbit arteries: impact on transgene expression and endothelial function. *Circ. Res.*, 82(12):1253–1262, 1998.

[146] G. H. Gibbons and V. J. Dzau. The emerging concept of vascular remodeling. *N Engl J Med*, 330(20):1431–1438, 1994.

[147] M. D. Rekhter, R. D. Simari, C. W. Work, G. J. Nabel, E. G. Nabel, and D. Gordon. Gene transfer into normal and atherosclerotic human blood vessels. *Circ. Res.*, 82(12):1243–1252, 1998.

[148] T. Ohno, D. Gordon, H. San, V. J. Pompili, M. J. Imperiale, G. J. Nabel, and E. G. Nabel. Gene therapy for vascular smooth muscle cell proliferation after arterial injury. *Science*, 265(5173):781–784, 1994.

[149] R. J. Guzman, E. A. Hirschowitz, S. L. Brody, R. G. Crystal, S. E. Epstein, and T. Finkel. In vivo suppression of injury-induced vascular smooth muscle cell accumulation using adenovirus-mediated transfer of the herpes simplex virus thymidine kinase gene. *Proc. Natl. Acad. Sci. USA*, 91(22):10732–10736, 1994.

[150] R. D. Simari, H. San, M. Rekhter, T. Ohno, D. Gordon, G. J. Nabel, and E. G. Nabel. Regulation of cellular proliferation and intimal formation following balloon injury in atherosclerotic rabbit arteries. *J. Clin. Invest.*, 98(1):225–235, 1996.

[151] P. G. Steg, O. Tahlil, N. Aubailly, J. M. Caillaud, J. F. Dedieu, K. Berthelot, A. Le Roux, L. Feldman, M. Perricaudet, P. Denefle, and D. Branellec. Reduction of restenosis after angioplasty in an atheromatous rabbit model by suicide gene therapy. *Circulation*, 96(2):408–411, 1997.

[152] M. W. Chang, E. Barr, J. Seltzer, Y. Q. Jiang, G. J. Nabel, E. G. Nabel, M. S. Parmacek, and J. M. Leiden. Cytostatic gene therapy for vascular proliferative disorders with a constitutively active form of the retinoblastoma gene product. *Science*, 267(5197):518–522, 1995.

[153] R. C. Smith, K. N. Wills, D. Antelman, H. Perlman, L. N. Truong, K. Krasinski, and K. Walsh. Adenoviral constructs encoding phosphorylation-competent full-length and truncated forms of the human retinoblastoma protein inhibit myocyte proliferation and neointima formation. *Circulation*, 96(6):1899–1905, 1997.

[154] P. P. Claudio, L. Fratta, F. Farina, C. M. Howard, G. Stassi, S. Numata, C. Pacilio, A. Davis, M. Lavitrano, M. Volpe, J. M. Wilson, B. Trimarco, A. Giordano, and G. Condorelli. Adenoviral RB2/p130 gene transfer inhibits smooth muscle cell proliferation and prevents restenosis after angioplasty. *Circ. Res.*, 85(11):1032–1039, 1999.

[155] M. W. Chang, E. Barr, M. M. Lu, K. Barton, and J. M. Leiden. Adenovirus-mediated overexpression of the cyclin/cyclin-dependent kinase inhibitor, p21 inhibits vascular smooth muscle cell proliferation and neointima formation in the rat carotid artery model of balloon angioplasty. *J. Clin. Invest.*, 96(5):2260–2268, 1995.

[156] Z. Y. Yang, R. D. Simari, N. D. Perkins, H. San, D. Gordon, G. J. Nabel, and E. G. Nabel. Role of the p21 cyclin-dependent kinase inhibitor in limiting intimal cell proliferation in response to arterial injury. *Proc. Natl. Acad. Sci. USA*, 93(15):7905–7910, 1996.

[157] H. Ueno, S. Masuda, S. Nishio, J. J. Li, H. Yamamoto, and A. Takeshita. Adenovirus-mediated transfer of cyclin-dependent kinase inhibitor-p21 suppresses neointimal formation in the balloon-injured rat carotid arteries in vivo. *Ann. N. Y. Acad. Sci.*, 811:401–411, 1997.

[158] Z. Luo, M. Sata, T. Nguyen, J. M. Kaplan, G. Y. Akita, and K. Walsh. Adenovirus-mediated delivery of fas ligand inhibits intimal hyperplasia after balloon injury in immunologically primed animals. *Circulation*, 99(14):1776–1779, 1999.

[159] D. Chen, K. Krasinski, A. Sylvester, J. Chen, P. D. Nisen, and V. Andres. Downregulation of cyclin-dependent kinase 2 activity and cyclin a promoter activity in vascular smooth muscle cells by p27(KIP1), an inhibitor of neointima formation in the rat carotid artery. *J. Clin. Invest.*, 99(10):2334–2341, 1997.

[160] Y. Yonemitsu, Y. Kaneda, S. Tanaka, Y. Nakashima, K. Komori, K. Sugimachi, and K. Sueishi. Transfer of wild-type p53 gene effectively inhibits vascular smooth muscle cell proliferation in vitro and in vivo. *Circ. Res.*, 82(2):147–156, 1998.

[161] M. Scheinman, E. Ascher, G. S. Levi, A. Hingorani, D. Shirazian, and P. Seth. p53 gene transfer to the injured rat carotid artery decreases neointimal formation. *J. Vasc. Surg.*, 29(2):360–369, 1999.

[162] Y. Shi, A. Fard, A. Galeo, H. G. Hutchinson, P. Vermani, G. R. Dodge, D. J. Hall, F. Shaheen, and A. Zalewski. Transcatheter delivery of c-myc antisense oligomers reduces neointimal formation in a porcine model of coronary artery balloon injury. *Circulation*, 90(2):944–951, 1994.

[163] M. Kibbe, T. Billiar, and E. Tzeng. Gene therapy and vascular disease. *Adv. Pharmacol.*, 46:85–150, 1999.

[164] H. Ueno, H. Yamamoto, S. Ito, J. J. Li, and A. Takeshita. Adenovirus-mediated transfer of a dominant-negative h-ras suppresses neointimal formation in balloon-injured arteries in vivo. *Arterioscler. Thromb. Vasc. Biol.*, 17(5):898–904, 1997.

[165] C. L. Cioffi, M. Garay, J. F. Johnston, K. McGraw, R. T. Boggs, D. Hreniuk, and B. P. Monia. Selective inhibition of A-raf and C-Raf mRNA expression by antisense oligodeoxynucleotides in rat vascular smooth muscle cells: role of A-Raf and C-Raf in serum-induced proliferation. *Mol. Pharmacol.*, 51(3):383–389, 1997.

[166] M. V. Autieri, T. L. Yue, G. Z. Ferstein, and E. Ohlstein. Antisense oligonucleotides to the p65 subunit of NF-kB inhibit human vascular smooth muscle cell adherence and proliferation and prevent neointima formation in rat carotid arteries. *Biochem. Biophys. Res. Commun.*, 213(3):827–836, 1995.

[167] R. Morishita, G. H. Gibbons, M. Horiuchi, K. E. Ellison, M. Nakama, L. Zhang, Y. Kaneda, T. Ogihara, and V. J. Dzau. A gene therapy strategy using a transcription factor decoy of the E2F binding site inhibits smooth muscle proliferation in vivo. *Proc. Natl. Acad. Sci. USA*, 92(13):5855–5859, 1995.

[168] L. Maillard, E. Van Belle, R. C. Smith, A. Le Roux, P. Denefle, G. Steg, J. J. Barry, D. Branellec, J. M. Isner, and K. Walsh. Percutaneous delivery of the gax gene inhibits vessel stenosis in a rabbit model of balloon angioplasty. *Cardiovasc. Res.*, 35(3):536–546, 1997.

[169] T. Mano, Z. Luo, S. L. Malendowicz, T. Evans, and K. Walsh. Reversal of GATA-6 downregulation promotes smooth muscle differentiation and inhibits intimal hyperplasia in balloon-injured rat carotid artery. *Circ. Res.*, 84(6):647–654, 1999.

[170] D. Stephan, H. San, Z. Y. Yang, D. Gordon, S. Goelz, G. J. Nabel, and E. G. Nabel. Inhibition of vascular smooth muscle cell proliferation and intimal hyperplasia by gene transfer of beta-interferon. *Mol. Med.*, 3(9):593–599, 1997.

[171] E. Van Belle, L. Maillard, F. O. Tio, and J. M. Isner. Accelerated endothelialization by local delivery of recombinant human vascular endothelial growth factor reduces in-stent intimal formation. *Biochem. Biophys. Res. Commun.*, 235(2):311–316, 1997.

[172] A. K. Hanna, J. C. Fox, D. G. Neschis, S. D. Safford, J. L. Swain, and M. A. Golden. Antisense basic fibroblast growth factor gene transfer reduces neointimal thickening after arterial injury. *J. Vasc. Surg.*, 25(2):320–325, 1997.

[173] M. G. Sirois, M. Simons, and E. R. Edelman. Antisense oligonucleotide inhibition of PDGFR-beta receptor subunit expression directs suppression of intimal thickening. *Circulation*, 95(3):669–676, 1997.

[174] J. Deguchi, T. Namba, H. Hamada, T. Nakaoka, J. Abe, O. Sato, T. Miyata, M. Makuuchi, K. Kurokawa, and Y. Takuwa. Targeting endogenous platelet-derived growth factor B-chain by adenovirus-mediated gene transfer potently inhibits in vivo smooth muscle proliferation after arterial injury. *Gene Ther.*, 6(6):956–965, 1999.

[175] H. E. von der Leyen, G. H. Gibbons, R. Morishita, N. P. Lewis, L. Zhang, M. Nakajima, Y. Kaneda, J. P. Cooke, and V. J. Dzau. Gene therapy inhibiting neointimal vascular lesion: in vivo transfer of endothelial cell nitric oxide synthase gene. *Proc. Natl. Acad. Sci. USA*, 92(4):1137–1141, 1995.

[176] L. Chen, G. Daum, R. Forough, M. Clowes, U. Walter, and A. W. Clowes. Overexpression of human endothelial nitric oxide synthase in rat vascular smooth muscle cells and in balloon-injured carotid artery. *Circ. Res.*, 82(8):862–870, 1998.

[177] S. Janssens, D. Flaherty, Z. Nong, O. Varenne, N. van Pelt, C. Haustermans, P. Zoldhelyi, R. Gerard, and D. Collen. Human endothelial nitric oxide synthase gene transfer inhibits vascular smooth muscle cell proliferation and neointima formation after balloon injury in rats. *Circulation*, 97(13):1274–1281, 1998.

[178] O. Varenne, S. Pislaru, H. Gillijns, N. Van Pelt, R. D. Gerard, P. Zoldhelyi, F. Van de Werf, D. Collen, and S. P. Janssens. Local adenovirus-mediated transfer of human endothelial nitric oxide synthase reduces luminal narrowing after coronary angioplasty in pigs. *Circulation*, 98(9):919–926, 1998.

[179] 2nd Shears, L. L., M. R. Kibbe, A. D. Murdock, T. R. Billiar, A. Lizonova, I. Kovesdi, S. C. Watkins, and E. Tzeng. Efficient inhibition of intimal hyperplasia by adenovirus-mediated inducible nitric oxide synthase gene transfer to rats and pigs in vivo. *J. Am. Coll. Surg.*, 187(3):295–306, 1998.

[180] M. Hedman, J. Hartikainen, M. Syvanne, J. Stjernvall, A. Hedman, A. Kivela, E. Vanninen, H. Mussalo, E. Kauppila, S. Simula, O. Narvanen, A. Rantala, K. Peuhkurinen, M. S. Nieminen, M. Laakso, and S. Yla-Herttuala. Safety and feasibility of catheter-based local intracoronary vascular endothelial growth factor gene transfer in the prevention of postangioplasty and in-stent restenosis and in the treatment of chronic myocardial ischemia: phase ii results of the kuopio angiogenesis trial (kat). *Circulation*, 107(21):2677–2683, 2003.

[181] D. W. Losordo, J. M. Isner, and L. J. Diaz-Sandoval. Endothelial recovery: the next target in restenosis prevention. *Circulation*, 107(21):2635–2637, 2003.

[182] G. Siegl, R. C. Bates, K. I. Berns, B. J. Carter, D. C. Kelly, E. Kurstak, and P. Tattersall. Characteristics and taxonomy of parvoviridae. *Intervirology*, 23(2):61–73, 1985.

[183] R. M. Buller, J. E. Janik, E. D. Sebring, and J. A. Rose. Herpes simplex virus types 1 and 2 completely help adenovirus-associated virus replication. *J. Virol.*, 40(1):241–247, 1981.

[184] H. D. Mayor and J. L. Melnick. Small deoxyribonucleic acid-containing viruses (picodnavirus group). *Nature*, 210(33):331–332, 1966.

[185] G. Gao, M. R. Alvira, S. Somanathan, Y. Lu, L. H. Vandenberghe, J. J. Rux, R. Calcedo, J. Sanmiguel, Z. Abbas, and J. M. Wilson. Adeno-associated viruses undergo substantial evolution in primates during natural infections. *Proc. Natl. Acad. Sci. USA*, 100(10):6081–6086, 2003.

[186] BernsKI. *Parvoviridae and their replication. Virology*, volume 158. Raven, New York, 1992.

[187] A. Srivastava. Replication of the adeno-associated virus dna termini in vitro. *Intervirology*, 27(3):138–147, 1987.

[188] R. J. Samulski, A. Srivastava, K. I. Berns, and N. Muzyczka. Rescue of adeno-associated virus from recombinant plasmids: gene correction within the terminal repeats of AAV. *Cell*, 33(1):135–43, 1983.

[189] T. R. Flotte, S. A. Afione, R. Solow, M. L. Drumm, D. Markakis, W. B. Guggino, P. L. Zeitlin, and B. J. Carter. Expression of the cystic fibrosis transmembrane conductance regulator from a novel adeno-associated virus promoter. *J. Biol. Chem.*, 268(5):3781–3790, 1993.

[190] Q. Xie, W. Bu, S. Bhatia, J. Hare, T. Somasundaram, A. Azzi, and M. S. Chapman. The atomic structure of adeno-associated virus (aav-2), a vector for human gene therapy. *Proc. Natl. Acad. Sci. USA*, 99(16):10405–10410, 2002.

[191] A. Srivastava, E. W. Lusby, and K. I. Berns. Nucleotide sequence and organization of the adeno-associated virus 2 genome. *J. Virol.*, 45(2):555–564, 1983.

[192] P. L. Hermonat and N. Muzyczka. Use of adeno-associated virus as a mammalian DNA cloning vector: transduction of neomycin resistance into mammalian tissue culture cells. *Proc. Natl. Acad. Sci. USA*, 81(20):6466–6470, 1984.

[193] K. I. Berns and C. Giraud. Biology of adeno-associated virus. *Curr Top Microbiol Immunol*, 218:1–23, 1996.

[194] Thomas FB Johnson FB Hoggan MD, Thomas GF. Continous "carriage" of adenovirus associated genome in cell cultures in the absence of helper adenovirus. In *Proceedeings of the 4th Lepetit Colloquium*, Cocoyac, Mexico, 1972. Proceedeings of the 4th Lepetit Colloquium, North Holland Publishing Co., Amsterdan.

[195] H. Handa, K. Shiroki, and H. Shimojo. Establishment and characterization of KB cell lines latently infected with adeno-associated virus type 1. *Virology*, 82(1):84–92, 1977.

[196] A. K. Cheung, M. D. Hoggan, W. W. Hauswirth, and K. I. Berns. Integration of the adeno-associated virus genome into cellular DNA in latently infected human Detroit 6 cells. *J. Virol.*, 33(2):739–748, 1980.

[197] N. Muzyczka. Use of adeno-associated virus as a general transduction vector for mammalian cells. *Curr Top Microbiol Immunol*, 158:97–129, 1992.

[198] R. M. Kotin, J. C. Menninger, D. C. Ward, and K. I. Berns. Mapping and direct visualization of a region-specific viral DNA integration site on chromosome 19q13-qter. *Genomics*, 10(3):831–834, 1991.

[199] R. M. Kotin, R. M. Linden, and K. I. Berns. Characterization of a preferred site on human chromosome 19q for integration of adeno-associated virus DNA by non-homologous recombination. *EMBO J.*, 11(13):5071–5078, 1992.

[200] R. J. Samulski. Adeno-associated virus: integration at a specific chromosomal locus. *Curr Opin Genet Dev*, 3(1):74–80, 1993.

[201] C. E. Walsh, J. M. Liu, X. Xiao, N. S. Young, A. W. Nienhuis, and R. J. Samulski. Regulated high level expression of a human gamma-globin gene introduced into erythroid cells by an adeno-associated virus vector. *Proc. Natl. Acad. Sci. USA*, 89(15):7257–7261, 1992.

[202] R. T. Surosky, M. Urabe, S. G. Godwin, S. A. McQuiston, G. J. Kurtzman, K. Ozawa, and G. Natsoulis. Adeno-associated virus rep proteins target dna sequences to a unique locus in the human genome. *J Virol*, 71(10):7951–7959, 1997.

[203] S. Lamartina, G. Roscilli, D. Rinaudo, P. Delmastro, and C. Toniatti. Lipofection of purified adeno-associated virus rep68 protein: toward a chromosome-targeting nonviral particle. *J Virol*, 72(9):7653–7658, 1998.

[204] M. D. Hoggan, N. R. Blacklow, and W. P. Rowe. Studies of small DNA viruses found in various adenovirus preparations: physical, biological, and immunological characteristics. *Proc. Natl. Acad. Sci. USA*, 55(6):1467–1474, 1966.

[205] S. E. Straus, E. D. Sebring, and J. A. Rose. Concatemers of alternating plus and minus strands are intermediates in adenovirus-associated virus DNA synthesis. *Proc. Natl. Acad. Sci. USA*, 73(3):742–746, 1976.

[206] K. I. Berns. Parvovirus replication. *Microbiol. Rev.*, 54(3):316–329, 1990.

[207] G. Seisenberger, M. U. Ried, T. Endress, H. Buning, M. Hallek, and C. Brauchle. Real-time single-molecule imaging of the infection pathway of an adeno-associated virus. *Science*, 294(5548):1929–1932, 2001.

[208] J. S. Bartlett, R. Wilcher, and R. J. Samulski. Infectious entry pathway of adeno-associated virus and adeno-associated virus vectors. *J. Virol.*, 74(6):2777–2785, 2000.

[209] C. Summerford and R. J. Samulski. Membrane-associated heparan sulfate proteoglycan is a receptor for adeno-associated virus type 2 virions. *J. Virol.*, 72(2):1438–1445, 1998.

[210] K. Qing, C. Mah, J. Hansen, S. Zhou, V. Dwarki, and A. Srivastava. Human fibroblast growth factor receptor 1 is a co-receptor for infection by adeno-associated virus 2. *Nat. Med.*, 5(1):71–77, 1999.

[211] C. Summerford, J. S. Bartlett, and R. J. Samulski. Alphavbeta5 integrin: a co-receptor for adeno-associated virus type 2 infection. *Nat. Med.*, 5(1):78–82, 1999.

[212] D. Duan, Q. Li, A. W. Kao, Y. Yue, J. E. Pessin, and J. F. Engelhardt. Dynamin is required for recombinant adeno-associated virus type 2 infection. *J Virol*, 73(12):10371–10376, 1999.

[213] A. M. Douar, K. Poulard, D. Stockholm, and O. Danos. Intracellular trafficking of adeno-associated virus vectors: routing to the late endosomal compartment and proteasome degradation. *J Virol*, 75(4):1824–1833, 2001.

[214] J. Hansen, K. Qing, and A. Srivastava. Adeno-associated virus type 2-mediated gene transfer: altered endocytic processing enhances transduction efficiency in murine fibroblasts. *J. Virol.*, 75(9):4080–4090, 2001.

[215] S. Sanlioglu, P. K. Benson, J. Yang, E. M. Atkinson, T. Reynolds, and J. F. Engelhardt. Endocytosis and nuclear trafficking of adeno-associated virus type 2 are controlled by rac1 and phosphatidylinositol-3 kinase activation. *J Virol*, 74(19):9184–9196, 2000.

[216] B. Sodeik, M. W. Ebersold, and A. Helenius. Microtubule-mediated transport of incoming herpes simplex virus 1 capsids to the nucleus. *J. Cell. Biol.*, 136(5):1007–1021, 1997.

[217] M. Suomalainen, M. Y. Nakano, S. Keller, K. Boucke, R. P. Stidwill, and U. F. Greber. Microtubule-dependent plus- and minus end-directed motilities are competing processes for nuclear targeting of adenovirus. *J. Cell. Biol.*, 144(4):657–672, 1999.

[218] W. Xiao, Jr. Warrington, K. H., P. Hearing, J. Hughes, and N. Muzyczka. Adenovirus-facilitated nuclear translocation of adeno-associated virus type 2. *J Virol*, 76(22):11505–11517, 2002.

[219] P. E. Monahan and R. J. Samulski. Aav vectors: is clinical success on the horizon? *Gene Ther.*, 7(1):24–30, 2000.

[220] C. S. Manno, A. J. Chew, S. Hutchison, P. J. Larson, R. W. Herzog, V. R. Arruda, S. J. Tai, M. V. Ragni, A. Thompson, M. Ozelo, L. B. Couto, D. G. Leonard, F. A. Johnson, A. McClelland, C. Scallan, E. Skarsgard, A. W. Flake, M. A. Kay, K. A. High, and B. Glader. Aav-mediated factor ix gene transfer to skeletal muscle in patients with severe hemophilia b. *Blood*, 101(8):2963–2972, 2003.

[221] L. H. McGee Sanftner, K. G. Rendahl, D. Quiroz, M. Coyne, M. Ladner, W. C. Manning, and J. G. Flannery. Recombinant aav-mediated delivery of a tet-inducible reporter gene to the rat retina. *Mol Ther*, 3(5 Pt 1):688–696, 2001.

[222] J. W. Bainbridge, A. Mistry, K. Binley, M. De Alwis, A. J. Thrasher, S. Naylor, and R. R. Ali. Hypoxia-regulated transgene expression in experimental retinal and choroidal neovascularization. *Gene Ther*, 10(12):1049–1054, 2003.

[223] S. Jiang, A. Altmann, D. Grimm, J. A. Kleinschmidt, T. Schilling, C. Germann, and U. Haberkorn. Tissue-specific gene expression in medullary thyroid carcinoma cells employing calcitonin regulatory elements and aav vectors. *Cancer Gene Ther*, 8(7):469–472, 2001.

[224] S. Z. Zhou, H. E. Broxmeyer, S. Cooper, M. A. Harrington, and A. Srivastava. Adeno-associated virus 2-mediated gene transfer in murine hematopoietic progenitor cells. *Exp. Hematol.*, 21(7):928–933, 1993.

[225] E. Mendelson, Z. Grossman, F. Mileguir, G. Rechavi, and B. J. Carter. Replication of adeno-associated virus type 2 in human lymphocytic cells and interaction with HIV-1. *Virology*, 187(2):453–463, 1992.

[226] M. P. Einerhand, M. Antoniou, S. Zolotukhin, N. Muzyczka, K. I. Berns, F. Grosveld, and D. Valerio. Regulated high-level human beta-globin gene expression in erythroid cells following recombinant adeno-associated virus-mediated gene transfer. *Gene Ther.*, 2(5):336–343, 1995.

[227] K. J. Fisher, K. Jooss, J. Alston, Y. Yang, S. E. Haecker, K. High, R. Pathak, S. E. Raper, and J. M. Wilson. Recombinant adeno-associated virus for muscle directed gene therapy. *Nat. Med.*, 3(3):306–312, 1997.

[228] P. D. Kessler, G. M. Podsakoff, X. Chen, S. A. McQuiston, P. C. Colosi, L. A. Matelis, G. J. Kurtzman, and B. J. Byrne. Gene delivery to skeletal muscle results in sustained expression and systemic delivery of a therapeutic protein. *Proc. Natl. Acad. Sci. USA*, 93(24):14082–14087, 1996.

[229] H. Nakai, Y. Iwaki, M. A. Kay, and L. B. Couto. Isolation of recombinant adeno-associated virus vector-cellular DNA junctions from mouse liver. *J. Virol.*, 73(7):5438–5447, 1999.

[230] W. Xiao, S. C. Berta, M. M. Lu, A. D. Moscioni, J. Tazelaar, and J. M. Wilson. Adeno-associated virus as a vector for liver-directed gene therapy. *J. Virol.*, 72(12):10222–10226, 1998.

[231] X. Xiao, J. Li, and R. J. Samulski. Efficient long-term gene transfer into muscle tissue of immunocompetent mice by adeno-associated virus vector. *J Virol*, 70(11):8098–8108, 1996.

[232] X. Xiao, J. Li, T. J. McCown, and R. J. Samulski. Gene transfer by adeno-associated virus vectors into the central nervous system. *Exp. Neurol.*, 144(1):113–124, 1997.

[233] A. Girod, M. Ried, C. Wobus, H. Lahm, K. Leike, J. Kleinschmidt, G. Deleage, and M. Hallek. Genetic capsid modifications allow efficient re-targeting of adeno-associated virus type 2. *Nat Med*, 5(12):1438, 1999.

[234] D. W. Russell. Aav loves an active genome. *Nat Genet*, 34(3):241–242, 2003.

[235] R. J. Samulski, K. I. Berns, M. Tan, and N. Muzyczka. Cloning of adeno-associated virus into pBR322: rescue of intact virus from the recombinant plasmid in human cells. *Proc. Natl. Acad. Sci. USA*, 79(6):2077–2081, 1982.

[236] J. D. Tratschin, M. H. West, T. Sandbank, and B. J. Carter. A human parvovirus, adeno-associated virus, as a eucaryotic vector: transient expression and encapsidation of the procaryotic gene for chloramphenicol acetyltransferase. *Mol. Cell. Biol.*, 4(10):2072–2081, 1984.

[237] T.R. Flotte, B. Carter, C. Conrad, W. Guggino, T.C. Reynolds, B. Rosenstein, G. Tylor, S. Walden, and R. Wetzel.

[238] M. A. Kay, C. S. Manno, M. V. Ragni, and et al. Evidence for gene transfer and expression of factor IX in haemophilia B patients treated with an AAV vector. *Nat. Genet.*, 24(3):257–261, 2000.

[239] J. A. Wagner, I. B. Nepomuceno, A. H. Messner, M. L. Moran, E. P. Batson, S. Dimiceli, B. W. Brown, J. K. Desch, A. M. Norbash, C. K. Conrad, W. B. Guggino, T. R. Flotte, J. J. Wine, B. J. Carter, T. C. Reynolds, R. B. Moss, and P. Gardner. A phase ii, double-blind, randomized, placebo-controlled clinical trial of tgaavcf using maxillary sinus delivery in patients with cystic fibrosis with antrostomies. *Hum Gene Ther*, 13(11):1349–1359, 2002.

[240] M. A. Kay and H. Nakai. Looking into the safety of aav vectors. *Nature*, 424(6946):251, 2003.

[241] R. J. Samulski, L. S. Chang, and T. Shenk. Helper-free stocks of recombinant adeno-associated viruses: normal integration does not require viral gene expression. *J Virol*, 63(9):3822–3828, 1989.

[242] W. T. Hermens, O. ter Brake, P. A. Dijkhuizen, M. A. Sonnemans, D. Grimm, J. A. Kleinschmidt, and J. Verhaagen. Purification of recombinant adeno-associated virus by iodixanol gradient ultracentrifugation allows rapid and reproducible preparation of vector stocks for gene transfer in the nervous system. *Hum Gene Ther*, 10(11):1885–1891, 1999.

[243] K. R. Clark, X. Liu, J. P. McGrath, and P. R. Johnson. Highly purified recombinant adeno-associated virus vectors are biologically active and free of detectable helper and wild-type viruses. *Hum Gene Ther*, 10(6):1031–1039, 1999.

[244] S. Zolotukhin, B. J. Byrne, E. Mason, I. Zolotukhin, M. Potter, K. Chesnut, C. Summerford, R. J. Samulski, and N. Muzyczka. Recombinant adeno-associated virus purification using novel methods improves infectious titer and yield. *Gene Ther*, 6(6):973–985, 1999.

[245] C. R. O'Riordan, A. L. Lachapelle, K. A. Vincent, and S. C. Wadsworth. Scaleable chromatographic purification process for recombinant adeno-associated virus (raav). *J Gene Med*, 2(6):444–454, 2000.

[246] A. Auricchio, M. Hildinger, E. O'Connor, G. P. Gao, and J. M. Wilson. Isolation of highly infectious and pure adeno-associated virus type 2 vectors with a single-step gravity-flow column. *Hum Gene Ther*, 12(1):71–76, 2001.

[247] N. Kaludov, K. E. Brown, R. W. Walters, J. Zabner, and J. A. Chiorini. Adeno-associated virus serotype 4 (aav4) and aav5 both require sialic acid binding for hemagglutination and efficient transduction but differ in sialic acid linkage specificity. *J Virol*, 75(15):6884–6893, 2001.

[248] E. A. Rutledge, C. L. Halbert, and D. W. Russell. Infectious clones and vectors derived from adeno-associated virus (aav) serotypes other than aav type 2. *J Virol*, 72(1):309–319, 1998.

[249] G. P. Gao, M. R. Alvira, L. Wang, R. Calcedo, J. Johnston, and J. M. Wilson. Novel adeno-associated viruses from rhesus monkeys as vectors for human gene therapy. *Proc Natl Acad Sci U S A*, 99(18):11854–1189, 2002.

[250] N. Kaludov, B. Handelman, and J. A. Chiorini. Scalable purification of adeno-associated virus type 2, 4, or 5 using ion-exchange chromatography. *Hum Gene Ther*, 13(10):1235–1243, 2002.

[251] K. R. Clark, F. Voulgaropoulou, D. M. Fraley, and P. R. Johnson. Cell lines for the production of recombinant adeno-associated virus. *Hum Gene Ther*, 6(10):1329–1341, 1995.

[252] C. Qiao, J. Li, A. Skold, X. Zhang, and X. Xiao. Feasibility of generating adeno-associated virus packaging cell lines containing inducible adenovirus helper genes. *J Virol*, 76(4):1904–1913, 2002.

[253] M. Urabe, C. Ding, and R. M. Kotin. Insect cells as a factory to produce adeno-associated virus type 2 vectors. *Hum Gene Ther*, 13(16):1935–1943, 2002.

[254] S. Hacein-Bey-Abina, C. von Kalle, M. Schmidt, F. Le Deist, N. Wulffraat, E. McIntyre, I. Radford, J. L. Villeval, C. C. Fraser, M. Cavazzana-Calvo, and A. Fischer. A serious adverse event after successful gene therapy for x-linked severe combined immunodeficiency. *N Engl J Med*, 348(3):255–6, 2003.

[255] N. Dutheil, F. Shi, T. Dupressoir, and R. M. Linden. Adeno-associated virus site-specifically integrates into a muscle-specific DNA region. *Proc. Natl. Acad. Sci. USA*, 97(9):4862–4866, 2000.

[256] D. G. Miller, E. A. Rutledge, and D. W. Russell. Chromosomal effects of adeno-associated virus vector integration. *Nat Genet*, 30(2):147–148, 2002.

[257] H. Nakai, E. Montini, S. Fuess, T. A. Storm, M. Grompe, and M. A. Kay. Aav serotype 2 vectors preferentially integrate into active genes in mice. *Nat Genet*, 34(3):297–302, 2003.

[258] D. W. Russell, I. E. Alexander, and A. D. Miller. Dna synthesis and topoisomerase inhibitors increase transduction by adeno-associated virus vectors. *Proc Natl Acad Sci U S A*, 92(12):5719–5723, 1995.

[259] L. Zentilin, A. Marcello, and M. Giacca. Involvement of cellular double-stranded DNA break binding proteins in processing of the recombinant adeno-associated virus genome. *J. Virol.*, 75(24):12279–12287, 2001.

[260] S. Song, P. J. Laipis, K. I. Berns, and T. R. Flotte. Effect of DNA-dependent protein kinase on the molecular fate of the rAAV2 genome in skeletal muscle. *Proc. Natl. Acad. Sci. USA*, 98(7):4084–4088, 2001.

[261] D. Duan, Y. Yue, and J. F. Engelhardt. Consequences of DNA-dependent protein kinase catalytic subunit deficiency on recombinant adeno-associated virus genome circularization and heterodimerization in muscle tissue. *J. Virol.*, 77(8):4751–4759, 2003.

[262] D. Duan, Y. Yue, Z. Yan, J. Yang, and J. F. Engelhardt. Endosomal processing limits gene transfer to polarized airway epithelia by adeno-associated virus. *J. Clin. Invest.*, 105(11):1573–1587, 2000.

[263] R. O. Snyder, S. K. Spratt, C. Lagarde, D. Bohl, B. Kaspar, B. Sloan, L. K. Cohen, and O. Danos. Efficient and stable adeno-associated virus-mediated transduction in the skeletal muscle of adult immunocompetent mice. *Hum. Gene Ther.*, 8(16):1891–1900, 1997.

[264] N. Vincent-Lacaze, R. O. Snyder, R. Gluzman, D. Bohl, C. Lagarde, and O. Danos. Structure of adeno-associated virus vector dna following transduction of the skeletal muscle. *J. Virol.*, 73(3):1949–1955, 1999.

[265] F. K. Ferrari, T. Samulski, T. Shenk, and R. J. Samulski. Second-strand synthesis is a rate-limiting step for efficient transduction by recombinant adeno-associated virus vectors. *J. Virol.*, 70(5):3227–3234, 1996.

[266] K. J. Fisher, G. P. Gao, M. D. Weitzman, R. DeMatteo, J. F. Burda, and J. M. Wilson. Transduction with recombinant adeno-associated virus for gene therapy is limited by leading-strand synthesis. *J. Virol.*, 70(1):520–532, 1996.

[267] K. Qing, J. Hansen, K. A. Weigel-Kelley, M. Tan, S. Zhou, and A. Srivastava. Adeno-associated virus type 2-mediated gene transfer: role of cellular fkbp52 protein in transgene expression. *J Virol*, 75(19):8968–8976, 2001.

[268] C. Mah, K. Qing, B. Khuntirat, S. Ponnazhagan, X. S. Wang, D. M. Kube, M. C. Yoder, and A. Srivastava. Adeno-associated virus type 2-mediated gene transfer: role of epidermal growth factor receptor protein tyrosine kinase in transgene expression. *J. Virol.*, 72(12):9835–9843, 1998.

[269] K. Qing, W. Li, L. Zhong, M. Tan, J. Hansen, K. A. Weigel-Kelley, L. Chen, M. C. Yoder, and A. Srivastava. Adeno-associated virus type 2-mediated gene transfer: role of cellular t-cell protein tyrosine phosphatase in transgene expression in established cell lines in vitro and transgenic mice in vivo. *J Virol*, 77(4):2741–2746, 2003.

[270] D. Duan, P. Sharma, J. Yang, Y. Yue, L. Dudus, Y. Zhang, K. J. Fisher, and J. F. Engelhardt. Circular intermediates of recombinant adeno-associated virus have defined structural characteristics responsible for long-term episomal persistence in muscle tissue. *J. Virol.*, 72(11):8568–8577, 1998.

[271] H. Nakai, T. A. Storm, and M. A. Kay. Recruitment of single-stranded recombinant adeno-associated virus vector genomes and intermolecular recombination are responsible for stable transduction of liver in vivo. *J. Virol.*, 74(20):9451–9463, 2000.

[272] H. Nakai, S. R. Yant, T. A. Storm, S. Fuess, L. Meuse, and M. A. Kay. Extrachromosomal recombinant adeno-associated virus vector genomes are primarily responsible for stable liver transduction in vivo. *J. Virol.*, 75(15):6969–6976, 2001.

[273] R. Hirata, J. Chamberlain, R. Dong, and D. W. Russell. Targeted transgene insertion into human chromosomes by adeno-associated virus vectors. *Nat. Biotechnol.*, 20(7):735–738, 2002.

[274] M. G. Kaplitt, X. Xiao, R. J. Samulski, J. Li, K. Ojamaa, I. L. Klein, H. Makimura, M. J. Kaplitt, R. K. Strumpf, and E. B. Diethrich. Long-term gene transfer in porcine myocardium after coronary infusion of an adeno-associated virus vector. *Ann Thorac Surg*, 62(6):1669–1676, 1996.

[275] D. Gnatenko, T. E. Arnold, S. Zolotukhin, G. J. Nuovo, N. Muzyczka, and W. F. Bahou. Characterization of recombinant adeno-associated virus-2 as a vehicle for gene delivery and expression into vascular cells. *J. Investig. Med.*, 45(2):87–98, 1997.

[276] Y. Maeda, U. Ikeda, Y. Ogasawara, M. Urabe, T. Takizawa, T. Saito, P. Colosi, G. Kurtzman, K. Shimada, and K. Ozawa. Gene transfer into vascular cells using adeno-associated virus (AAV) vectors. *Cardiovasc. Res.*, 35(3):514–521, 1997.

[277] F. Rolling, Z. Nong, S. Pisvin, and et al. Adeno-associated virus-mediated gene transfer into rat carotid arteries. *Gene. Ther.*, 4(8):757–761, 1997.

[278] C. M. Lynch, P. S. Hara, J. C. Leonard, J. K. Williams, R. H. Dean, and R. L. Geary. Adeno-associated virus vectors for vascular gene delivery. *Circ. Res.*, 80(4):497–505, 1997.

[279] M. Richter, A. Iwata, J. Nyhuis, Y. Nitta, A. D. Miller, C. L. Halbert, and M. D. Allen. Adeno-associated virus vector transduction of vascular smooth muscle cells in vivo. *Physiol. Genomics*, 2(3):117–127, 2000.

[280] Zacchigna Serena. Sviluppo di un vettore AAV per il trasferimento del gene hTimp1 e sue applicazioni in terapia genica, 2000.

[281] D. Grimm, A. Kern, K. Rittner, and J. A. Kleinschmidt. Novel tools for production and purification of recombinant adenoassociated virus vectors. *Hum. Gene Ther.*, 9(18):2745–2760, 1998.

[282] S. Diviacco, P. Norio, L. Zentilin, S. Menzo, M. Clementi, G. Biamonti, S. Riva, A. Falaschi, and M. Giacca. A novel procedure for quantitative polymerase chain reaction by coamplification of competitive templates. *Gene*, 122(2):313–320, 1992.

[283] A. Lafont, E. Durand, J. L. Samuel, B. Besse, F. Addad, B. I. Levy, M. Desnos, C. Guerot, and C. M. Boulanger. Endothelial dysfunction and collagen accumulation: two independent factors for restenosis and constrictive remodeling after experimental angioplasty. *Circulation*, 100(10):1109–1115, 1999.

[284] A. Albini, I. Paglieri, G. Orengo, S. Carlone, M. G. Aluigi, R. DeMarchi, C. Matteucci, A. Mantovani, F. Carozzi, S. Donini, and R. Benelli. The beta-core fragment of human chorionic gonadotrophin inhibits growth of kaposi's sarcoma-derived cells and a new immortalized kaposi's sarcoma cell line. *AIDS*, 11(6):713–721, 1997.

[285] B. H. Strauss, R. J. Chisholm, F. W. Keeley, A. I. Gotlieb, R. A. Logan, and P. W. Armstrong. Extracellular matrix remodeling after balloon angioplasty injury in a rabbit model of restenosis. *Circ. Res.*, 75(4):650–658, 1994.

[286] D. Duan, Z. Yan, Y. Yue, and J. F. Engelhardt. Structural analysis of adeno-associated virus transduction circular intermediates. *Virology*, 261(1):8–14, 1999.

[287] C. Castro, A. Diez-Juan, M. J. Cortes, and V. Andres. Distinct regulation of mitogen-activated protein kinases and p27kip1 in smooth muscle cells from different vascular beds. a potential role in establishing regional phenotypic variance. *J Biol Chem*, 278(7):4482–4490, 2003.

[288] F. Rolling, Z. Nong, S. Pisvin, and et al. Adeno-associated virus-mediated gene transfer into rat carotid arteries. *Gene. Ther.*, 4(8):757–761, 1997.

[289] M. R. Ward, G. Pasterkamp, A. C. Yeung, and C. Borst. Arterial remodeling. mechanisms and clinical implications. *Circulation*, 102(10):1186–1191, 2000.

[290] Y. Hojo, U. Ikeda, T. Katsuki, O. Mizuno, H. Fujikawa, and K. Shimada. Matrix metalloproteinase expression in the coronary circulation induced by coronary angioplasty. *Atherosclerosis*, 161(1):185–192, 2002.

[291] A. Kranzhofer, A. H. Baker, S. J. George, and A. C. Newby. Expression of tissue inhibitor of metalloproteinase-1, -2, and -3 during neointima formation in organ cultures of human saphenous vein. *Arterioscler. Thromb. Vasc. Biol.*, 19(2):255–265, 1999.

[292] D. Godin, E. Ivan, C. Johnson, R. Magid, and Z. S. Galis. Remodeling of carotid artery is associated with increased expression of matrix metalloproteinases in mouse blood flow cessation model. *Circulation*, 102(23):2861–2866, 2000.

[293] H. J. Cho, I. H. Chae, K. W. Park, J. R. Ju, S. Oh, M. M. Lee, and Y. B. Park. Functional polymorphism in the promoter region of the gelatinase b gene in relation to coronary artery disease and restenosis after percutaneous coronary intervention. *J. Hum. Genet.*, 47(2):88–91, 2002.

[294] M. P. Bendeck, M. Conte, M. Zhang, N. Nili, B. H. Strauss, and S. M. Farwell. Doxycycline modulates smooth muscle cell growth, migration, and matrix remodeling after arterial injury. *Am. J. Pathol.*, 160(3):1089–1095, 2002.

[295] J. J. Wentzel, J. Kloet, I. Andhyiswara, J. A. Oomen, J. C. Schuurbiers, B. J. de Smet, M. J. Post, D. de Kleijn, G. Pasterkamp, C. Borst, C. J. Slager, and R. Krams. Shear-stress and wall-stress regulation of vascular remodeling after balloon angioplasty: effect of matrix metalloproteinase inhibition. *Circulation*, 104(1):91–96, 2001.

[296] D. W. Seo, H. Li, L. Guedez, P. T. Wingfield, T. Diaz, R. Salloum, B. Y. Wei, and W. G. Stetler-Stevenson. Timp-2 mediated inhibition of angiogenesis: an mmp-independent mechanism. *Cell*, 114(2):171–180, 2003.

[297] J. H. Qi, Q. Ebrahem, N. Moore, G. Murphy, L. Claesson-Welsh, M. Bond, A. Baker, and B. Anand-Apte. A novel function for tissue inhibitor of metalloproteinases-3 (timp3): inhibition of angiogenesis by blockage of vegf binding to vegf receptor-2. *Nat Med*, 9(4):407–415, 2003.

[298] L. J. Feldman, M. Mazighi, A. Scheuble, J. F. Deux, E. De Benedetti, C. Badier-Commander, E. Brambilla, D. Henin, P. G. Steg, and M. P. Jacob. Differential expression of matrix metalloproteinases after stent implantation and balloon angioplasty in the hypercholesterolemic rabbit. *Circulation*, 103(25):3117–3122, 2001.

[299] A. W. Clowes, M. A. Reidy, and M. M. Clowes. Kinetics of cellular proliferation after arterial injury. I. smooth muscle growth in the absence of endothelium. *Lab. Invest.*, 49(3):327–333, 1983.

[300] A. W. Clowes and S. M. Schwartz. Significance of quiescent smooth muscle migration in the injured rat carotid artery. *Circ. Res.*, 56(1):139–145, 1985.

[301] M. A. Reidy, J. Fingerle, and V. Lindner. Factors controlling the development of arterial lesions after injury. *Circulation*, 86(6 Suppl):III43–46, 1992.

[302] A. B. Pardee. G1 events and regulation of cell proliferation. *Science*, 246(4930):603–608, 1989.

[303] R. C. Braun-Dullaeus, M. J. Mann, and V. J. Dzau. Cell cycle progression: new therapeutic target for vascular proliferative disease. *Circulation*, 98(1):82–89, 1998.

[304] V. Lindner, R. A. Majack, and M. A. Reidy. Basic fibroblast growth factor stimulates endothelial regrowth and proliferation in denuded arteries. *J. Clin. Invest.*, 85(6):2004–2008, 1990.

[305] A. J. Nauta, B. Bottazzi, A. Mantovani, G. Salvatori, U. Kishore, W. J. Schwaeble, A. R. Gingras, S. Tzima, F. Vivanco, J. Egido, O. Tijsma, E. C. Hack, M. R. Daha, and A. Roos. Biochemical and functional characterization of the interaction between Pentraxin 3 and C1q. *Eur. J. Immunol.*, 33(2):465–473, 2003.

[306] E. Napoleone, A. Di Santo, A. Bastone, G. Peri, A. Mantovani, G. de Gaetano, M. B. Donati, and R. Lorenzet. Long pentraxin ptx3 upregulates tissue factor expression in human endothelial cells: a novel link between vascular inflammation and clotting activation. *Arterioscler. Thromb. Vasc. Biol.*, 22(5):782–787, 2002.

[307] R. Singh, S. Pan, C. S. Mueske, T. Witt, L. S. Kleppe, T. E. Peterson, A. Slobodova, J. Y. Chang, N. M. Caplice, and R. D. Simari. Role for tissue factor pathway in murine model of vascular remodeling. *Circ. Res.*, 89(1):71–76, 2001.

[308] S. Bhakdi. Complement and atherogenesis: the unknown connection. *Ann. Med.*, 30(6):503–507, 1998.

[309] T. Chakraborti, A. Mandal, M. Mandal, S. Das, and S. Chakraborti. Complement activation in heart diseases. role of oxidants. *Cell. Signal.*, 12(9-10):607–617, 2000.

[310] A. B. Reiss, N. W. Awadallah, S. Malhotra, M. C. Montesinos, E. S. Chan, N. B. Javitt, and B. N. Cronstein. Immune complexes and IFN-gamma decrease cholesterol 27-hydroxylase in human arterial endothelium and macrophages. *J. Lipid. Res.*, 42(11):1913–1922, 2001.

[311] G. Rodriguez, A. Sulli, M. Cutolo, P. Vitali, and F. Nobili. Carotid atherosclerosis in patients with rheumatoid arthritis: a preliminary case-control study. *Ann. N. Y. Acad. Sci.*, 966:478–482, 2002.

[312] K. S. Kilgore, E. Schmid, T. P. Shanley, C. M. Flory, V. Maheswari, N. L. Tramontini, H. Cohen, P. A. Ward, H. P. Friedl, and J. S. Warren. Sublytic concentrations of the membrane attack complex of complement induce endothelial interleukin-8 and monocyte chemoattractant protein-1 through nuclear factor-kappa B activation. *Am. J. Pathol.*, 150(6):2019–2031, 1997.

[313] B. D. Klugherz, P. L. Jones, X. Cui, W. Chen, N. F. Meneveau, S. DeFelice, J. Connolly, R. L. Wilensky, and R. J. Levy. Gene delivery from a dna controlled-release stent in porcine coronary arteries. *Nat. Biotechnol.*, 18(11):1181–1184, 2000.

[314] R. Mendoza-Maldonado, L. Zentilin, R. Fanin, and M. Giacca. Purging of chronic myelogenous leukemia cells by retrovirally expressed anti-bcr-abl ribozymes with specific cellular compartmentalization. *Cancer Gene Ther*, 9(1):71–86, 2002.

[315] I. J. Kullo, G. Mozes, R. S. Schwartz, P. Gloviczki, M. Tsutsui, Z. S. Katusic, and T. O'Brien. Enhanced endothelium-dependent relaxations after gene transfer of recombinant endothelial nitric oxide synthase to rabbit carotid arteries. *Hypertension*, 30(3 Pt 1):314–320, 1997.

[316] S. P. Janssens, K. D. Bloch, Z. Nong, R. D. Gerard, P. Zoldhelyi, and D. Collen. Adenoviral-mediated transfer of the human endothelial nitric oxide synthase gene reduces acute hypoxic pulmonary vasoconstriction in rats. *J. Clin. Invest.*, 98(2):317–324, 1996.

[317] C. Wang, L. Chao, and J. Chao. Direct gene delivery of human tissue kallikrein reduces blood pressure in spontaneously hypertensive rats. *J. Clin. Invest.*, 95(4):1710–1716, 1995.

[318] P. Zoldhelyi, J. McNatt, X. M. Xu, D. Loose-Mitchell, R. S. Meidell, Jr. Clubb, F. J., L. M. Buja, J. T. Willerson, and K. K. Wu. Prevention of arterial thrombosis by adenovirus-mediated transfer of cyclooxygenase gene. *Circulation*, 93(1):10–17, 1996.

[319] M. J. Mann, G. H. Gibbons, R. S. Kernoff, F. P. Diet, P. S. Tsao, J. P. Cooke, Y. Kaneda, and V. J. Dzau. Genetic engineering of vein grafts resistant to atherosclerosis. *Proc. Natl. Acad. Sci. USA*, 92(10):4502–4506, 1995.

[320] H. Shimano, J. Ohsuga, M. Shimada, Y. Namba, T. Gotoda, K. Harada, M. Katsuki, Y. Yazaki, and N. Yamada. Inhibition of diet-induced atheroma formation in transgenic mice expressing apolipoprotein e in the arterial wall. *J. Clin. Invest.*, 95(2):469–476, 1995.

[321] B. D. Klugherz, C. Song, S. DeFelice, X. Cui, Z. Lu, J. Connolly, J. T. Hinson, R. L. Wilensky, and R. J. Levy. Gene delivery to pig coronary arteries from stents carrying antibody-tethered adenovirus. *Hum. Gene. Ther.*, 13(3):443–454, 2002.

[322] T. E. Arnold, D. Gnatenko, and W. F. Bahou. In vivo gene transfer into rat arterial walls with novel adeno-associated virus vectors. *J. Vasc. Surg.*, 25(2):347–355, 1997.